Nitrogen Storage and Removal in Catchments on the Eastern Shore of Virginia

Samuel Austin Flewelling
Brandywine, Maryland, USA

B.A., University of Virginia, 2001

A Dissertation presented to the Graduate Faculty
of the University of Virginia in Candidacy for the Degree of
Doctor of Philosophy

Department of Environmental Sciences

University of Virginia
December, 2009

_____

_____

_____

_____

Abstract

In this dissertation, I developed several approaches to understand how nitrogen is stored and removed from coupled groundwater-stream systems in the Mid-Atlantic Coastal Plain. I found that there is substantial storage of nitrogen in groundwater and that this storage results in lag times between nitrogen inputs and outputs ranging from decades to centuries. A major implication of this finding is that many of these catchments will experience large increases in groundwater nitrate concentrations in the coming decades, even if anthropogenic nitrogen inputs remain constant. Fortunately, not all nitrate in groundwater discharges to streams. Rather, a portion of nitrate is removed by microorganisms that naturally inhabit streambed and riparian zone sediments. The extent of nitrate removal that occurred in the streambed was a function of groundwater travel time, which varied widely in space. Greater removal occurred where groundwater moved more slowly through nitrate removal zones. Taking the stream as a whole, the extent of nitrate removal was describable by a single rate coefficient applied to high-flow regions of the streambed. Locations of lower flow were not important since they did not contribute significant amounts of nitrate to the stream. But even at a single location in the streambed, the rate of groundwater flow is not constant through time. I found that evapotranspiration can act as a pump in the riparian zone, drawing down the water table and driving patterns in groundwater travel time through the streambed. These patterns in groundwater travel time affected the extent of nitrate removal in the streambed and ultimately stream nitrate concentrations. Thus, the physical interactions between the climate, vegetation, groundwater, and streams determine the fate of nitrogen deposited on the land surface.

Table of Contents

List of Figures

List of Tables

Acknowledgments

This dissertation has been an agonizing process, but in the end, I am glad that I did it. Each of my committee members (Aaron Mills, Janet Herman, George Hornberger, and Teresa Culver) has contributed significantly to this project and I thank each of you. Aaron Mills, who became my committee chair, has been a sounding board for ideas and a strong supporter of my work, even when my ideas did not pan out or led to dead ends. We have had many productive discussions about new ways to approach old problems and his support for creative thinking has been particularly helpful. I am enormously grateful for his continued input, support, and patience over the years. Janet Herman has also been a strong supporter of my work and has been instrumental in helping me organize my ideas and keeping my project moving forward. At times when I felt somewhat alone in the graduate program, Janet helped me realize that my project was, indeed, interesting and that there were many important questions that needed answers. She has been an excellent mentor and I especially thank her for the time that she spent introducing me to others in my field during the 2007 GSA meeting. George Hornberger has fundamentally improved many of the ideas and analyses in this dissertation. I have never met anyone with George's ability to hear a new idea, instantly grasp it, and then be able to immediately improve upon it in a significant way. He has a seemingly endless breadth of knowledge, personable nature, and provides a constant input of ideas. This dissertation improved dramatically from his input and creativity and I am glad to have had the chance to work with him.

Several other faculty members and graduate students have also helped me through the course of this work. Chuanhui Gu has been an excellent friend and colleague and our

discussions helped form the basic understanding of the interactions amongst Cobb Mill Creek, groundwater, and nitrate. Many of the ideas that we developed together are reflected in Chapter 3 of this dissertation. John Maben and Susy Maben have helped me keep our lab running over the years and generously donated their equipment when ours was broken. Jim Galloway helped me put my work in a broader context and Paolo D'Odorico helped with some conceptual and theoretical aspects of derived distributions. I have consulted with Hank Shugart over the years regarding plant-solute interactions at the root-soil interface. Many friends and graduate students have helped me in the lab and field as well, including: Holly Galavotti, Joe Battistelli, Dan Muth, Joel Antonioli, Wendy Robertson, Travis Robertson, Meg Miller, and Matt Long. One undergraduate student, George McFadden, helped me immensely during my last season of field work. Lastly, I thank my loving partner, Rachel Ghent, who has always kept me grounded and reminded me of the things that are most important in life—your family and loved ones.

This research was supported by several funding sources, including: the NSF transient hydrology grant, the LTER grant, a Graduate Assistance in Areas of National Need (GAANN) Felowship, the UVA Environmental Sciences Department, and the UVA Graduate School of Arts & Sciences.

Chapter 1: Introduction and Research Objectives

1.1. The Global Nitrogen Cycle

Famine was predicted in Europe. The year was 1898. William Crookes, incoming president of the British Academy of Sciences, challenged his colleagues to harness the abundant supply of nitrogen in the atmosphere by developing a way to convert nitrogen gas into fertilizer. This challenge was ultimately met by a young German chemist, Fritz Haber, who devised a method to create ammonia synthetically — an essential plant nutrient that could greatly enhance agricultural production. Haber was successful in his quest, and the legacy of his discovery would prove to be one of the greatest boons to human existence in recent history. His discovery would also lead to widespread changes in global environmental processes—a consequence unseen at the time [*Hager*, 2008].

Haber's success led to a Nobel Prize in chemistry in 1918. Carl Bosch, a German chemist and industrialist, modified and increased the scale of Haber's nitrogen fixation process. Bosch's efforts led to the creation of the fertilizer production industry and similar to Haber, Bosch was rewarded with the Nobel Prize in Chemistry in 1931 [*Hager*, 2008]. These two advances made nitrogen fertilizer available to sustain the growing population of Europe and then to the world. Currently, over half of the food eaten by the world's population derives from nitrogen fixed in the Haber-Bosch process [*Galloway and Cowling*, 2002].

The Haber-Bosch process unlocks the vast reservoir of atmospheric (elemental) nitrogen and makes it available (termed fixation) to organisms. Elemental nitrogen, N_2, is abundant, yet un-reactive due to the strong triple bond between nitrogen atoms. Most

organisms cannot use the large reservoir of atmospheric nitrogen; rather, it must be fixed to become useful. Fixation occurs when elemental nitrogen is either oxidized or reduced. The fixation of nitrogen is a critical step that allows life on Earth to exist as we know it.

There are only two natural processes that can fix nitrogen: biological fixation and lightning. Biological fixation is the dominant natural source of fixed nitrogen, and it is accomplished by microorganisms that either work in symbiosis with plants or by themselves. The nitrogen fixed by microbes is reduced, entering the environment either as ammonia or, after assimilation, as organic nitrogen (amines). Lightning, a much smaller natural source, fixes nitrogen through oxidation. The high temperatures and pressures associated with the lightning plasma cause elemental oxygen and nitrogen in the atmosphere to react and form nitrogen oxides [*Galloway et al.*, 1995]. These nitrogen oxides reach the biosphere through a combination of wet and dry deposition [*Russell et al.*, 2003]. Natural nitrogen fixation dominated nitrogen inputs to the environment until the early 20th century, but that dominance has now changed [*Galloway and Cowling*, 2002].

To understand how the nitrogen cycle has changed since then, one needs to consider the primary driver of change—global population. Global population has increased exponentially through time. To feed that growing population requires grain and, not surprisingly, global grain production has mimicked the trend in global population [*Galloway et al.*, 1995]. Since plants (*i.e.,* grain) need nitrogen to grow, there is an indirect link between population and nitrogen use.

The significance of the plant-nitrogen link in agricultural production becomes apparent when one considers the trend in the world's arable and permanent cropland. From 1890 to approximately 1965, the amount of arable and permanent cropland increased proportional to population and grain production. After 1965, the amount of arable and permanent cropland changed little, while grain production almost tripled [*Galloway et al,*. 1995]. That dramatic increase in grain production on essentially the same amount of land was accomplished by the use of nitrogen fertilizers. Humans, through the necessity to eat, have mobilized large amounts of fixed nitrogen.

Fertilizer is not the only source of anthropogenic nitrogen, however. Humans also fix nitrogen by cultivating nitrogen fixing legumes and through combustion process (combustion oxidizes nitrogen in a similar way as lightning). These combined anthropogenic sources currently input fixed nitrogen to the environment at a greater rate than natural processes. Over the past 200 years, humans have gone from a small fixed nitrogen source to being the dominant one [*Galloway and Cowling*, 2002].

Fixed nitrogen is very reactive and once dispersed into the environment, it participates in many oxidation-reduction (redox) reactions. Those redox reactions transform nitrogen into different chemical species, each with different properties and effects. As a result, a single atom of nitrogen can move through the environment, change speciation, and have multiple environmental effects in sequence [*Galloway et al.*, 2003].

The range of nitrogen species and environmental effects has been documented in a wide range of studies. Nitric oxide in the troposphere can catalyze the formation of ground-level ozone, a component of photochemical smog [*Fowler et al.*, 1998], whereas nitrous oxide in the stratosphere can catalyze the destruction of the ozone layer [*Rowland*,

1991]. Nitric acid in the atmosphere increases the acidity of precipitation [*Galloway and Likens*, 1981] and, upon deposition, acidifies surface waters [*Murdoch and Stoddard*, 1992]. Nitrate can contaminate groundwater above drinking water standards, a common occurrence in intensive agricultural areas [*Denver et al.*, 2003]. Both oxidized and reduced nitrogen species contribute to surface water eutrophication [*Vitousek et al.*, 1997], which can cause hypoxia, anoxia, and fish kills. There is, arguably, no other element that has such a wide-spread impact on all environmental compartments as nitrogen.

Because global population is predicted to increase in the future, there will undoubtedly be an increase in reactive nitrogen dispersed to the environment [*Galloway*, 1998]. The question that remains unanswered is: What will be the effects of additional nitrogen inputs to the environment in the future? At present, the scientific community is unable to predict the magnitude or timing of those effects [*Galloway and Cowling*, 2002]. The reason is that we, as a community, are unable to quantify the fate of nitrogen dispersed in the environment with any amount of certainty. The fate of nitrogen depends on microorganisms that recycle fixed nitrogen back into N_2 and physical transport processes that control the storage of nitrogen in the environment. Better quantifying nitrogen's fate depends on improving what is known about these microbial removal and physical storage processes.

1.2. Microbial Nitrate Removal

Fixed nitrogen may exist in a range of oxidation states and chemical species. The chemical species that are biologically useful are referred to as reactive nitrogen (Nr). While Nr is a broad range of species, there are only two processes that can remove that

nitrogen from the reactive pool. Both of these processes, anammox and denitrification, are carried out by microorganisms.

The anammox pathway simultaneously converts NH_3 and NO_2^- to N_2. Anammox is considered most important in the low-organic matter conditions of the deep oceans [*Schmidt et al.*, 2003] and is probably not as important on the continents where organic matter is more abundant. Very little terrestrial nitrogen reaches the open ocean [*Chen and Wang*, 1999; *Nixon*, 1996; *Seitzinger and Giblin*, 1996], such that terrestrial and oceanic nitrogen cycles are essentially decoupled. The terrestrial environment is the main focus here, where the highest rates of nitrogen deposition occur and denitrification is the dominant nitrate removal mechanism.

Denitrification is the dissimilatory reduction of NO_3^- to N_2 [*Zumft*, 1997] and is a fairly ubiquitous process which can occur in virtually any near-surface environment, provided that the right conditions exist. Most denitrifiers are heterotrophic facultative anaerobic bacteria that use oxygen as the terminal electron acceptor when present, but switch to using nitrate when oxygen becomes limiting [*Zumft*, 1997]. Electron donors for denitrification include organic carbon, sulfide, and ferrous iron. The approximate stoichiometry for denitrification by organic carbon [*Freeze and Cherry*, 1979], sulfide, and ferrous iron [*Tesoriero et al.*, 2000] oxidation are given in Equations (1)-(3), respectively.

$$CH_2O + \tfrac{4}{5} NO_3^- \rightarrow \tfrac{2}{5} N_{2(g)} + HCO_3^- + \tfrac{1}{5} H^+ + \tfrac{2}{5} H_2O \qquad (1)$$

$$5FeS_2 + 14NO_3^- + 4H^+ \rightarrow 5Fe^{2+} + 7N_2 + 10SO_4^{2-} + 2H_2O \qquad (2)$$

$$5Fe^{2+} + NO_3^- + 7H_2O \rightarrow 5FeOOH + \tfrac{1}{2} N_2 + 9H^+ \quad (3)$$

Most denitrification is heterotrophic and tends to follow a stoichiometric relationship of the form of Equation (1). Thus, locations with high concentrations of dissolved organic carbon (DOC), nitrate and low dissolved oxygen are generally favorable for denitrification.

These denitrifying conditions are often found in the riparian zones and streambeds of agricultural watersheds. High rates of denitrification often occur in riparian zones where nitrate-rich groundwater mixes with DOC-rich groundwater [*Hill et al.*, 2000] or comes in contact with organic-rich peat deposits [*Hedin et al.*, 1998]. The organic matter in both cases serves to remove dissolved oxygen and to provide the energy to drive denitrification. Similarly, denitrification in streambed sediments can potentially remove all nitrate in groundwater, provided that there is sufficient organic matter [*Mills et al.*, 2008] or reduced minerals [*Bohlke and Denver*, 1995] to supply denitrifiers with the requisite reducing power. Thus, the rate of denitrification depends on the activity of microorganisms as moderated by their surroundings.

In concert with denitrification rates, the extent of nitrate removal is controlled by the contact time between nitrate and denitrifiers. Riparian zone and streambed environments consist of saturated soils and sediments. Nitrate is dissolved in the interstitial waters of those saturated porous media. The flow of water through these pores is controlled by hydrological processes and therefore, so is the residence time of nitrate. Thus, the extent of nitrate removal depends on denitrifier activity and hydrological controls on nitrate's residence time within denitrifying zones.

1.2.1. Residence Time

It is generally understood that longer residence time leads to a greater extent of nitrate removal. This is true of nitrate in surface water (e.g. Seitzinger et al. [2002]) and in groundwater within riparian zones (e.g. Willems et al. [1997]) and streambeds [*Gu et al.*, 2008]. Residence time is never a constant, however, since hydrological conditions are always changing.

Short-term perturbations may occur in stream and groundwater flow due to storms [*Cooper and Rorabaugh*, 1963] or daily evapotranspiration cycles [*Troxell*, 1936; *White*, 1932]. Intermediate-scale transience may result from seasonal climatic patterns that drive changes in precipitation, evapotranspiration, and stream flow [*Thornthwaite*, 1948]. Longer-term fluctuations in the climate due to large-scale ocean-atmosphere feedbacks can also affect hydrological conditions. Thus, catchment hydrology is always in a state of change.

Constantly changing hydrological conditions must have some effect on nitrate removal since hydrology controls the residence time of the nitrate-containing water in active zones of denitrification. Storms, for example, can alter the residence time of groundwater nitrate in the denitrifying zone of streambeds and this can either increase or decrease the flux of nitrate from groundwater [*Gu, et al.*, 2008]. The change in nitrate flux depends on the hydraulic diffusivity of the streambed and the size of the storm. Seasonal climatic patterns also affect the rate of groundwater flow through the riparian zone, such that lower stream nitrate concentrations may be found in the summer, when residence time is longer [*Lischeid et al.*, 2007]. The effects of diurnal evapotranspiration

cycles and inter-annual hydrological transience on groundwater residence time and, therefore, nitrate removal have not been studied.

1.3. Nitrogen Storage

Reactive nitrogen that is not removed by microorganism is stored in the environment. Storage can occur in any environmental compartment, such as soils, trees, and groundwater. The magnitude of storage observed in these different compartments varies, and some compartments are larger than others.

Agricultural soils receive large inputs of nitrogen fertilizer. Much of this nitrogen is either taken up by plants [*Smil*, 1999] or leached downward to the water table [*Denver, et al.*, 2003]. Therefore, agricultural soils generally do not retain much of this fertilizer nitrogen over the long term, so N storage in agricultural soils is not considered to be large. This is in contrast to significant N storage that has been observed in some forest soils [*Neirynck et al*., 2008].

Storage of N in biota depends primarily on accumulation in woody biomass. Although trees may take up large quantities of nitrogen during the growing season, much of this is returned to the soil when leaves senesce [*Kozlowski*, 1997]. Therefore, only a small fraction of nitrogen taken up by trees remains in the woody biomass and in some cases, this makes trees a small component of N storage [*Neirynck et al*., 2008]. In catchments dominated by agricultural land use, forest coverage is generally low, further reducing the potential for nitrogen storage in woody biomass. N storage in trees must be small in agricultural areas.

Little work has been done on the subject of N storage in groundwater. Howarth *et al.* [1996] ignored the effects of groundwater storage on N transport, since their

calculated groundwater N storage was only a small fraction of annual N inputs. These estimates may not be accurate however, since they were generalized for the North American continent and were based on very low groundwater storage estimates (*i.e.* a continental average storage of 7.8 cm). In agricultural catchments with permeable soils overlying unconfined aquifers, widespread leaching of N to groundwater has been observed [*Denver et al.*, 2003]. Significant lag times between catchment N inputs and outputs in streams have also been observed in similar agricultural catchments [*Bohlke*, 2002]. Given these observations, it seems likely that groundwater is either a significant reservoir for N storage, a major moderator in the timing of N transport, or both. In any case, there is a need to better understand how the storage and release of groundwater N affects stream N concentrations.

1.4 Research Objectives and Dissertation Summary

The goal of the present research was to develop a better understanding of three critical issues:

1. **Lag times created by nitrogen storage in groundwater,**
2. **The control of residence time on nitrate removal in streambed sediments, and**
3. **The effects of temporal variations in residence time on stream nitrate concentrations.**

This work focused on the Cobb Mill Creek watershed on the Eastern Shore of Virginia, with an emphasis on nitrate removal in streambed sediments. Nitrate removal in

streambeds of gaining streams has only been studied to a limited extent. Groundwater travel time through streambed sediments can vary spatially [*Kennedy et al.*, 2007] and temporally [*Gu, et al.*, 2008]. Because the extent of nitrate removal depends on time, variations in groundwater travel time may result in distinct patterns in nitrate fluxes in stream flow. It is important to understand the aggregate effects of those spatial and temporal variations on nitrate fluxes in streams so that better quantitative predictions of the effects of future nitrogen inputs can be determined.

This work fills a critical gap in our existing knowledge of nitrogen cycling in coastal plain catchments. Hydrology is a seldom-studied cause for temporal and spatial variations in nitrate concentrations in near-stream zones, despite the important role that hydrology plays in nitrogen biogeochemistry [*Cirmo and McDonnell*, 1997]. Unfortunately, the predictive models used to estimate nitrogen discharge from streams [*Caraco and Cole*, 1999; *Howarth et al.*, 1996] or nitrate removal during in-stream transport [*Seitzinger et al.*, 2006] tend to rely more on statistical regressions than fundamental relationships between hydrology and nitrogen biogeochemistry. Groundwater and streams interact [*Winter et al.*, 1998] and there is a need to develop a mechanistic understanding of those interactions among streams, groundwater, and nitrogen inputs to catchments. In order to do so, the hydrological setting needs to be more carefully considered.

In the following chapters, I present several approaches to help understand the hydrological controls on nitrate accumulation in groundwater and nitrate's residence time within key removal zones. These approaches are as mechanistic and as physically based as practicable in an effort to reduce some of the limitations of previous statistical

approaches. I first developed a simple theory in Chapter 2 that predicts considerable increases in groundwater nitrate concentrations in the Mid-Atlantic Coastal Plain.

With large predicted increases, there are likely to be impacts on streams as well. But the effects on streams cannot be determined without first knowing how much nitrate discharges from groundwater to streams. This subject is addressed in Chapters 3 and 4, where I report the tremendous variability in groundwater travel time through streambed sediments in space and time. However, despite the large amount of spatial variation in travel time, the system as a whole was still describable by an average reaction rate coefficient (Chapter 3).

These findings allow one to subsume the enormous spatial variability into effective or averaged quantities so that simple, low-dimensional models can be used to interpret nitrate concentrations that are driven by groundwater-stream interactions. In Chapter 4, a modeling approach was used to show that evapotranspiration drives diurnal fluctuations in stream discharge and nitrate concentrations. These findings provide a new perspective on how streambeds and riparian zones work to retain nitrate and the importance that hydrology plays in controlling the extent of retention. This work, combined with previous research by Gu *et al.* [2008; 2007], Mills et al. [2008], and Galavotti [2004] provides a compendium of the controls on nitrate transport and removal near the groundwater-surface water interface of Cobb Mill Creek and, by extension, similar coastal plain settings. The discoveries reported here provide a range of tools for understanding and predicting the impacts of agricultural nitrogen use on groundwater and streams.

Chapter 2: Groundwater Nitrogen Dynamics in the Mid-Atlantic Coastal Plain

Abstract

A dynamic catchment-scale mass-balance model for nitrogen was developed to predict how catchments in the Mid-Atlantic Coastal plain would respond to changing nitrogen (N) inputs through time. The model was developed in a way that explicitly links the hydrological cycle to the N cycle in catchments and was used to estimate the catchment response time (the time required to achieve steady state) to a step change in N inputs. Predictions of groundwater N concentrations by the model were then compared to historical groundwater N concentrations near Locust Grove, MD. Catchment response times varied from decades to centuries and depended on aquifer thicknesses. The slow response time of catchments suggests that most on the Delmarva Peninsula are probably far from steady state conditions. The model reproduced the historical trend in groundwater N concentrations near Locust Grove and predicted that catchments in that area would require about 50 years to reach steady state after N inputs stabilized. Furthermore, the model predicted that groundwater N concentrations in that area would increase from about 17 mg L^{-1} in 1990 to 25 mg L^{-1} at steady state in 2040. Intense agricultural activities will likely continue on the Delmarva Peninsula, and groundwater N concentrations will increase substantially in the future as catchments in the region move closer to steady state. The transfer of that N to coastal waters will only worsen problems with surface water eutrophication.

2.1 Introduction

Nitrogen (N) is a ubiquitous contaminant of groundwater worldwide [*Spalding and Exner*, 1993]. In agricultural watersheds, groundwater N concentrations have changed over time, reflecting the historical use of N fertilizers [*Bohlke and Denver*, 1995]. Groundwater ultimately discharges to streams and other surface water features where this nitrogen can adversely affect aquatic ecosystems. The discharge of groundwater with high N concentrations to streams may persist long after application of N fertilizers ceases due to long travel times from recharge areas to discharge areas [*Tomer and Burkart*, 2003]. This persistence of N in groundwater suggests that significant storage of anthropogenic N may occur. Developing a better understanding of this groundwater storage mechanism will improve the prediction of future patterns of eutrophication associated with groundwater N discharging to surface waters.

To better understand downstream N migration, there have been many models proposed for describing stream N fluxes (*e.g. Howarth et al*. [1996], *Smith et al.,* [1997], *Caraco and Cole* [1999], *Green et al*. [2004]). Surprisingly, none of these models included storage of N within catchments or the potential lag time between inputs and outputs that may result from long groundwater travel times. All these models are based on statistical regression and when used in a predictive fashion, this can be problematic because the regression coefficients are dependent on the data set used to produce the regression. There is no guarantee that one set of regression coefficients will work for a different set of streams or even for the same streams during a different time period. Therefore, making predictions of past or future N discharge from streams is a dubious

task with regression models because it is never assured that regression coefficients will remain sufficiently constant under new or changing conditions.

In addition to the limitations inherent to regression analyses, mass balance is not a constraint in any of these models and this means that predictions can defy physical reality. Violation of the mass balance is clearly seen in the model proposed by Green *et al*. (2004). The governing equation of the Green model is, in simplified notation,

$$F_{riv} = p_{riv} p_{res} p_{lake} \left(F_P + \frac{Q}{P} p_{soil} F_{NP} \right), \tag{4}$$

F = N fluxes, with subscripts pertaining to:

riv – riverine export

P – point sources

NP – non-point sources

p = transfer coefficient (i.e. the fraction of N transferred downstream), with subscripts for:

riv – transport through stream and river networks

res – transport through reservoirs

lake – transport through lakes

soil – transport through soils

Q – stream discharge

P – precipitation

As a demonstrative example, consider a catchment with absolutely no N removal mechanisms (*i.e.* 100% of the N input gets transferred to the stream), so all of the delivery coefficients (p's) equal unity. The ratio Q/P is always less than unity and, for

this example, assume that *Q/P* equals 1/3. In this case, the Green equation simplifies to the following expression.

$$F_{riv} = F_P + \frac{1}{3} F_{NP} \tag{5}$$

Thus, with no mechanisms to remove N in the catchment, the Green model would predict that only one-third of non-point N sources reach the stream. This does not make sense, but clearly demonstrates the importance of mass-balance constraints when quantifying N transport and removal. The net effect is that this model inflates the fraction of N inputs that are removed in the watershed.

One way to address the shortcomings of regression analyses, including the mass balance issue, is to develop more physically-based approaches for describing N storage and removal in catchments that rely on meaningful characteristics of catchments as model parameters. In this chapter is developed a simple dynamic mass balance model for nitrogen in coastal plain agricultural watersheds. The model takes the form of a first-order differential equation whose solution predicts the N concentration of groundwater through time. Inputs to the model can be easily measured or estimated from readily available data on hydrological fluxes and N fertilizer use. The model was applied to catchments in the Mid-Atlantic Coastal Plain to answer three important questions:

1. **How long does it take groundwater N concentrations to respond to a step change in N inputs?**
2. **What controls this response time?**

3. **What effects have historical N inputs had on groundwater N concentrations in the Mid-Atlantic Coastal Plain and what changes might be expected in the future?**

Model predictions indicated that it may take decades to centuries for catchments in the Mid-Atlantic Coastal Plain to respond to a step change in N inputs. Response times were controlled by aquifer thickness, where thicker aquifers take longer to respond than thinner ones.

Historical N inputs to the Mid-Atlantic Coastal Plain have changed gradually, rather than the step increase used to estimate catchment response times. The gradual change in N inputs near Locust Grove, MD was used to reconstruct groundwater N concentrations between 1940 and 1990. This historical reconstruction matched the observed record of groundwater N concentrations, suggesting that the model captures the major processes governing groundwater N storage and that this approach is useful as a predictive tool for this coastal plain setting. Extending beyond the period of record, the model predicted that groundwater N concentrations will increase by approximately 40% over the next 50 years if fertilizer application rates remain constant. As a result, the current rates of nitrogen export from groundwater to streams will likely increase over that time period. This increased nitrogen export to surface waters may exacerbate the eutrophication of Mid-Atlantic coastal waters.

2.2 Development of a Dynamic Catchment-Scale Mass Balance for Nitrogen

As the simplest case, catchments within the Mid-Atlantic Coastal Plain were conceptualized as simple reservoirs with a mass of stored nitrogen (M) and some volume of stored water (S). The average concentration of nitrogen in the reservoir, N, is the

stored nitrogen mass divided by the stored volume of water. These are fundamental variables used in the following section to derive a nitrogen mass-balance expression for coastal plain watersheds.

Before proceeding to that derivation, these variables need to be clearly defined. The total mass of nitrogen in a catchment (*M*) is defined as all of the nitrogen contained in soils, soil water, groundwater, and surface water. Catchment storage (S) is the total volume of water stored in the catchment from the land surface down to the confining layer and from the catchment divide to the point on the stream that defines the catchment outlet. Storage includes all water contained in the surficial aquifer, vadose-zone (liquid water and water vapor), and surface water.

The properties of catchments in the Mid-Atlantic Coastal Plain allow some simplifying assumptions to be made. The underlying geology in this area is dominated by an unconsolidated sand layer on the order of 10 m thick, most of which is saturated (*i.e.* the unconfined aquifer). The unconfined aquifer is the largest pool of stored water in Mid-Atlantic Coastal Plain catchments, contains appreciable nitrogen, and interacts with surface waters. I assume, therefore, that storage (*S*) is the water stored in the unconfined aquifer. When storage is normalized by catchment area, it equals aquifer thickness multiplied by porosity. Porosity for these aquifers was assumed to be 0.3, a value representative of sands. In addition to these thick aquifers being the primary location of water storage, groundwater likely stores the majority of aqueous nitrogen as well. Thus, the average watershed nitrogen concentration, *N*, would mimic the average concentration of nitrogen in groundwater. These assumptions carry forward through the rest of this chapter.

The solution of the dynamic catchment mass-balance model predicts the average groundwater nitrogen concentration (N) through time (see Section 2.2.1 and 2.2.2 for the derivation). As inputs, the model requires the terms in the water balance for a catchment and the individual fluxes of nitrogen into and out of a catchment. The sources of data used to estimate the hydrological variables contained in the catchment water balance are described in Section 2.2.3. The nitrogen fluxes into and out of a catchment are estimated in Section 2.2.4. Several model scenarios are then described in Sections 2.2.5 and 2.2.6 that were used to explore how nitrogen concentrations in catchments in the Mid-Atlantic Coastal Plain might respond to changing nitrogen fertilizer inputs through time and what controls lags times.

2.2.1 A Dynamic Catchment-Scale Mass Balance for Nitrogen

The basic concept of the model begins with a balance of inputs (I) and outputs (O) of nitrogen for a catchment, *i.e.* the catchment mass balance for nitrogen.

$$\frac{dM}{dt} = I - O \tag{6}$$

The left hand side can be written in different terms since the mass of nitrogen in the catchment (M) can also be expressed as the product of a water volume and a concentration of nitrogen. Therefore, the time derivative in Equation (6) can be rewritten to depend on the product of aquifer storage (S) and the average groundwater nitrogen concentration (N).

$$M = SN \tag{7}$$

$$\frac{dM}{dt} = \frac{d\left(SN\right)}{dt} \tag{8}$$

$$\frac{d(SN)}{dt} = S\frac{dN}{dt} + N\frac{dS}{dt} \tag{9}$$

The time derivative of storage in Equation (9), $\frac{dS}{dt}$, is a function of precipitation (P), evapotranspiration (E), and stream discharge (Q) according to the water balance for the catchment.

$$\frac{dS}{dt} = P - E - Q \tag{10}$$

Combining Equations (9) and (10) yields an expression of the time derivative of the mass of nitrogen stored in the catchment as a function of the average groundwater nitrogen concentration and the terms from the water balance.

$$\frac{dM}{dt} = S\frac{dN}{dt} + N(P - E - Q) \tag{11}$$

The time derivative of mass in Equation (11) is also equal to the fluxes of nitrogen into and out of the catchment (*i.e. I-O* on the right hand side Equation (6)). Those individual fluxes (F_i) are listed in Table 2-1 and in Equation (12) as the sum of inputs minus the sum of outputs. Catchment area (A) appears in Equation (12) because the nitrogen fluxes are all expressed per unit catchment area.

$$\frac{dM}{dt} = A(F_{atm} + F_{agr}) - A(F_{crp} + F_{str} + F_{net}) \tag{12}$$

The net input or removal term (Fnet) represents the net nitrogen flux due to a suite of processes that are difficult or impossible to measure at the catchment scale (Table 2-2). Previous steady-state nitrogen mass-balance calculations suggested that denitrification and plant uptake would be much larger than volatilization, nitrogen fixation in forests, and septic tank discharge [Barnes, 2004; Stanhope, 2003]. Therefore, it was assumed for

this analysis that Fnet would be a net removal term and was grouped with the other nitrogen output terms in Equation (12).

Table 2-1. Inputs and outputs of nitrogen to a catchment expressed as fluxes. The net input or removal term is a collection of processes that are difficult or impossible to measure at the catchment scale. The dimensions of the fluxes are M L^{-2} T^{-1}.

Inputs	**Notation**
Agricultural input (fertilizer plus legume N fixation)	F_{agr}
Atmospheric deposition (wet plus dry)	F_{atm}
Outputs	
Crop export	F_{crp}
Stream export	F_{str}
Net N input or removal due to immeasurable processes	F_{net}

Table 2-2. Processes that contribute to F_{net}

Process	**Input or Output**
Denitrification	Output
Plant uptake	Output
Volatilization	Output
Nitrogen fixation in forests	Input
Septic tank discharge	Input

The right hand sides of Equations (11) and (12) are equal and can be combined and rearranged into a single expression describing the time derivative of the average groundwater nitrogen concentration $\left(\frac{dN}{dt}\right)$. Catchment area ($A$) in Equation (12) cancels out of the equation because S, P, E, and Q are now expressed per unit catchment area.

$$\frac{dN}{dt} = \frac{1}{S}\left(F_{atm} + F_{agr} - F_{crp} - F_{str} - F_{net}\right) - N\frac{\left(P - E - Q\right)}{S} \tag{13}$$

Equation (13) is a first-order differential equation with respect to N and can be solved numerically as long as all the other terms are known.

The time scale for solving Equation (13) is not inherently restricted, although most of the nitrogen fluxes would be easiest to measure or observe at a yearly time scale. For that reason, I focus the remainder of this paper on yearly averaged or summed values for the variables in Equation (13).

2.2.2 Solution of the Mass Balance

While there are too many unknowns in Equation (13) to solve it directly, simplifications can be made for catchments within the Mid-Atlantic Coastal Plain so that Equation (13) can ultimately be solved.

Consider dividing a catchment into two reservoirs: a near-stream zone and a distal-stream zone. The near-stream zone would comprise the riparian zone and streambed. These are areas of focused groundwater discharge [*Angier et al.*, 2005] and also where nitrogen removal primarily occurs [*Cirmo and McDonnell*, 1997]. The distal-stream zone would then represent the rest of the catchment where recharge and transport of nitrogen through the aquifer takes place. In this scenario, the near-stream zone would act as an in-line reactor that removes nitrogen that discharges from groundwater. A schematic drawing of this two-reservoir system is illustrated in Figure 2-1.

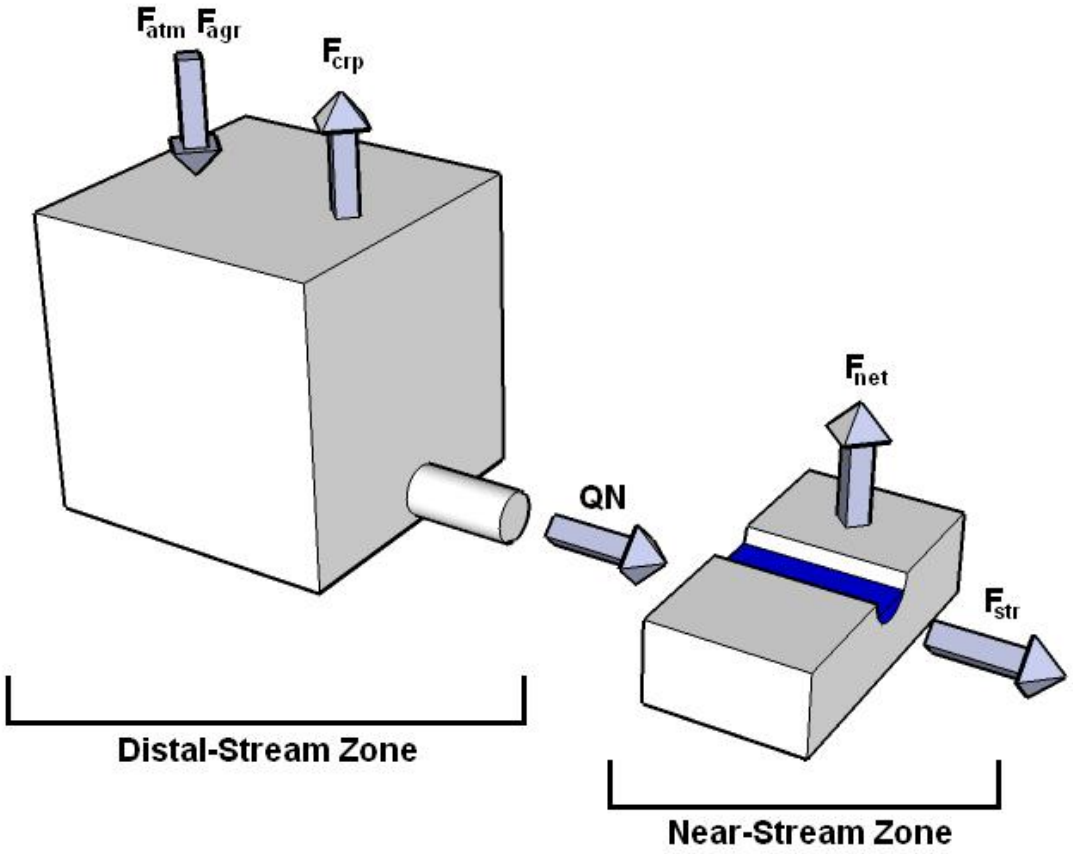

Figure 2-1. Schematic illustration of a catchment represented by a two-reservoir system. In the distal-stream zone, there is no nitrate attenuation and the mean catchment nitrogen concentration (*N*) leaves that reservoir as a stream flux. In the near-stream zone, the only influx of nitrogen is what leaves the distal-stream zone (*QN*) and the fluxes out of the near-stream zone are the actual stream nitrogen flux (F_{str}) and the lumped removal term, F_{net}.

Using the two-reservoir system, the stream nitrogen flux out of the distal-stream zone can now be approximated as the product *QN*. *QN* would also be the only nitrogen flux into the near-stream zone. This flux into the near-stream zone has only a few possible fates; it can leave in stream flow (F_{str}) or be removed by vegetation and denitrification (F_{net}). As a result of these assumptions, the nitrogen mass balance for the distal-stream zone becomes:

$$\frac{dN}{dt} = \frac{1}{S}\left(F_{atm} + F_{agr} - F_{crp} - QN\right) - N\frac{\left(P - E - Q\right)}{S}, \quad (14)$$

which can be simplified to:

$$\frac{dN}{dt} = \frac{1}{S}\left(F_{atm} + F_{agr} - F_{crp}\right) - N\frac{\left(P - E\right)}{S}. \quad (15)$$

The solution of the mass-balance model for the distal-stream zone, Equation (15), is now tractable, because all of the independent variables can be estimated. Thus, the temporal trend in groundwater nitrogen concentrations can now be predicted for different scenarios of nitrogen use and for a range of hydrological conditions.

2.2.3 Hydrological Data

Stream discharge data were obtained for Guy Creek from the USGS National Water Information System (NWIS). Guy Creek is located on the Eastern Shore of Virginia near the town of Painter and drains towards Chesapeake Bay. Stream discharge was measured on the non-tidal freshwater portion of the creek. Complete stream discharge data were available from 1964 to 1995. Stream discharge was reported in cubic feet per second and was converted to cm per year by dividing yearly total discharge by catchment area. Catchment area, 4.9 km^2, was provided in the USGS NWIS database. Discharge from Guy Creek varied from 9 to 63 cm yr^{-1} over the period of record (Figure 2-2).

Daily precipitation and temperature data were obtained from the weather station at Painter, VA. Data were available from 1956 to 2002. Monthly precipitation totals were used to estimate potential evapotranspiration (PET); yearly precipitation totals were used in the dynamic mass-balance model. The weather station only reported minimum

(T_{min}) and maximum (T_{max}) daily temperatures. Average daily temperature was assumed to be the mean of T_{min} and T_{max}. Mean monthly temperatures were calculated by taking the mean of the average daily temperatures and those monthly means were used to estimate potential evapotranspiration (*PET*) with the Thornthwaite [1948; 1955; 1957] method,

$$PET = \begin{cases} 0 & \text{when T < 0 °C} \\ 1.6L\left(\dfrac{10T}{I}\right)^{a} & \text{when 0 ≤ T < 26.5 °C} \\ -415.85 + 32.25T - 0.43T^{2} & \text{when T ≥ 26.5 °C} \end{cases} \quad (16)$$

with

$$L = \frac{d}{30}\frac{h_J}{12}, \quad (17)$$

where d is the number of days in the month and h_J is the number of hours of daylight on the middle day of the month. The variables I and a are defined as follows,

$$I = \sum_{i=1}^{12}\left(\frac{T_i}{5}\right)^{1.514} \quad (18)$$

$$a = \left(6.75x10^{-7}\right)T^3 - \left(7.71x10^{-5}\right)T^2 + \left(1.79x10^{-2}\right)T + 0.49 \quad (19)$$

with the number of daylight hours on the middle day of each month equal to

$$h_J = \frac{24\omega_s}{\pi}. \quad (20)$$

The sunset hour angle (ω_s) is a function of latitude (φ) and solar declination (δ) on day J (Julian day) of the year.

$$\omega_s = \arccos\left(-\tan\phi\tan\delta\right) \quad (21)$$

$$\delta = 0.4093 \sin\left(\frac{2\pi}{365} J - 1.405\right) \tag{22}$$

This approach for estimating PET is somewhat coarse, but was chosen due to the availability of historical climatological data. Multi-decadal historical records of the full set of variables that actually drive evapotranspiration were unavailable such that a more sophisticated estimate of PET (*e.g.* the Penman-Monteith equation) was unattainable. Despite its simplicity and use of mean monthly temperature, the Thornthwaite method still performs well in comparison to other methods that require more extensive data sets [Rosenberry *et al*., 2004].

The *PET* estimates from the Thornthwaite [1948; 1955; 1957] approach were used in a simple water-balance calculation to estimate actual evapotranspiration (E). The water-balance calculation moves at monthly time steps and assumes that the water available for evapotranspiration is a combination of precipitation (P) and water stored in the soil root zone (S_{rz}). All quantities in the water balance are expressed as volume per unit catchment area, that is, as depths. Records of precipitation are available, but the maximum amount of water that can be stored in the root zone is a parameter that must be varied until the predicted runoff from the water balance model agrees closest to observed runoff.

The physical meaning of root zone storage (S_{rz}) is analogous to soil moisture. If S_{rz} were at a maximum in a given month and then in the following month P exceeded *PET*, then the excess water is lost to runoff. Similarly, water supplied to a saturated soil would be lost as runoff. On the other hand, if S_{rz} were below its maximum and P exceeds *PET*, then the excess water would be used to fill up S_{rz} before contributing to runoff. In

the same way, water supplied to a partially-saturated soil would be stored in the soil in addition to contributing to runoff. That logic allows for S_{rz} to vary from month to month between its maximum (a fitted parameter) and its minimum (zero), and is calculated at each monthly time step.

$$S_{rz,i} = S_{rz,i-1} + P_i - PET_i \tag{23}$$

It was assumed that S_{rz} was at a maximum on the first January of simulation. Moving at monthly time steps from that first January, S_{rz} was updated by implementing Equation (23). S_{rz} may only fluctuate between zero and its maximum allowable value. It is physically impossible for *PET* to extract more water than is stored in the soil, so the lower limit of S_{rz} must be equal to zero. If Equation (23) estimates S_{rz} less than zero or greater than its maximum, then a simple instruction was used:

if at any time, $S_{rz} < 0$, then $S_{rz} = 0$;

if at any time, $S_{rz} > \max(S_{rz})$, then $S_{rz} = \max(S_{rz})$.

For any given month of the simulation, S_{rz} at the previous month (time *i-1*) is available to be lost as evapotranspiration in addition to water entering the catchment as precipitation during the current month (time *i*). At each monthly time step, *E* was estimated as follows and then monthly *E* was integrated for each year. Estimated values of annual *E* are shown graphically in Figure 2-2.

$$E_i = \begin{cases} PET_i & \text{when } PETi \le P_i + S_{rz,i-1} \\ P_i + S_{rz,i-1} & \text{when } PET_i > P_i + S_{rz,i-1} \end{cases} \tag{24}$$

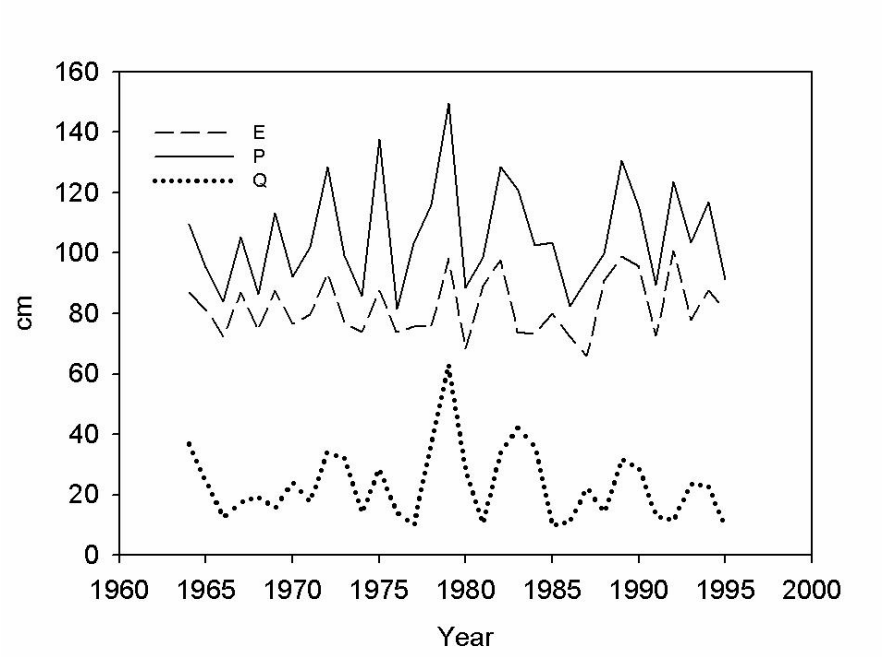

Figure 2-2. Time series of historical precipitation (*P*), modeled evapotranspiration (*E*), and historical stream discharge (*Q*) from Guy Creek that were used in the nitrogen mass-balance model.

At each monthly time step there is some amount of precipitation in excess of water lost to evapotranspiration and S_{rz}. That amount of water is lost as runoff (*R*) and is an estimate of stream discharge that is calculated at each monthly time step.

$$R_i = P_i + S_{rz,i} - S_{rz,i-1} - E_i \tag{25}$$

The maximum value of S_{rz} was varied until the modeled yearly runoff was closest to observed yearly stream discharge. The plot of modeled yearly runoff versus observed stream discharge clustered around a 1:1 line (Figure 2-3A). The modeled runoff also captured the general temporal patterns of peaks and troughs in observed stream discharge (Figure 2-3B). The value of maximum S_{rz} that created a best fit between modeled runoff and observed stream discharge was 11.8 cm.

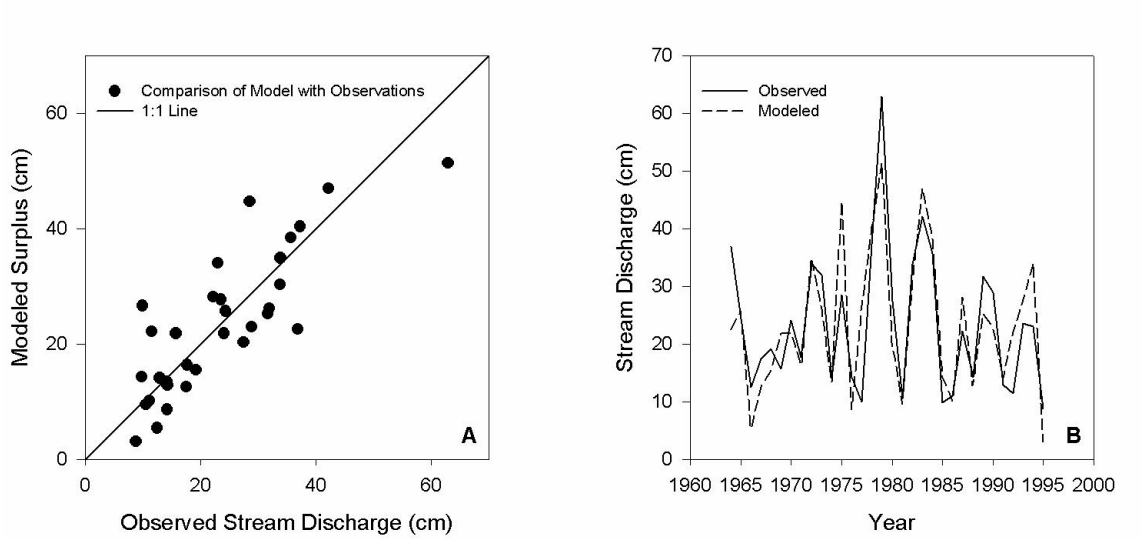

Figure 2-3. Comparison of modeled runoff and observed stream discharge for maximum S_{rz} set to 11.8 cm.

Total catchment storage (S) is the only other hydrological variable required by the nitrogen mass-balance model. Initial storage (S_0 at $t = 0$) was left as a user specified initial condition. This can be estimated from the average aquifer thickness multiplied by porosity. At subsequent yearly time steps, storage was calculated from the water balance equation.

$$S_i = S_{i-1} + P_i - E_i - Q_i \tag{26}$$

2.2.4 Nitrogen Flux Estimates

The nitrogen fluxes that require estimation are atmospheric deposition (F_{atm}), agricultural inputs due to fertilizers and symbiotic N fixation (F_{agr}), and crop export (F_{crp}). This section describes how each of those quantities was estimated.

Atmospheric nitrogen deposition is a combination of wet and dry deposition. Data on wet deposition were taken from the National Atmospheric Deposition Program (NADP). The NADP had data available for wet deposition from 1983-2006 at Wye MD,

from 2001-2006 at Assateague MD, and from 2003-2006 at Trap Pond State Park (TPSP) DE. All of the data overlap (Figure 2-4) and it was assumed that wet deposition at the three sites would be similar to that on the Eastern Shore of Virginia. For simplicity, wet deposition in the nitrogen mass-balance model was assumed constant through time. The constant value was taken as the mean rate of wet atmospheric deposition at Wye, MD (5 kg-N ha^{-1} yr^{-1}). A detailed study of dry deposition at Lewes, Delaware, showed that dry deposition was 43% of total atmospheric nitrogen deposition [*Russell, et al.*, 2003]. To account for dry deposition, the wet deposition was doubled so that total atmospheric deposition (F_{atm}) was 10 kg-N ha^{-1} yr^{-1}.

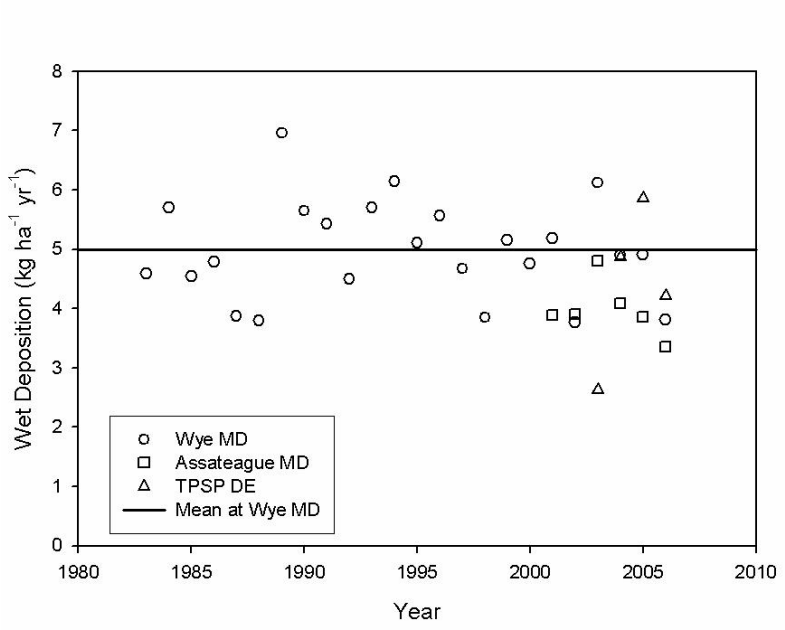

Figure 2-4. Yearly totals of atmospheric nitrogen deposition to National Atmospheric Deposition Program (NADP) monitoring sites close to the Eastern Shore of Virginia.

Agricultural nitrogen inputs were estimated by multiplying the percent of land area in agricultural use (p_{agr}) by the nitrogen input per unit agricultural area (U_{agr}).

$$F_{agr} = \frac{p_{agr}}{100} U_{agr} \tag{27}$$

Based on agricultural loading estimates performed by Stanhope [2003], 150 kg ha^{-1} yr^{-1} was selected as a representative nitrogen input per unit agricultural area (U_{agr}). Stanhope [2003] estimated agricultural nitrogen inputs based on a crop rotation of corn, winter wheat, and soybean.

The flux of nitrogen lost as crop export was assumed to be 50 percent of N inputs (fertilizer plus atmospheric deposition), the same as the global mean fraction of N inputs taken up by agricultural crops [*Smil*, 1999].

$$F_{crp} = 0.5\left(F_{agr} + F_{atm}\right) \tag{28}$$

2.2.5 Response Times in the Mid-Atlantic Coastal Plain

As the simplest scenario, consider a catchment that undergoes a step change in nitrogen inputs, while the hydrological fluxes (*i.e.* P, E, Q, and S) are long-term averages (constants). Under those conditions, the dynamic mass balance (Equation (15)) can be solved analytically with the substitutions,

$$f = \frac{1}{S}\left(F_{atm} + F_{agr} - F_{crp}\right) \tag{29}$$

$$k = \frac{P - E}{S} \tag{30}$$

where f is the net nitrogen flux per unit storage and k is the rate of turnover of groundwater. The reciprocal of k is the hydraulic residence time. Equation (15) can then be rewritten as,

$$\frac{dN}{dt} = f - kN \tag{31}$$

with the solution,

$$N = N_0 + \frac{f}{k}\left(1 - e^{-kt}\right) \quad (32)$$

Holding all other things constant, a range of storages were input to the model to see how this variable affected the response time of groundwater nitrate concentrations to a step change in nitrogen inputs. Aquifer thicknesses in the Mid-Atlantic Coastal Plain range from a few meters to tens of meters [*Trapp*, 1992]. Storages were estimated by multiplying these aquifer thicknesses by an approximate porosity of 0.3 for sand.

2.2.6 Historical and Future Predictions of Groundwater Nitrate Concentrations in the Mid-Atlantic Coastal Plain

The model output from Equation (15) was compared to data on historical groundwater nitrogen concentrations. Bohlke and Denver [1995] inferred the age and measured the nitrate concentrations of groundwater samples near Locust Grove, MD. Locust Grove is within the Mid-Atlantic Coastal Plain, on the Delmarva Peninsula north of the Eastern Shore of Virginia. The historical records of nitrogen fertilizer application and atmospheric N deposition at Locust Grove (data reported by Bohlke and Denver [1995]) were used as inputs to the model. Average P, E, and Q were used from Guy Creek as described in Section 2.2.3. Initial storage was assumed to be 4.5 m (i.e. an aquifer 15 m thick with porosity equal to 0.3) and initial groundwater nitrate concentration before agricultural activity was estimated from Equation 13 for steady-state conditions before agricultural activity began (*i.e.* $dN/dt = 0$ and P and E are constants). With no agricultural activity, fertilizer inputs would be zero and during this earlier time period, atmospheric deposition was assumed half of the current rate (*i.e.* 5 kg ha^{-1} yr^{-1}). With these assumptions, the initial N concentration in groundwater was set to 2.5 mg L^{-1}.

The model was solved for the above conditions during the period of record. Predictions were then made for future groundwater nitrate concentrations by holding nitrogen fertilizer use constant at the 1990 rate for the next 200 years. All other model inputs were the same as described above.

2.3 Results

2.3.1 Response Times

There are two special cases of Equation (32) that provide some insight into how quickly catchments respond to nitrogen inputs and how those inputs affect groundwater at steady state.

The first special case is when t is equal to the hydraulic residence time ($t = 1/k$). For this case, the groundwater nitrogen concentration would be:

$$N = N_0 + 0.63\frac{f}{k} \tag{33}$$

That is, the hydraulic residence time indicates how long it would take for 63% of a step change in nitrogen inputs to be realized in the output. The time required for 95% of nitrogen inputs to be realized in the output is equal to three times the hydraulic residence time ($3/k$). Therefore, the hydraulic residence time is a measure of the response time of a catchment to changing nitrogen inputs.

As a second case, assume that catchments were able to approach steady state, which occurs as t approaches infinity. In that case, the steady state concentration of nitrogen in groundwater (N_{ss}) is:

$$N_{ss} = \lim_{t\to\infty} N_0 + \frac{f}{k}\left(1 - e^{-kt}\right)$$
$$N_{ss} = N_0 + \frac{f}{k} \quad . \tag{34}$$

At steady state, N_{ss} is a simple linear function of nitrogen inputs (f), since hydraulic residence time ($1/k$) is constant for any catchment at steady state. Thus, the linear regression model developed by Howarth *et al*. [1996] for the major basins draining to the North Atlantic Ocean is in the proper mathematical form for catchments at steady state. The accuracy of that regression relationship, however, would depend on how close catchments were to steady state at the time of that study and whether hydraulic residence time could be reasonably assumed constant in all basins draining to the North Atlantic. On the Eastern Shore of Virginia, a much smaller and more homogeneous area, f would primarily reflect agricultural nitrogen inputs to catchments. Agricultural inputs would be related to land use or, more specifically, the percent of land area that is cropped. For catchments at steady state with similar hydraulic residence times, there would be a linear relationship between percent agricultural area and groundwater nitrogen concentrations.

Returning to the idea of catchment response, the response time required for catchment outputs to reflect 95% of a step change in nitrogen inputs was plotted for the range of aquifer thickness in the Mid-Atlantic Coastal Plain. As indicated by Equation (33), a doubling of the amount of water initially stored in the catchment resulted in a doubling of this response time (Figure 2-5). Water stored in aquifers, which is a large component of storage, varies considerably throughout the Mid-Atlantic Coastal Plain [*Trapp*, 1992]. For example, aquifer thickness in Northern Maryland and Northern Delaware is approximately 6 m and then thickens to greater than 12 m in the

Southeastern portions of those states [*Vroblesky and Fleck*, 1991]. Based on the thickness of the surficial deposits near Oyster, VA [*Richardson*, 1994] and the depth to the water table measured in the Cobb Mill Creek catchment, it was inferred that the aquifer thickness was about 11 m in that watershed. Assuming a porosity of 0.3, storage in the Cobb Mill Creek aquifer would be 3.3 m and would correspond to a 95% response time of more than 40 years. With that same assumption, aquifer storage in Northern MD and DE would be 1.8 m and would increase to between 3.6 and 15 m in the Southeastern regions of those states. Those storages are labeled in Figure 2-5 and correspond to 95% response times ranging from decades to centuries.

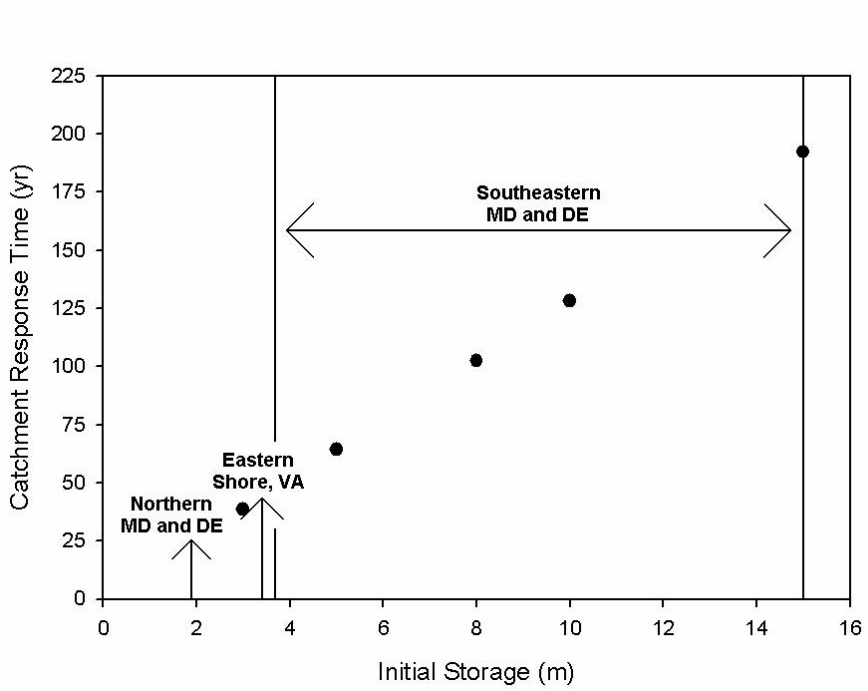

Figure 2-5. The linear relationship between catchment response time and initial storage is linear. Aquifer thicknesses in selected areas of the Delmarva Peninsula were multiplied by a porosity of 0.3 and are labeled by the arrows. In Southeastern Maryland and Delaware, the aquifer thickness can range from 12 m to greater than 50 m [*Vroblesky and Fleck*, 1991] and when multiplied by a porosity of 0.3 corresponds to 3.6-15 m of storage.

The evolution of the mean catchment nitrogen concentration with steady-state and non-steady-state hydrological conditions was calculated with equation (15), assuming

each month obtains a quasi-steady state. These transient simulations are shown in Figure 2-6. The 95% response time for this steady-state scenario was 38 yr (for an aquifer thickness of 10 m). When non-steady-state hydrology is included in the model, there can be 10- to 20-year time intervals where the trend in mean catchment nitrogen concentrations is counter to the long-term multi-decadal pattern. For example, around year 20 in Figure 2-6 (solid line), there were about 10 years when the mean catchment nitrogen concentration leveled off even though the catchment had not yet reached an approximate steady-state. After the catchment had reached an approximate steady state (i.e. after 38 years in Figure 2-6), there were still upward and downward fluctuations that persisted for as long as a decade.

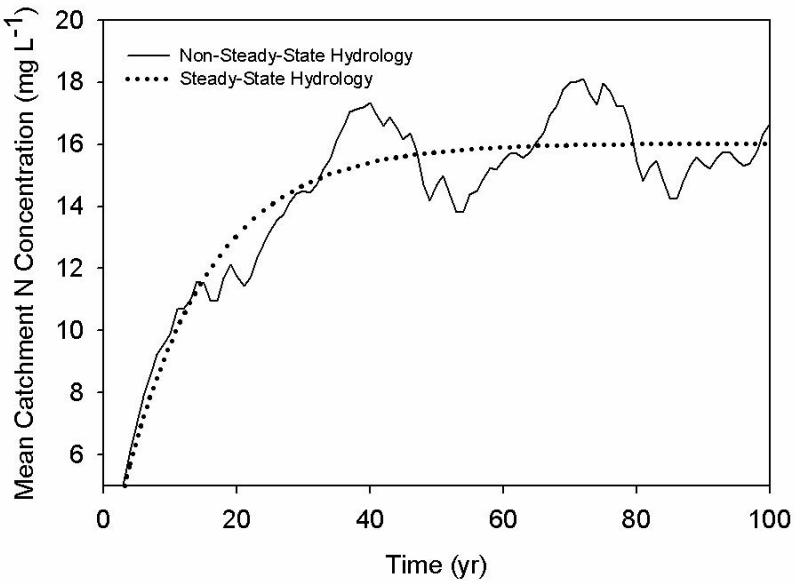

Figure 2-6. Simulated mean catchment N concentration for steady-state and non-steady-state hydrological conditions. The hydraulic residence time (1/*k*) for the steady-state example was 13 yr and the net nitrogen input per unit storage (*f*) was 1.2 g m^3 yr^{-1}.

2.3.2 Predicted Groundwater Nitrate Concentrations: Past, Present, and Future

The dynamic nitrogen mass-balance model (Equation 15) was compared with observed groundwater nitrate concentrations near Locust Grove, MD, that were presented by Bohlke and Denver [1995]. The model reproduced the pattern of historical groundwater nitrate concentrations (Figure 2-7A).

Matching past observations is important, but the true power of the dynamic mass-balance model is in its ability to predict nitrogen concentrations into the future. It is remarkable that the already high groundwater nitrate concentrations found near Locust Grove are predicted to increase far into the future, even though nitrogen inputs were held constant at 1990 levels (*circa* 120 kg ha^{-1} yr^{-1}). It may take another 40 to 50 years before groundwater nitrate concentrations near Locust Grove begin to approach steady state (Figure 2-7B). At steady state, groundwater nitrogen concentrations near Locust Grove will be approximately 40% higher than they were in 1990.

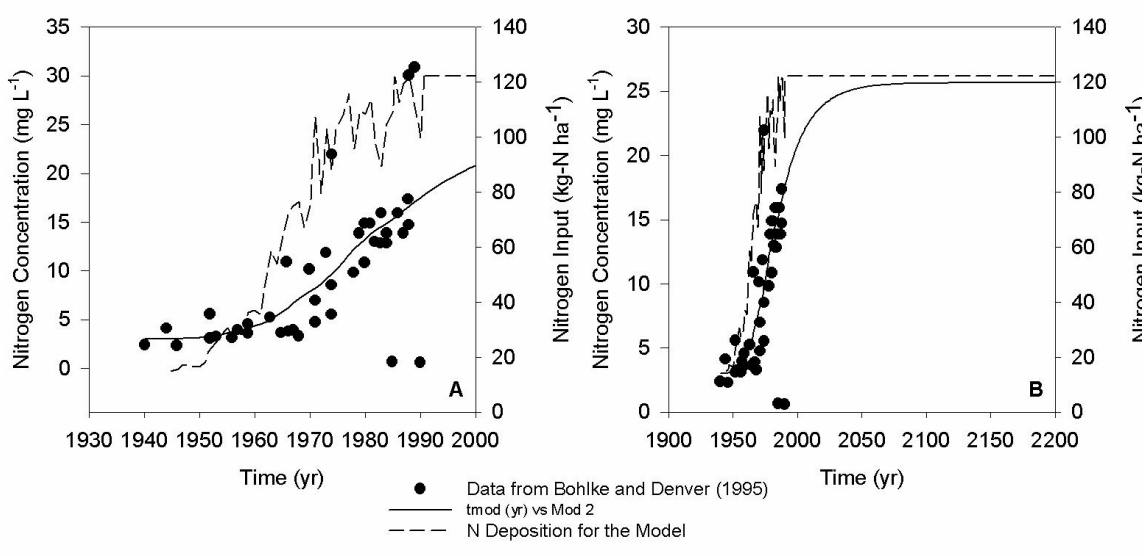

Figure 2-7. Comparison of the dynamic catchment nitrogen mass-balance model to historical groundwater nitrate concentration data collected by Bohlke and Denver [1995]. The history of nitrogen input was also taken from Bohlke and Denver [1995] up to 1990 and was then held constant through 2200. (A) A close up shows detail during the historical record of groundwater nitrate concentrations. (B) The dynamic model predicts that it may take an additional 50 years before groundwater nitrogen concentrations in the Locust Grove, MD, area begin to approach steady state.

2.4 Discussion

There are several implications of the predicted catchment response times. From a management and regulatory standpoint, that response (or lag) time indicates how long it would take for a new regulation or best management practice to achieve its full effect on stream and groundwater quality. Moreover, in a single state or locality, response time may vary considerably. For example, response times in the Maryland Coastal Plain may vary by an order of magnitude depending on geographic location within that state (Figure 2-5). Fortunately, physical constraints on the effective aquifer thickness that were presented by Phillips [2003] constrain the effective aquifer thickness in the Mid-Atlantic Coastal Plain to ~30 m. This constraint also restricts the maximum response time of

these coastal plain catchments to approximately 100 years. Thus, there is at least an upper bound to the response time for these coastal plain catchments.

From a research perspective, the time lag between nitrogen inputs and outputs in catchments is important for explaining environmental observations. There have been numerous linear regressions of annual stream nitrogen export (or stream nitrate concentration) on nitrogen inputs to catchments [*Barnes*, 2004; *Caraco and Cole*, 1999; *Howarth, et al.*, 1996; *Stanhope*, 2003]. None of these approaches considers groundwater nitrogen storage or the lag times resulting from this storage mechanism. They all inherently assume steady state conditions. Under steady state, a linear relationship between inputs and outputs would be expected. Thus, only under the limiting assumption of steady state do these approaches agree with the theory presented here.

It is not clear that all streams used in those regression studies were close to steady state, however. Non-steady-state conditions would add scatter to those relationships and could possibly cause the regression equations to change over time. Several data sets of stream nitrogen fluxes and percentage agricultural area on the Easter Shore of Virginia are plotted in Figure 2-8 (data synthesized from Barnes [2004], Olson et al. [2006], and Stanhope [2003]). All of these plots show positive correlations, but none of these would make a strong regression, nor would a single regression equation fit all three data sets. These inconsistencies may be due, in part, to non-steady-state conditions in these watersheds. Additional research is needed to understand better these observations and the underlying causes for their variability.

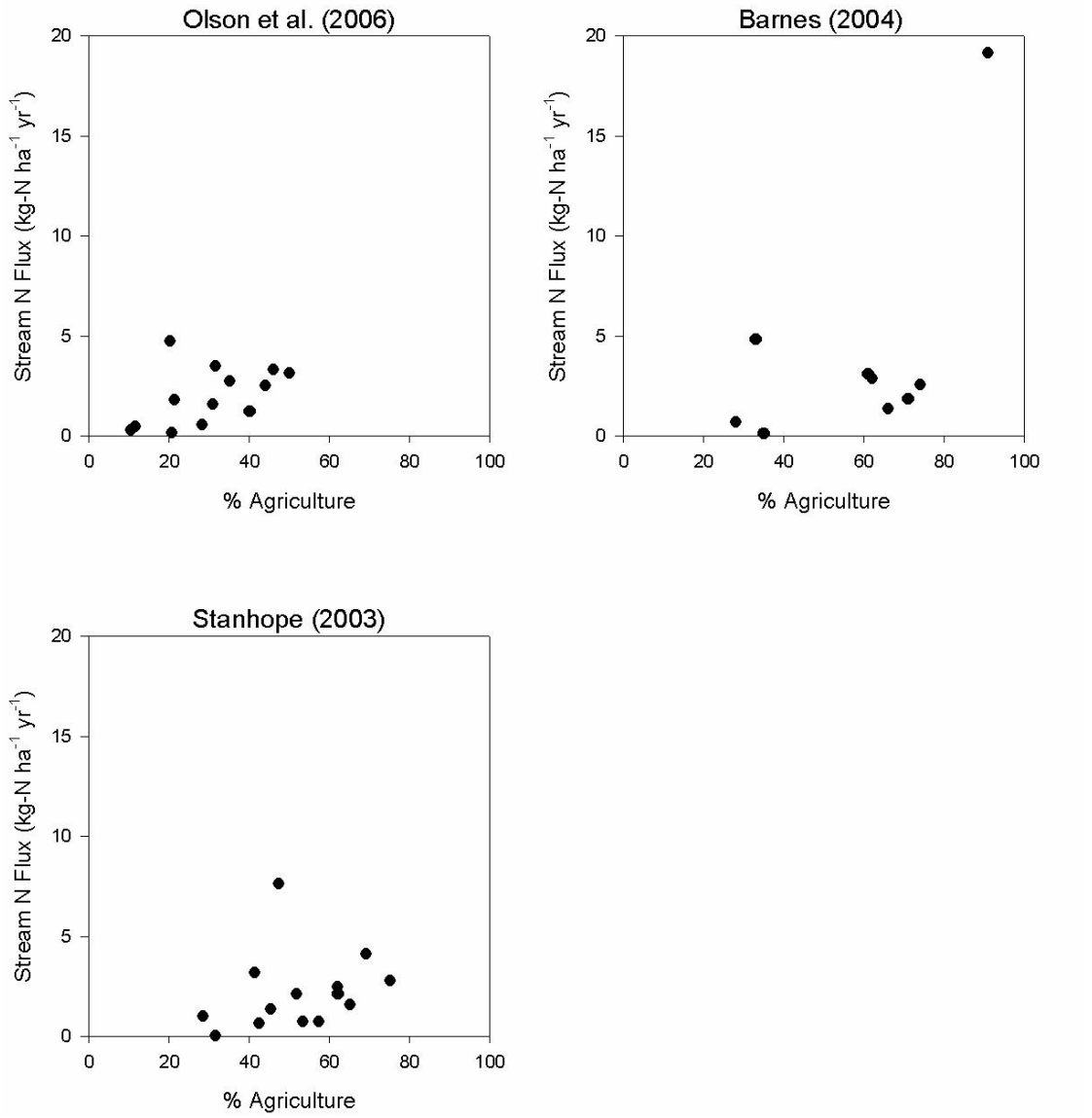

Figure 2-8: Three data sets containing stream nitrogen fluxes and percent agricultural area within the catchments sampled. There appears to be a positive correlation between these two variables, but there is a lot of scatter in the data. The theory presented here suggests that there should be a linear relationship, but that this relationship is only valid for catchments that are in steady state.

An additional inference derived from this analysis is that interpretations of long-term data sets of groundwater nitrogen concentrations should consider the effects of hydrological variability. Apparent trends in groundwater nitrate concentrations may occur even though a watershed is near steady state. This is seen in Figure 2-6 between

years 40 and 55, 55 and 70, and 70 and 80, for example. One would find increasing or decreasing trends during those periods, even though the catchment is in approximate steady state. Only when the groundwater nitrogen concentration is changing rapidly can data sets several years long indicate a reliable trend—*i.e.* between 0 and 13 years in Figure 2-6. Thirteen years is the hydraulic residence time for that particular example. That is, a large change in nitrogen inputs will overwhelm hydrological variability and cause a clear trend in groundwater nitrogen concentrations only within 1 hydraulic residence time of that change. If a groundwater monitoring program were initiated more than 1 hydraulic residence time beyond a large change in nitrogen inputs, it would require a data set several hydraulic residence times long to detect a reliable trend.

Bohlke and Denver [1995] reconstructed a multi-decadal set of groundwater nitrate observations using groundwater age-dating techniques. They found an increasing trend in groundwater nitrate concentrations that lagged behind nitrogen inputs to the Locust Grove area. I predicted that nitrate concentrations would continue to increase for decades, even if nitrate inputs to the catchment were to stabilize. The future for groundwater quality in agricultural catchments is not promising.

But how will these increasing groundwater nitrate concentrations affect streams and coastal areas that ultimately receive this water? Nitrate in aerobic groundwater in the Mid-Atlantic Coastal Plain tends to behave conservatively [*Denver, et al.*, 2003], however, groundwater nitrate that discharges to streams must traverse the reduced conditions in riparian zones and streambed sediments [*Bohlke and Denver*, 1995; *Mills, et al.*, 2008; *Ocampo et al.*, 2006]. Nitrate will not behave conservatively under these reduced conditions. Rather, denitrification will remove some nitrate from groundwater

before it discharges to streams. Thus, the ultimate effect of these increasing groundwater nitrate concentrations on streams will require a more thorough understanding of what controls nitrate removal in streambeds and riparian zones.

Chapter 3: Travel Time Control on Nitrate Discharge from Groundwater to Streams on the Eastern Shore of Virginia, Mid-Atlantic Coastal Plain

Abstract

Groundwater discharge from the streambed of Cobb Mill Creek, VA was measured with seepage meters to determine the effect of groundwater residence time in the streambed on the extent of nitrate removal. Measurements made at the decimeter scale showed a large amount of spatial variability, with travel time in the streambed varying by orders of magnitude (0.2 to 480 cm d^{-1}) and nitrate concentrations in groundwater discharge ranging from nearly zero to more than ten mg L^{-1}. Chloride concentrations varied from 13.5 to 39.5 mg L^{-1}, which was unexpected. The chloride distribution did, however, provide a means of separating groundwater discharge into source components, assuming that riparian processes (*e.g.* evapotranspiration) would increase groundwater chloride concentrations. Based on this assumption, approximately 66% of discharging groundwater was influenced by processes in the riparian zone, whereas 34% bypassed the riparian zone and discharged directly through the streambed. Damkohler numbers (*Da*, a quantity that captures the relative importance of the hydrological transport rate and the denitrification reaction rate) were calculated for non-riparian influenced groundwater and were found to be a linear function of groundwater travel time through the streambed for the locations of highest flow (*i.e.* when travel time was less than 6.7 days). The linear relationship means that the extent of nitrate removal varies spatially with travel time in the streambed and also that an average denitrification rate coefficient could be used for the streambed as a whole. At locations of lower

groundwater flow, a linear relationship between Da and travel time was not apparent. Those locations that deviated from a linear trend did not contribute a significant amount of nitrate to the stream and therefore, the flux of nitrate was dominated by high flow regions of the streambed (*i.e.* where $t < 6.7$ d).

3.1 Introduction

Eutrophication is becoming increasingly problematic in coastal zones [*Nixon*, 1995] that are under pressure from high nitrate loads. Nitrate that leaches from croplands in coastal plain settings enters the groundwater system [*Denver*, 1989] and that water ultimately supplies flow to streams [*Bachman et al.*, 1998] that drain to the coastal bays and lagoons.

Understanding the controls on groundwater nitrate delivery to streams is difficult due to the complex nature of the nitrogen (N) cycle. Nitrate is a reactive solute that is taken up by vegetation [*Kozlowski*, 1997] and microorganisms for the synthesis of proteins. Additionally, nitrate is used as a terminal electron acceptor by some facultative anaerobic bacteria [*Zumft*, 1997]. Because nitrate is a mobile aqueous solute, hydrological transport is a major determinant of the distribution of nitrate in the environment as well. A ratio of the time scales for hydrological transport to biological reaction has been used successfully to explain the extent of nitrate removal in riparian zones and streambeds [*Gu, et al.*, 2007; *Ocampo, et al.*, 2006]. The ability of this simple ratio to explain the extent of nitrate removal across a range of environmental settings (streambeds and riparian zones) and scales (centimeters to decameters) is a significant simplification of the complicated and multi-faceted nitrate transport problem.

Due to natural heterogeneity, the physical transport of nitrate in groundwater near streams may be spatially variable. Groundwater flow depends upon sedimentary architecture [*Bridge*, 1977], which dictates the spatial distribution of hydraulic conductivity (*i.e.* the primary control on groundwater flow rates) [*Cardenas and Zlotnik*, 2003]. The rates of groundwater discharge through streambed deposits, in turn, vary widely at the stream reach scale (meters to decameters) [*Kennedy, et al.*, 2007] and that variability influences solute transport as well [*Conant et al.*, 2004]. In some catchments, heterogeneity can cause focused areas of rapid groundwater discharge that are adjacent to areas with effectively no flow [*Angier et al.*, 2005]. These focused areas of groundwater discharge are also focused areas of solute discharge to streams.

For nitrate, focused groundwater discharge is not the only factor affecting its transport. Nitrate removal is also important. Permanent nitrate removal in streams and riparian zones is accomplished by microorganisms capable of denitrification, the dissimilatory reduction of NO_3^- to N_2. Denitrification in streambed sediments has largely been studied in settings where nitrate-rich stream water enters the streambed as a result of diffusive transport [*Hill*, 1988; *Hill and Sanmugadas*, 1985; *Kellman and Hillaire-Marcel*, 1998; *Swank and Caskey*, 1982] or advection-driven hyporheic exchange [*McMahon and Bohlke*, 1996]. Few studies have investigated the loss of nitrate to denitrification in the streambed of gaining streams where groundwater discharges vertically (upward) and hyporheic exchange is suppressed [*Seitzinger*, 1988].

The few studies that have examined denitrification during advective efflux of groundwater in gaining streams report a range of results. In some cases, nitrate in discharging groundwater passes virtually unaltered through streambed sediments [*Bohlke*

and Denver, 1995; *Denver, et al.*, 2003], whereas other studies have found large reductions in nitrate concentrations [*Jacobs and Gilliam*, 1985; *Lee and Hynes*, 1978; *Mills, et al.*, 2008].

The availability of electron donors has been shown to be part of the cause for the ambiguous role of streambed sediments in nitrate removal [*Bohlke and Denver*, 1995; *Hedin, et al.*, 1998; *Hill, et al.*, 2000]. A seldom studied cause for the ambiguity is the variability of groundwater travel time through active nitrate reduction zones in streambeds. In Cobb Mill Creek (see Fig. 3.1), NO_3^- concentrations in the stream channel are much lower than the ground water concentrations a meter below the bed surface, and profiles of NO_3^- show that the NO_3^- concentration decreases as the water discharges through the surficial sediments in to the stream [*Gallavotti,* 2004; *Mills et al,.* 2008]. Laboratory experiments using intact sediment cores from Cobb Mill Creek [*Gu, et al.*, 2007] demonstrated that groundwater travel time through the streambed sediments plays a major role in determining the nitrate concentrations in groundwater discharging through these sediments. Short residence times can allow significant nitrate to pass through active reduction zones, whereas long residence times may permit complete removal of nitrate to occur.

Several authors have reported that riparian-zone activity is insufficient to remove NO_3^- in groundwater discharging to local streams and have attributed the cause to local hydrology. Whereas, McCarty *et al.* [2008] indicated that water from upland agricultural fields often flows to the stream beneath the riparian zone, thus bypassing the biologically active soils and sediments. Willems *et al.* [1997] speculated that local hydrology, i.e. the presence of groundwater flow paths with short residence times, was responsible for

allowing a portion of groundwater nitrate to pass through the riparian zone in spite of high denitrification potentials measured in the lab. Obviously, either, or both, of these processes may function at any given site, such that nitrate loading to the stream is greater than anticipated based on measurement of biological activity in small samples extracted from the site.

In this paper, the dependency of nitrate removal on groundwater travel time in the streambed of a small coastal-plain stream on the Eastern Shore of Virginia (Cobb Mill Creek) is examined. Cobb Mill Creek is a gaining stream and the strong vertical upwelling of groundwater suppresses hyporheic exchange. Spatial variations in groundwater travel time were inferred from direct measurements of specific discharge from the streambed of Cobb Mill Creek. An extensive set of groundwater seepage samples and the associated solute concentrations of seepage water revealed complex spatial patterns of nitrate and chloride transport, similar to the findings of Conant *et al.* [2004] regarding PCE discharge from a streambed. Almost all nitrate transported from groundwater to the stream in our study reach occurred along flow paths with short (< 6.7 days) residence times in the sediments. Moreover, Damkohler numbers in these areas of rapid flow were a direct linear function of groundwater travel time through the sediment nitrate reduction zone. These observations imply that a single denitrification rate coefficient described our stream reach on average and that hydrology plays an important role in controlling the spatial pattern of the extent of nitrate removal in this system.

3.2 Methods

A multi-step approach was required to measure, and then interpret, groundwater seepage from the streambed of Cobb Mill Creek. In the following sections is described:

1. the general setting of Cobb Mill Creek within the Eastern Shore of Virginia,
2. the collection and analysis of groundwater seepage from the streambed,
3. the determination of subsurface hydraulic head and solute distributions,
4. a first-order rate law for nitrate removal in the streambed, and
5. an empirical method for differentiating groundwater affected by very shallow riparian processes from groundwater that effectively bypasses these soil-based processes.

3.2.1 Research Site Description

The Cobb Mill Creek catchment is approximately 19 km north of the mouth of Chesapeake Bay. The catchment is located on the Eastern Shore of Virginia comprising part of the Anheuser-Busch Coastal Research Center (ABCRC; Figure 3-1).

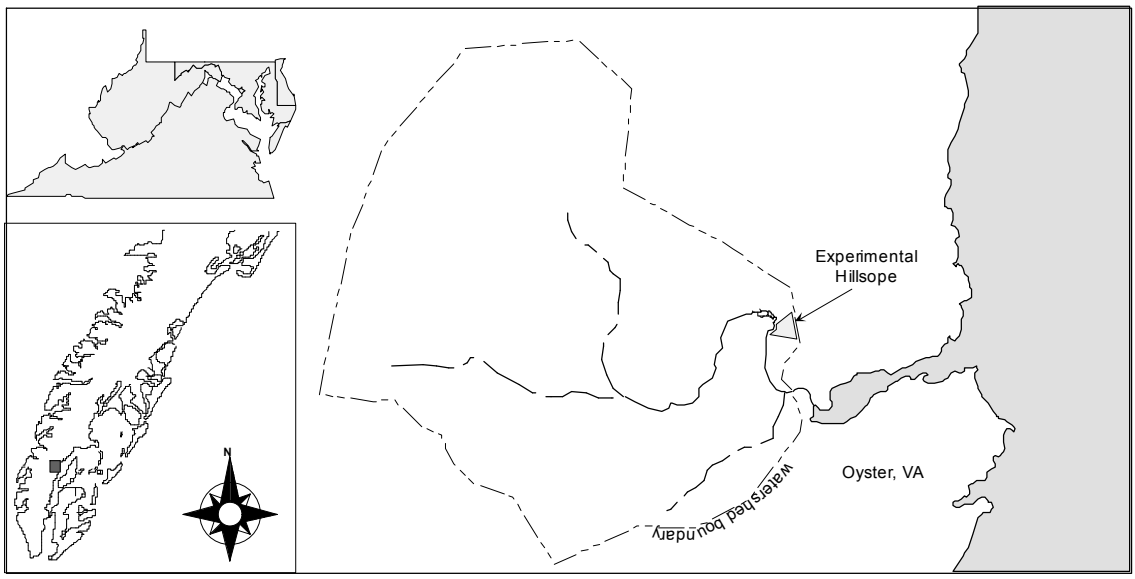

Figure 3-1. Location of the Cobb Mill Creek study area at the Anheuser-Busch Coastal Research Center in Oyster, VA

Cobb Mill Creek is 4.96 km^2 in area and it has low topographic relief, sloping from approximately 45 ft elevation down to sea level. Land use is dominated by forested

(62%) and agricultural (34%) areas, with the remaining 4% of land area in residential and other uses. Cobb Mill Creek discharges into Oyster Harbor, a component of the system of lagoons that is situated between the mainland and the chain of barrier islands between which the lagoons exchange water with the Ocean.

Approximately 50% of Virginia's Eastern Shore is agricultural land, with 80% of agricultural area in row crops [*USDA Census of Agriculture*, 2002]. Cropland is preferentially situated on well drained soils [*Phillips et al.*, 1993] where nitrate fertilizers readily leach to generally aerobic groundwater [*Denver, et al.*, 2003]. Commercial fertilizer use (59%) and manure application to land (35%) account for over 94% of the nitrogen load to catchments on the Delmarva Peninsula (the geographic region encompassing the eastern shores of Delaware, Maryland, and Virginia) [*Brakebill and Preston*, 1999].

Agriculturally derived nitrogen has leached to the unconfined Columbia aquifer [*Denver*, 1989] that supplies flow to the small coastal streams on the Eastern Shore of Virginia [*Bachman, et al.*, 1998]. Nitrate concentrations in the Columbia aquifer often exceed the US EPA primary drinking water standard of 10 mg NO_3^--N L^{-1} [*Denver, et al.*, 2003]. The Columbia aquifer is composed of Pleistocene-aged unconsolidated sands (generally 8-30 m thick; [*Calver*, 1968; *Mixon et al.*, 1989]) with high hydraulic conductivity ($5.53 \times 10^{-5} \pm 1.56 \times 10^{-8}$ m s^{-1}; [*Hubbard et al.*, 2001]). The aquifer is generally aerobic, resulting in little attenuation of nitrate concentrations during transport through the groundwater system.

The fairly unabated transport of nitrate through the Columbia aquifer leaves the riparian zone and streambed as the final barriers to nitrate transport to streams on the

Eastern Shore of Virginia. Due to the significant depth of the Columbia aquifer, a portion of groundwater bypasses the riparian zone and discharges vertically through the streambed [*Bohlke and Denver*, 1995]. Galavotti [2004] and Gu [2007] found that most or all of the nitrate in groundwater discharging vertically through the streambed of Cobb Mill Creek could be denitrified in a 30-cm thick organic-rich layer directly beneath the sediment surface.

3.2.2 Groundwater Discharge Sample Collection and Analysis

Seepage meters were used to measure specific discharge of groundwater from the streambed and to determine the concentrations of chloride and nitrate in groundwater seepage. Arrays of seepage meters were installed in several different reaches of Cobb Mill Creek during base flow conditions in late summer and early fall of 2006 and 2007. Seepage meter use and design has been described elsewhere [*Lee*, 1977], so only a brief description will be given here. Seepage meters were constructed from 10-cm diameter steel cylinders (food cans) and were 10 cm tall. One end of the cylinder was open and was inserted into the streambed. The other end of the cylinder was closed except for a ½ inch diameter nozzle, where all groundwater vented to a 150-mL latex bladder (condom, Figure 3-2).

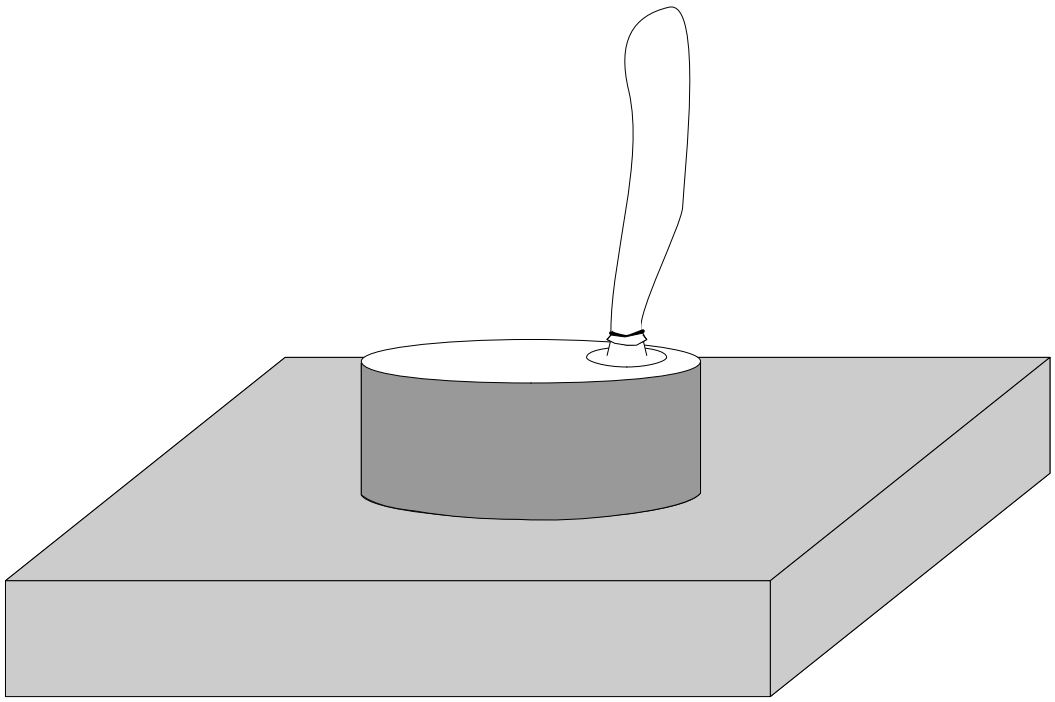

Figure 3-2. Seepage meter in place in the stream bed. Discharging water is displaced into the condom which is attached, empty, to the cylinder after emplacement and equilibration. Condoms were removed and sampled before reaching their maximum non-elastic volume to avoid any resistance to discharge.

The seepage meters were deployed without the condom attached 24 hours prior to making measurements in order to purge the remnant stream water from the seepage meter. At each seepage meter location, two sequential measurements were made. Specific discharge was measured first using a powder-coated condom. Then, an acid-washed condom was used to collect a water sample for determination of nitrate and chloride concentrations in seepage water.

To acid wash the condoms, each one was filled with approximately 100 mL of 10% nitric acid or hydrochloric acid, shaken by hand, and then emptied. That procedure was repeated 3 times for each condom. Then, the condoms were rinsed 3 times with deionized water (DIW) and placed in a 2-gal tank filled with DIW for 1 hour. The tank

was drained, the condoms were rinsed an additional 10 times with DIW, and then stored in clean Zip Lock® bags. All acid washing was done in the lab the day before field measurements were made. The powdering of the latex condom prevents the walls from sticking together and was considered reliable, even preferable, for estimating flow rates. The powder could, however, contaminate water samples, so the acid-washed condom was used to collect seepage water for chemical analysis.

Water samples were analyzed for nitrate and chloride on a Dionex® Ion Chromatograph equipped with a Gilson® 234 Autoinjector and a Dionex IonPac AS4A® 4 × 250-mm Analytical Column preceded by a Dionex IonPac AG4A-SC® 4 × 50-mm Guard Column. Each sample injection loaded 40 μL of sample onto the column. The eluent was 1.44 mM Na_2CO_3 and 1.36 mM $NaHCO_3$. The regenerant was 0.028 N H_2SO_4. Prior to ion-chromatography analysis, water samples were centrifuged at approximately 6900 × g for 20 min to remove particles in suspension.

A total of 158 seepage measurements were made in the late summer over the course of 8 sampling events on the following dates: 8/11/2006, 9/9/2006, 9/21/2006, 9/22/2006, 7/10/2007, 7/26/2007, 8/2/2007, and 8/25/2007. Samples were transferred from the condoms to clean 25-mL glass scintillation vials in the field and stored on ice until returned to the laboratory, where they were refrigerated until analyzed. Scintillation vials were cleaned with Alconox® soap and rinsed 10 times with DIW in the laboratory prior to sample collection. Anion concentrations in samples were determined in the laboratory within one month of collection.

On three of the eight sampling events, specific discharge from the streambed was mapped: 7/26/07, 8/02/07, and 8/24/07. Specific discharged was mapped by deploying multiple transects of seepage meters in three different stream reaches (2.5 – 4 m long). Each of the three reaches was mapped on a different day. Seepage meters in transects were spaced 20 cm apart and the spacing between transects varied from 0.29 to 1.12 m. These data were interpolated onto an evenly spaced 10-cm grid using a cubic spline procedure in Matlab. These interpolations were then plotted as contour maps using Sigma Plot.

Sequential measurements of groundwater seepage and nitrate concentrations for one array of seepage meters (sampling on 8/11/2006) demonstrated the precision of this sampling procedure (Figure 3-3).

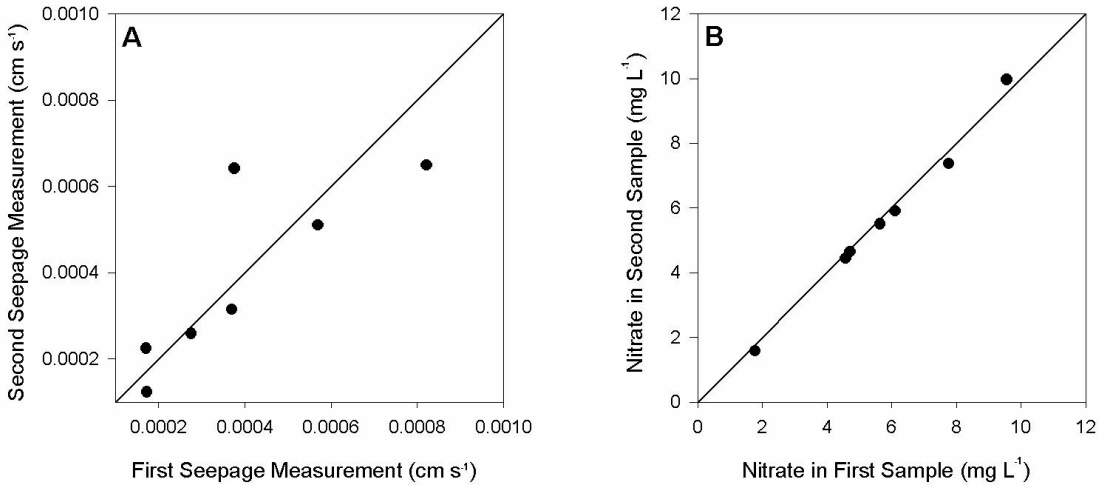

Figure 3-3. Comparison of 2 sequential specific discharge measurements (A) and NO_3^- measurements (B) for 7 seepage meters in Cobb Mill Creek that were sampled on 8/11/2006. Black dots are measurements; solid lines are 1:1 lines.

3.2.3 Measurement of Subsurface Hydraulic Head and Groundwater Solute Concentrations

Wells and piezometers (1-inch diameter) were installed in the stream and adjacent riparian zone of Cobb Mill creek. A hand auger was used to bore through the unsaturated zone and then wells and piezometers were driven down to a desired depth below the water table. In the stream, piezometers were opened at depths ranging from 0.4 – 0.9 m beneath the streambed surface. In the riparian zone, wells and piezometers were installed to depths of 0.76 – 4.6 m below the ground surface. The locations of wells and piezometers were previously described by Gu [2007]. After installation, wells and piezometers were pumped until the extracted fluid was free of visually detectable suspended sediments.

Hydraulic head was measured periodically in wells to map the elevation of the water table and in piezometers to infer the distribution of hydraulic head near the water table. The static water level in each well or piezometer was measured with a Solinst water level meter to the nearest 0.25 cm. Hydraulic heads were measured on 38 separate occasions from 1/9/2001 through 7/21/2006, representing a mixture of monthly and quarterly sampling events. The patterns of hydraulic head were similar for all sampling dates and showed vertical upwelling of groundwater beneath the stream and lateral groundwater flow towards the stream in the shallow riparian zone (Figure 3-4).

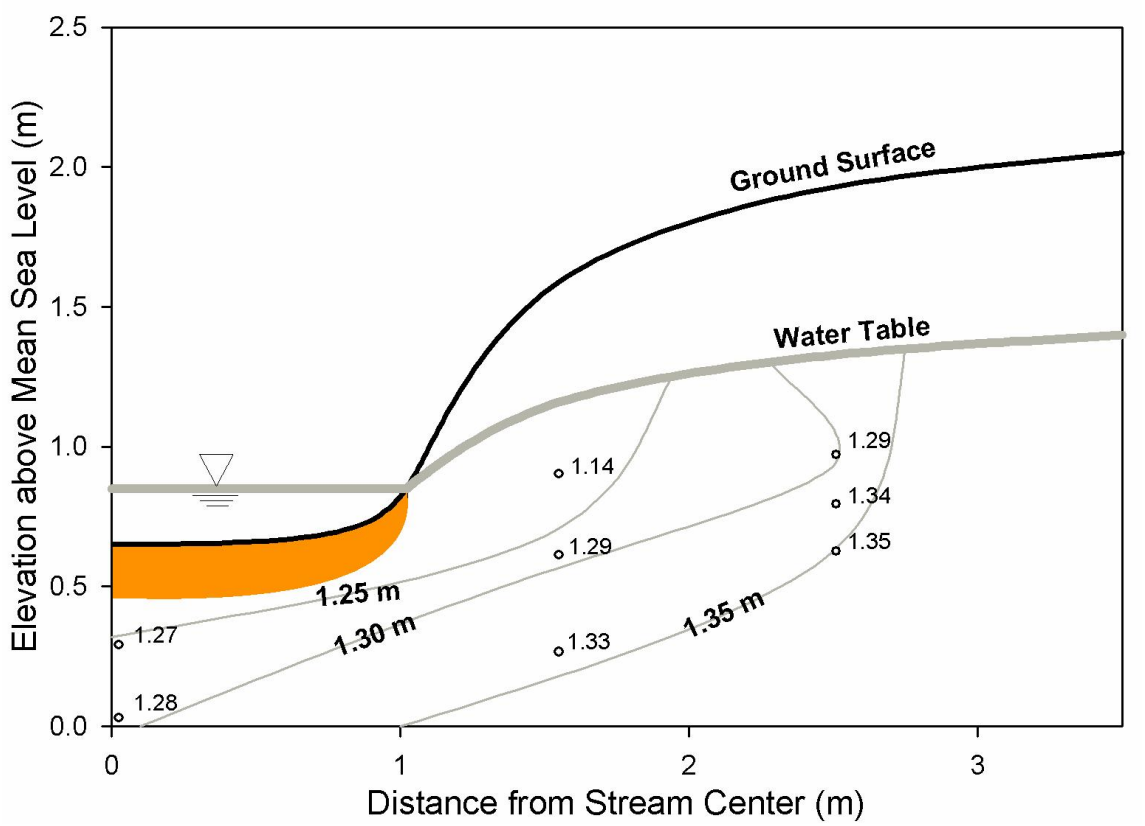

Figure 3-4. A cross-sectional map of the stream and riparian zone of Cobb Mill Creek showing vertical upwelling of groundwater beneath the stream and lateral flow of groundwater towards the stream in the shallow riparian zone on 2/3/2003. Black circles are the locations of piezometers with the measured values of hydraulic head labeled to the right. The heavy gray line indicates the position of the stream surface and water table (as measured in wells). Thinner gray lines are the approximate locations of equipotentials, whose magnitudes are labeled in bold. The equipotentials were drawn by hand. Although the equipotentials suggest the general direction of flow, the heterogeneous and anisotropic nature of the sediments results in high spatial variability in flow paths. The shaded region represents the zone of active denitrification in the streambed.

Water samples were collected from the entire array of wells and piezometers on 11 sampling events between 11/30/2003 and 7/19/2005. Piezometers beneath the streambed were sampled on 18 occasions between 11/30/2003 and 8/25/2007. Prior to sampling, 3 well volumes were purged from wells and piezometers with a peristaltic pump. Water samples were stored in 25-mL glass or polypropylene scintillation vials and refrigerated (4°C) within 2 hours of collection. Chloride and nitrate concentrations were

quantified for all water samples by ion chromatography (as described earlier) within one month of collection.

3.2.4 First-Order Model for Nitrate Removal in the Near-Stream Zone

Nitrate attenuation in the streambed was represented as a first-order kinetic process with respect to nitrate.

$$\frac{dN}{dt} = -kN \tag{35}$$

$N\left[ML^{-3}\right]$ is nitrate concentration and $k\left[T^{-1}\right]$ is a first-order rate coefficient.

Rearranging and integrating Equation (35) leads to a description of exponential decay over time,

$$N = N_0 e^{-kt} \tag{36}$$

where N_0 is the initial (influent) nitrate concentration. Groundwater travel time, t, through the streambed is a characteristic timescale for transport and the reaction rate coefficient, k, is the reciprocal of a characteristic timescale for reaction. The product kt is equivalent to a Damkohler number, Da, a ratio of the timescale for transport to the timescale for reaction.

$$Da = kt \tag{37}$$

By rearranging Equation (36) so that all the nitrate concentration terms are on the left hand side, Da can be computed directly from measured initial and final concentrations of nitrate along a flow path.

$$\frac{N}{N_0} = e^{-Da} \tag{38}$$

or,

$$Da = -\ln\left(\frac{N}{N_0}\right) \tag{39}$$

Damkohler numbers were estimated at all seepage meter locations with Equation (39) by taking measured nitrate concentrations in seepage water as N and the nitrate concentration in piezometers beneath the streambed as N_0. The initial nitrate concentration entering the nitrate reduction zone, N_0, was assumed constant at 12.2 mg L^{-1}, the average nitrate concentration in four piezometers (mean ± S.E.M: 12.2 ± 0.2 mg L^{-1}, n = 52) opened 40-80 cm beneath the streambed between October 2003 and May 2005.

The travel time component of the Damkohler number was estimated from specific discharge measurements in Cobb Mill Creek. Galavotti [2004] and Gu [2007] showed that nitrate removal occurs over a finite length scale in the streambed—i.e. the organic-rich zone near the streambed surface. The thickness of that organic-rich zone (L) is fairly constant so that travel time (t) is inversely proportional to specific discharge from the streambed.

$$t = \frac{L}{q} \tag{40}$$

The thickness of the organic-rich zone of the streambed (L) was taken to be a constant 30 cm based on previous measurements of organic carbon content of streambed sediments [*Galavotti*, 2004; *Gu*, 2007].

3.2.5 Separating riparian influenced and non-riparian influenced flows

Chloride concentrations in the shallowest groundwater directly beneath the riparian zone are higher than concentrations in upwelling groundwater beneath the

streambed at Cobb Mill Creek [*Gu, et al.*, 2008]. Riparian-zone groundwater may have a different chloride signature than deeper groundwater due to several factors:

1. infiltration of low-chloride and nitrate rain water;
2. concentration of chloride due to evapotranspiration;
3. differences in groundwater source region or age.

It is not clear which of these processes is the dominant cause for the observed differences in chloride concentrations, but the net effect is that shallow riparian-zone groundwater contains higher chloride concentrations and lower nitrate concentrations than does upwelling groundwater beneath the streambed. The observed difference in chloride concentrations was used as a basis for separating groundwater seepage that originated from the riparian zone and upwelling of relatively deeper groundwater. Such differences in groundwater sources have been observed elsewhere and used to identify source components [e.g., *Clement et al.*, 2003].

I compiled all chloride concentration measurements from seepage meters and used kernel density estimation (KDE) and a bootstrapping technique to test for multimodality in the chloride distribution [*Efron and Tibshirani*, 1993; *Silverman*, 1981]. KDE uses a bandwidth parameter to smooth distributions of observed data. Larger bandwidths lead to more smoothing (fewer modes) and smaller bandwidths lead to less smoothing (more modes). There is a critical bandwidth that defines the break point between a distribution with one mode and a distribution with multiple modes. A bootstrapping technique can be applied to a KDE made with the critical bandwidth to test whether that cutoff point is large or small at a defined level of significance. Here, I used

this technique to test for bimodality and trimodality in the observed chloride distribution at a statistical significance of $\alpha = 0.05$.

3.3 Results

3.3.1 Separating groundwater source components

Qualitative comparison of the maps of chloride (Figure 3-5A) and nitrate (Figure 3-5B) concentrations in groundwater seepage suggested that nitrate concentrations were low where chloride concentrations were high. The contours in Figures 3-5A and 3-5B showed that areas of the streambed where chloride concentrations were greater than 20 mg L^{-1} corresponded to nitrate concentrations less than 2 mg L^{-1}.

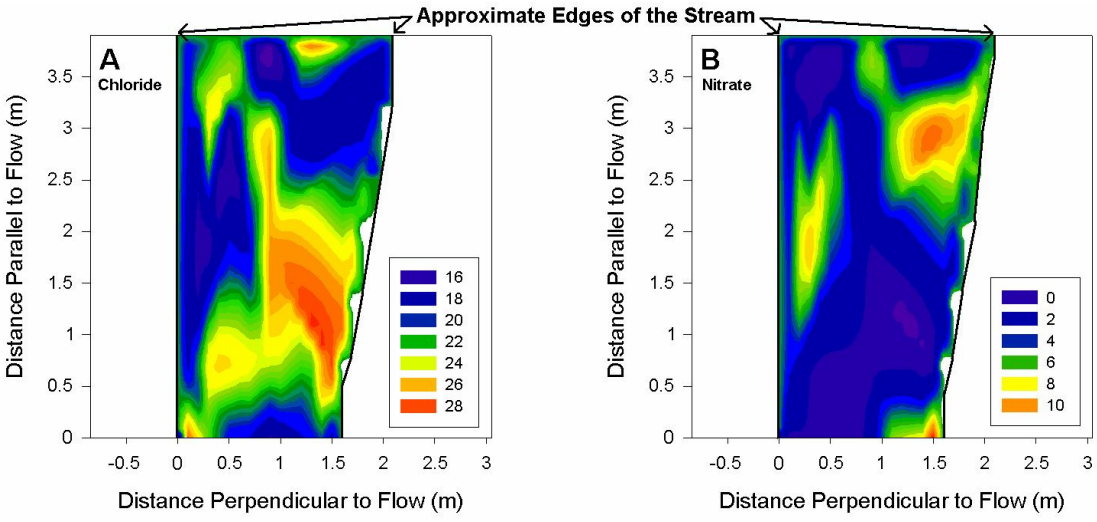

Figure 3-5. Map of chloride concentrations (A) and nitrate concentrations (B) in mg L^{-1} in groundwater discharge from the streambed on 8/02/2007.

Further analysis of the complete chloride distribution for all sampling locations revealed a complicated distribution with three significant modes ($\alpha = 0.05$, $p = 0.014$). The lowest mode was assumed to represent groundwater uninfluenced by processes in the riparian zone, with a cutoff concentration of 20.9 mg L^{-1} (Figure 3-6). The two modes

associated with higher chloride concentrations were assumed to represent groundwaters influenced by processes in the riparian zone. On the whole, 66% of groundwater flow was influenced by the riparian zone while 34% was not.

Separation of all data into the two inferred flow groups using the 20.9 mg/L Cl^- cutoff yielded a log-linear relationship between nitrate concentrations in water discharging from the streambed and groundwater travel time for non-riparian-influenced flow (Figure 3-7A). The log-linear relationship was consistent with the first order rate law for nitrate removal (Equation (36)). A log-linear relationship between nitrate concentrations and groundwater travel time was lacking for samples categorized as riparian-influenced flow (Figure 3-7B), *i.e.*, water with chloride concentrations below 20.9 mg/L.

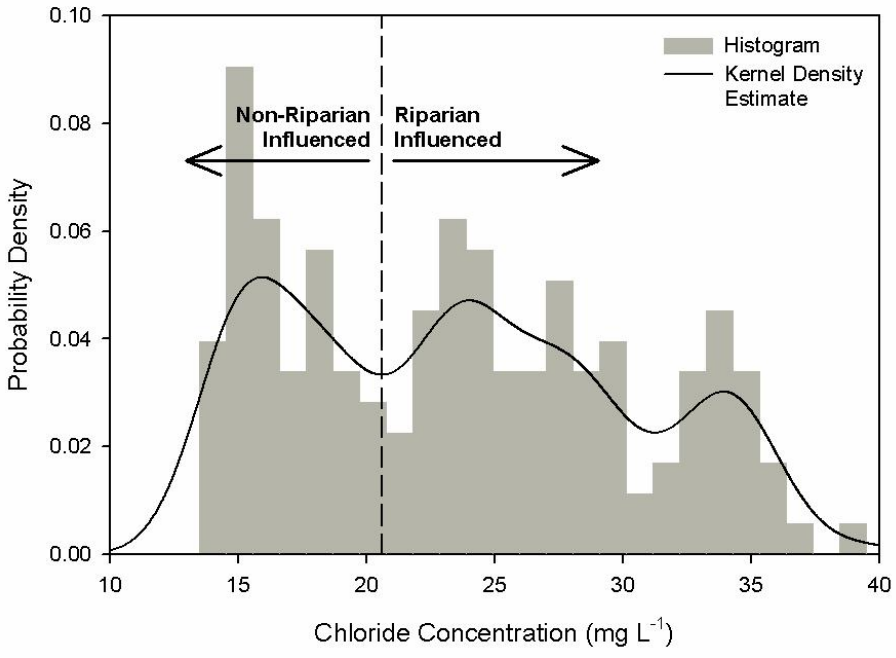

Figure 3-6: Histogram (gray bars) and kernel density estimate (solid line) of the chloride concentration in groundwater seepage into Cobb Mill Creek. The vertical dashed line indicates the inferred cutoff between riparian influenced and non-riparian influenced groundwaters.

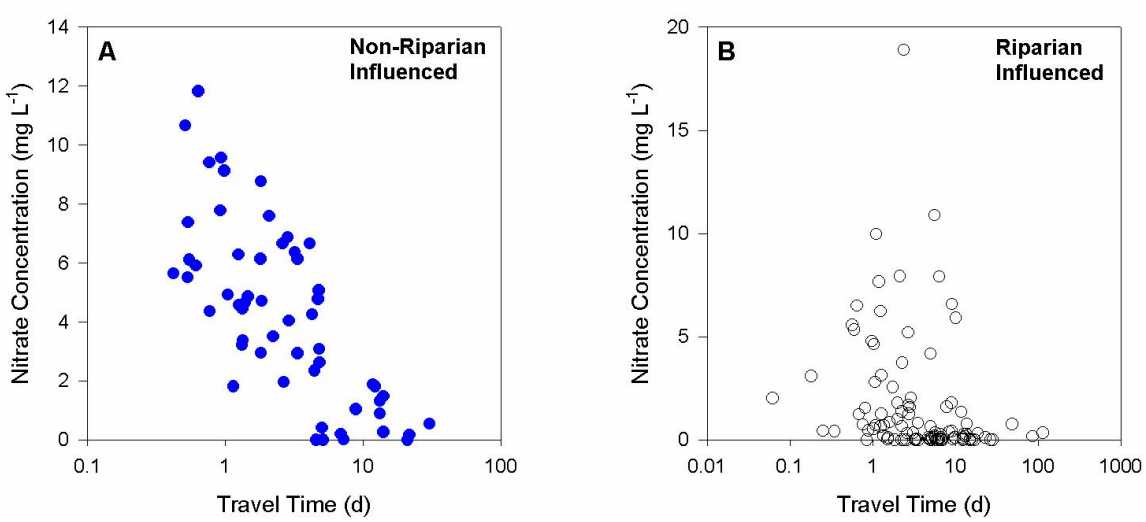

Figure 3-7. Relationship between nitrate concentrations and groundwater travel time for non-riparian influenced groundwater (solid blue circles) (A) and non-riparian influenced groundwater (open black circles) (B).

3.3.2 Spatial distributions of specific discharge through the streambed

Specific discharge varied by several orders of magnitude and large variations occurred over small spatial scales in the streambed (Figure 3-8). In some cases, specific discharge measurements made 20 cm apart differed by more than an order of magnitude. There tended to be high and low specific discharge regions in the streambed and those regions tended to be elliptical in shape, with the major axes of the ellipses oriented in the downstream direction.

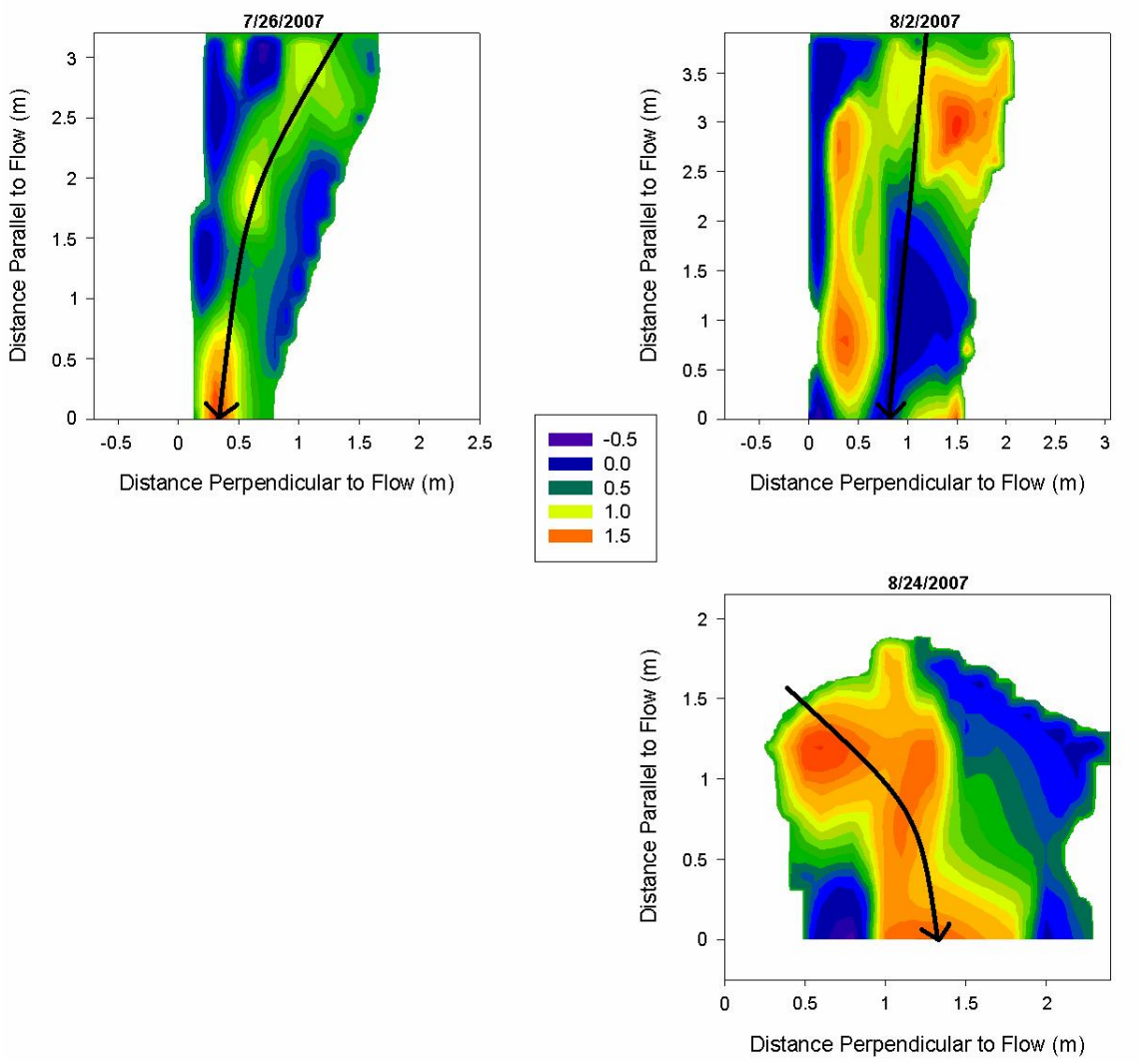

Figure 3-8. Maps of specific discharge observed in three different stream reaches on three different dates: 7/26/2007, 8/2/2007, and 8/24/2007. The large black arrow in each figure indicates the direction of stream flow and the approximate center of the channel. All maps are in units of the natural logarithm of specific discharge in cm d^{-1}.

3.3.3 The Damkohler number and its dependence on travel time

Damkohler numbers (*Da*) for the streambed of Cobb Mill Creek were directly computed from measured nitrate concentrations (Equation (39)). *Da* plotted as a function of *t* was best described by a segmented linear relationship (Figures 3-9A and 3-9B). The segmented linear regression had a slope of 0.50 day^{-1}, representing the average nitrate

removal rate coefficient for the streambed. The optimal break point was at 6.7 days. After 6.7 days, *Da* appeared to be constant at 3.2 (unitless). A semi-log plot of *Da* as a function of *t* (Figure 3-9B) shows greater detail of the relationship at lower travel times.

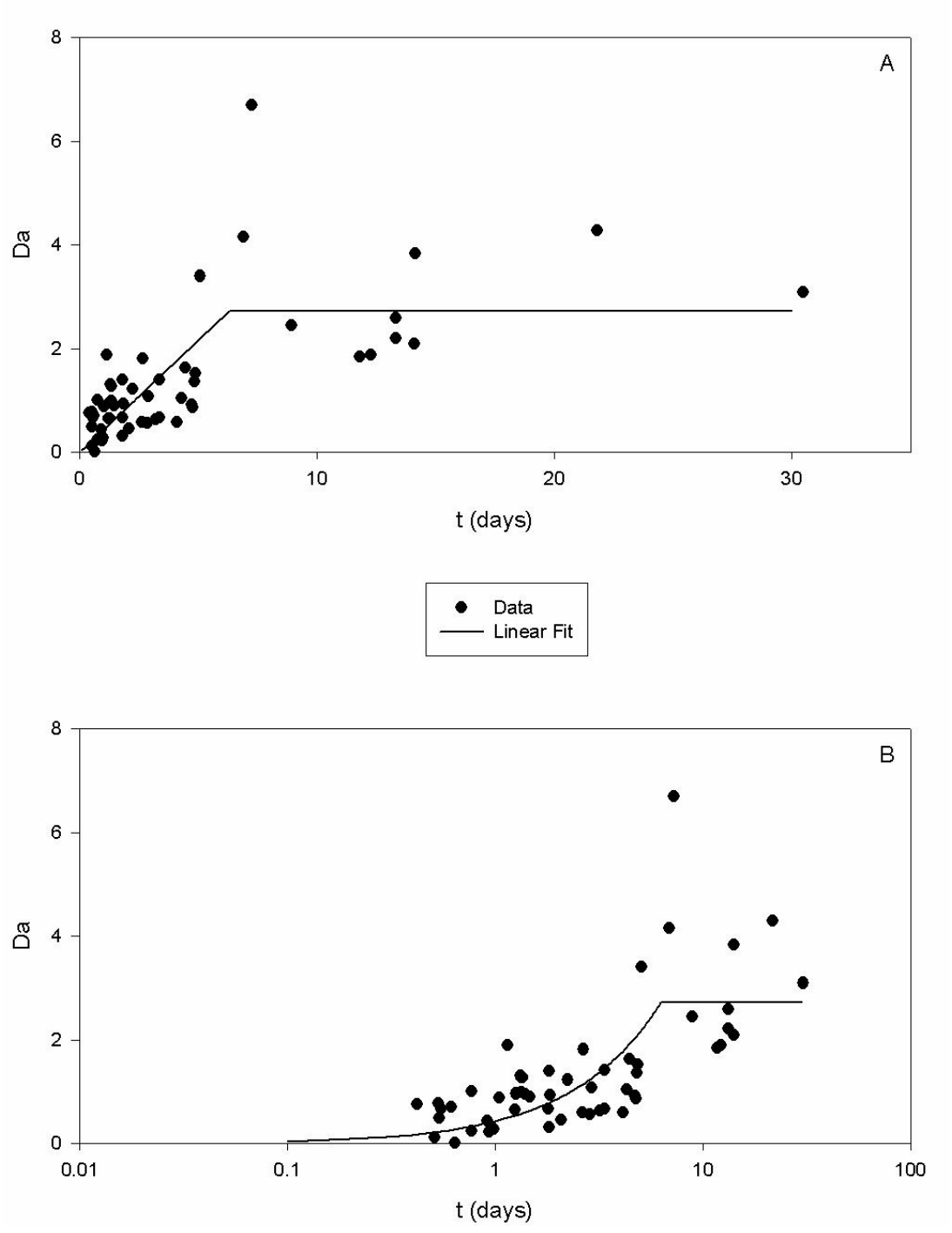

Figure 3-9. Relationship between *Da* and *t*. The trend line represents a linear relationship that reaches an asymptote between *Da* and *t* in linear space (A) and semi-log space (B).

3.4 Discussion

3.4.1 Differences in riparian influenced and non-riparian influenced flows

The transport of nitrate through the riparian zone could be complicated by a suite of microbially mediated N transformations (mineralization, nitrification, and denitrification) and plant interactions (evapotranspiration and plant uptake). Therefore, nitrate concentrations in riparian-influenced groundwater would be altered prior to discharging through the streambed. The nitrate concentration in groundwater seepage originating from those flow paths would not be a simple function of travel time through the streambed. Thus, a relationship between travel time and nitrate concentration was lacking for riparian influenced groundwater (Figure 3-7B). Upwelling groundwater that is not influenced by riparian processes and that discharges vertically through the streambed would be affected by denitrification only. Nitrate concentrations of groundwater seepage affected solely by denitrification would be expected to obey a log-linear relationship with travel time, as indicated by Figure 3-7A.

The occurrence of higher chloride concentrations in shallow riparian zone groundwater relative to deeper groundwater was used as the basis for separating source components. Gu [2007] showed that chloride concentrations in shallow riparian zone groundwater were consistently elevated relative to deeper groundwater. Others have found that chloride concentrations near the water table fluctuate seasonally, but that concentrations in deeper groundwater are more constant [*Legout et al.*, 2007]. Thus, a consistent pattern of dynamic chloride concentrations in shallow groundwater seems to be emerging.

Yet, the cause of high chloride concentrations in riparian influenced groundwater is not known. The trimodality of the chloride distribution at Cobb Mill Creek (Figure 3-6) was unexpected and suggests that chloride transport through riparian zones and streambeds may be extremely complicated. Here, I was only able to rationalize one of the three modes in that distribution (that representing a deep groundwater source). The other two modes with higher chloride concentrations were lumped into a single riparian influenced group for lack of a better classification scheme. Two important questions that still remain are what do those two higher chloride modes represent and what processes caused them?

There are many processes that may affect the concentration of chloride, including evapotranspiration [*Claassen and Halm*, 1996], plant uptake [*Xu et al.*, 2004], microbial cycling of organic and inorganic chlorine [*Bastviken et al.*, 2006], and infiltration of chloride-poor precipitation. These processes may not always have an effect in the same direction and may operate at different temporal and spatial scales. The aggregate effect on groundwater chloride concentrations is not obvious. Clearly there is a need to study the cycling and transport of chloride in greater detail, especially since it is so widely used as a passive conservative tracer in field studies.

3.4.2 Spatial distributions of specific discharge through the streambed

Variations in local hydrology can affect specific discharge through the streambed. Measurements of specific discharge from a 262.5 m stream reach in North Carolina by Kennedy et al. [2007] (q = -0.3-1.8 m d^{-1}) suggest that the large variations found in Cobb Mill Creek (q = 0-4.8 m d^{-1}) are likely a common occurrence in small coastal plain streams.

The primary cause of variations in hydraulic conductivity can be inferred from a simple analysis with Darcy's law, $q = K \, dh/dl$. Specific discharge is the product of hydraulic conductivity (K) and the hydraulic head gradient dh/dl across the streambed. Measured hydraulic head gradients across the streambed of Cobb Mill Creek are in the range of 0.1 – 0.3 and are similar to hydraulic head gradients measured in other streambeds on the Delmarva Peninsula, e.g. Bohlke and Denver [1995]. Phillips [2003] determined through a theoretical argument that one should expect a hydraulic head gradient close to 0.2 near regions of groundwater discharge on the Delmarva Peninsula. The large (orders of magnitude) spatial variability in specific discharge must therefore occur primarily as a result of heterogeneity in the hydraulic conductivity field in the streambed.

Since the head gradient falls within a narrow range, the hydraulic conductivities in the streambed can be estimated from Darcy's law. Assuming a mean hydraulic head gradient of 0.2, the mean of the hydraulic conductivity distribution for all seepage measurements would be 4.4×10^{-6} m s^{-1}, within an order of magnitude of the mean hydraulic conductivity of 1.7×10^{-5} m s^{-1} measured on three intact sediment cores by Gu [2007] at Cobb Mill Creek. Minimum and maximum hydraulic conductivities would be 1.3×10^{-7} m s^{-1} and 2.8×10^{-4} m s^{-1}, respectively. The mean, minimum, and maximum estimated hydraulic conductivities all fall in the range expected for a silty sand [*Hornberger et al.*, 1998], such as those found in sediments throughout the catchment.

There are several physical processes that can affect hydraulic conductivity of bed material. Organic matter in the streambed exists both as fine particles and also as coarse

debris (leaves and sticks). The different sizes and geometries of organic matter may affect the permeability of the streambed and, as a result, those organic inclusions may affect the distributions of specific discharge and travel time. Erosional and depositional processes operating in the stream channel can also affect hydraulic conductivity. The elliptical patterns in specific discharge in the streambed (Figure 3-8) may reflect hydraulic conductivity variations associated with dune formation in the channel. Channel geomorphology is an important control on sedimentary architecture [*Bridge*, 1977; *Cardenas and Zlotnik*, 2003], which strongly influences local hydrology [*Cardenas and Wilson*, 2004].

3.4.3 Da and its dependence on t

Hydraulic conductivity will exert the dominant control on retention times in biogeochemically active zones. The travel time of groundwater determines how long nitrate remains in denitrifying zones and this determines the extent of nitrate removal for a give rate coefficient. Since hydraulic conductivity is controlled by geomorphology (discussed above), there is an indirect link between geomorphology and nitrate dynamics. Local hydrology controls groundwater travel times, and those travel times strongly influence *Da* (the dominant control on the extent of nitrate removal).

The variability in *Da* may be influenced by changes in travel times, rate coefficients, or both. When travel times are short (less than 6.7 days for Cobb Mill Creek), travel time exerts the dominant control on *Da* (Figure 3-9). At longer travel times, other factors (*e.g.* dispersion) may become more important for those lower-flow regions of the streambed and there is also the potential for complete nitrate removal to

occur over a linear distance less than 30 cm—the assumed thickness of the nitrate reduction zone (Figure 3-9).

The need to account for different processes in high-flow and low-flow regions is completely negated by the fact that nearly 100% of the nitrate flux in vertically discharging groundwater was contributed by regions of the streambed with travel times shorter than 6.7 days (Figure 3-10). Therefore, the assumption that *Da* is a simple linear function of *t* holds true for regions of the streambed that contribute significantly to the groundwater nitrate flux. The processes that control *Da* at locations where travel times are greater than 6.7 days may be interesting, but they are of little practical importance to total groundwater nitrate export.

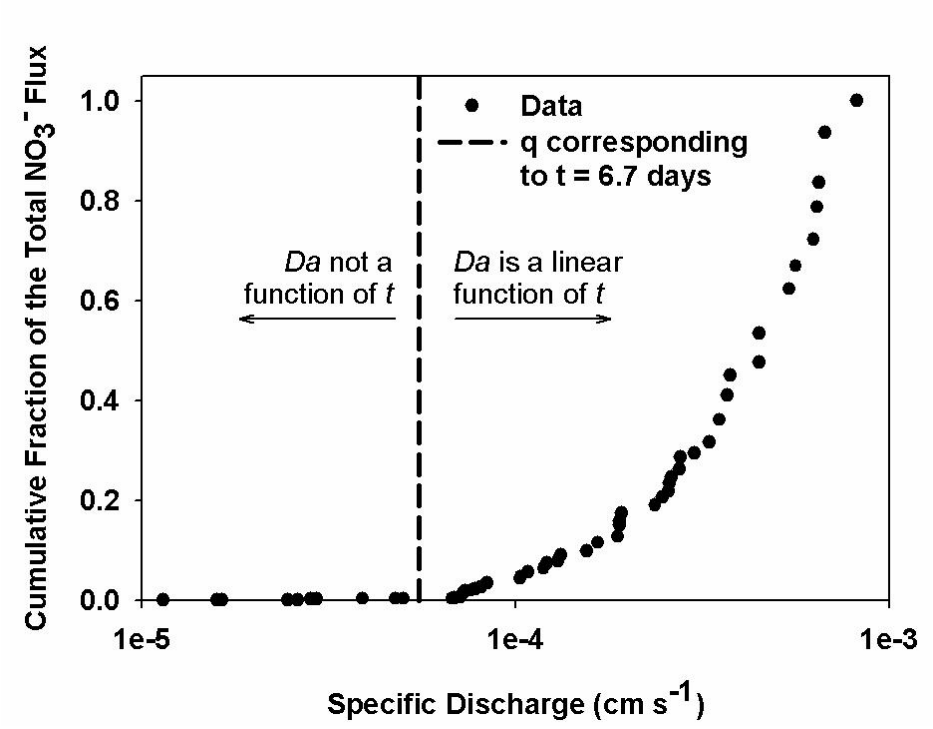

Figure 3-10. The cumulative fraction of the total nitrate flux from the streambed versus specific discharge. Higher flow locations (i.e. specific discharge corresponding to travel times less than 6.7 days) account for virtually all of the nitrate flux in vertical groundwater flow.

At Cobb Mill Creek, approximately 66% of groundwater passes through the riparian zone while the remainder bypasses this area and discharges directly through the streambed, a pattern consistent with the findings of others [*Bohlke and Denver*, 1995]. The riparian influenced and non-riparian influenced groundwater source components were inferred from the chloride distribution in groundwater seepage, although the trimodality of that distribution was unexpected and requires further investigation. Evapotranspiration may be one factor influencing the chloride distribution, but other aspects of chlorine cycling, *e.g.* microbial and plant interactions, need to be quantified to better understand the controls on this distribution.

Nearly all nitrate discharge from the streambed to Cobb Mill Creek occurs through high-flow regions with travel times of less than 6.7 days in the active nitrate reduction zone. Previous studies accurately predicted the extent of nitrate removal in the riparian zone and streambed sediments with the Damkohler number (*Da*), a ratio of the timescale for transport to reaction. In this study, it was clear that *Da* is a linear function of travel time through the active nitrate reduction zone in high-flow regions of the streambed. This means that an average or effective rate coefficient is sufficient for describing nitrate removal in the streambed as a whole and that spatial variability in nitrate flux from the streambed is primarily driven by hydrology. This is important, since denitrification rates themselves vary widely in general [*Gu, et al.*, 2007], and in Cobb Mill Creek specifically [*Mills, et al.*, 2008]. This finding reveals that there are multiple causes of temporal variations in denitrification extent, since dynamic changes in hydrology, rate coefficients, or both could result in temporal denitrification patterns.

These findings have important management implications as well, especially for cases that focus on the riparian zone as a nitrogen sink. At Cobb Mill Creek, a significant portion of groundwater discharge (34%) bypasses the riparian zone and this bypassing flow may be even greater at other streams in the Mid-Atlantic Coastal Plain [*e.g. Bolhke and Denver*, 1995]. Even though a significant portion of groundwater bypasses the riparian zone and discharges directly through the streambed, the riparian zone is still necessary for denitrification to occur in the streambed. Organic matter produced by vegetation in the riparian zone falls into the stream and accumulates in sediments, thus fueling the denitrification process in the streambed. Hence, the optimal size of a riparian zone for maximizing nitrate removal would depend on several factors, including plant N uptake, denitrification in groundwater affected by the riparian zone, and the supply of organic matter to streambed sediments. Even though hydrology appears to control spatial variations in N removal, it is the supply of organic matter that allows microorganisms to perform this vital ecosystem service. Soils, groundwater, riparian zones, and streambeds are parts of an integrated system that must be managed in concert to achieve maximum N removal.

Chapter 4: The Effect of Riparian Evapotranspiration on Groundwater Flow and Implications for Diurnal Nitrate Signals

Abstract

Evapotranspiration can cause diurnal fluctuations in the elevation of the water table and the magnitude of local stream flow. Those fluctuations were examined with a numerical model of transient saturated-unsaturated groundwater flow to explore the effect of temporal flow patterns on nitrate concentrations in streams. Nitrate that discharges from the groundwater system passes through zones in the streambed and riparian zone where nitrate can be removed and where the extent of nitrate removal is determined by groundwater travel time. The model predicted a diurnal saw-toothed pattern in specific discharge through the streambed and riparian zone (the nitrate-removal zones). This pattern caused groundwater travel times through nitrate reduction zones to vary temporally and this affected stream nitrate concentrations. The resulting temporal pattern in stream nitrate concentrations did not simply mimic the predicted patterns in specific discharge, however. Stream velocity affected the transit time of water through the stream network, such that low stream velocities dampened the signal produced by ET and high velocities allowed it to remain. Stream nitrate concentrations in Cobb Mill Creek were predicted to reach a peak at 11:00 a.m. and decline to a minimum at 5 p.m., only slightly offset from the initiation and cessation of ET. These findings indicate that the benefit of forested riparian zones goes beyond plant nitrogen uptake, since ET can increase groundwater residence time and thereby indirectly increase denitrification.

4.1 Introduction

Sediments in streambeds and riparian zones are focal points for nitrate removal in small streams [*Cirmo and McDonnell*, 1997]. The extent of nitrate removal in those zones is controlled by the ratio of time scales for transport to reaction [Chapter 3; *Ocampo, et al.*, 2006]. Stream base flow derives from groundwater discharge through streambed and riparian zones and so the removal of nitrate in those zones affects the concentration of nitrate in stream water.

In systems where the near-stream zone for nitrate reduction is of constant thickness, groundwater travel time is inversely proportional to the rate of groundwater flow (specific discharge). Groundwater travel time through nitrate reduction zones is an important factor controlling the concentration of nitrate that discharges from groundwater to streams [Chapter 3; *Gu et al.*, 2007]. Since specific discharge can vary through time [*Cooper and Rorabaugh*, 1963], it is important to consider how these variations might affect the extent of nitrate removal in streambed sediments.

Temporal changes in specific discharge through streambeds have been observed during storm events. For example, Squillace [1996] observed that base flow to a stream was reversed during a storm event and, after the passage of the storm, there was rapid flow of groundwater back towards the stream. Such transient groundwater flow can affect the concentration and efflux of nitrogen from the groundwater system. Storms can either increase or decrease the flux of nitrate from groundwater to streams, depending on the hydraulic diffusivity of the streambed [*Gu, et al.*, 2008].

Storm events are not the only cause of transient hydrology, however. During the growing season, evapotranspiration (ET) can draw down the water table and cause diurnal saw-toothed patterns in the elevation of the water table [*Butler et al.*, 2007; *Loheide et al.*, 2005; *White*, 1932] and in the magnitude of stream flow [*Bond et al.*, 2002; *Burt*, 1979; *Troxell*, 1936]. Just as storms drive temporal patters in specific discharge through nitrate reduction zones, evapotranspiration does too. These patterns in specific discharge would change the residence time of nitrate in reducing zones and that may affect stream nitrate concentrations.

Diurnal patterns in stream nitrate concentrations have been documented in a range of environmental settings, such as forested catchments in the Northeast USA [*Burns*, 1998] and in mixed land-use moorland catchments in the South West of the UK [*Scholefield et al.*, 2005]. Burns [1998] attributed the diurnal patterns to the activity of photoautotrophs . Scholefield et al. [2005] suggested the diurnal patterns may be related to temperature and light availability, and also attributed the observation to in-stream biological processes; the diurnal patterns in specific discharge were not considered as an explanatory factor.

There are clear diurnal fluctuations in summertime stream discharge at Cobb Mill Creek, an experimental catchment within the Anheuser Busch Coastal Research Center (ABCRC). Cobb Mill Creek is a gaining stream on the Eastern Shore of Virginia, and the diurnal fluctuations in summertime discharge are thought to be driven by ET in the riparian zone. Groundwater that supplies flow to Cobb Mill Creek is enriched with nitrate from adjacent agricultural lands, although previous research has shown that near-surface streambed sediments denitrify a portion of groundwater nitrate before it enters the

stream [*Galavotti*, 2004; *Gu*, 2007; *Mills, et al.*, 2008]. The portion removed depends on groundwater residence time in those reduced surface sediments (Chapter 3). Therefore, fluctuations in travel time induced by ET could affect the concentration of nitrate observed in the stream.

This chapter explores diurnal patterns in specific discharge and the effect that those patterns might have on nitrate concentrations in Cobb Mill Creek. To achieve that goal, two questions were addressed.

1. **What is the effect of ET on specific discharge to the stream?**
2. **What effect do specific discharge patterns have on stream nitrate concentrations?**

To examine these questions, a numerical model of 2-D, time-dependent saturated-unsaturated groundwater flow was developed for a cross-section of Cobb Mill Creek and the adjacent riparian zone. Potential evapotranspiration (PET, estimated with the Penman-Monteith equation) was applied to the vadose zone as a driver of transient flow patterns in the groundwater system. The groundwater flow model showed that PET caused diurnal fluctuations in groundwater discharge to the stream that matched the observed pattern of stream discharge. Specific discharge affects the residence time of nitrate in surface sediments, and the model further demonstrated the subsequent effect on the concentration of nitrate in the stream. The predicted pattern of stream nitrate concentrations depended on mean channel velocity, however. At low velocities, the transit time through the stream channel tended to cancel out the diurnal fluctuations, whereas shorter transit times allowed these diurnal patterns to persist.

4.2 Methods

4.2.1 Research Site Description

The experimental site was the Cobb Mill Creek watershed, which is 12 miles north of the mouth of the Chesapeake Bay on the Eastern Shore of Virginia in the Anheuser-Busch Coastal Research Center (ABCRC). The Eastern Shore of Virginia is bounded to the West by Chesapeake Bay and to the East by the Atlantic Ocean.

The Cobb Mill Creek watershed is 4.96 km^2 and has low topographic relief. Land use in the catchment is dominated by forested (62%) and agricultural (34%) areas, with the remaining 4% of land area in residential and other uses.

Cobb Mill Creek is one of many eastward draining coastal streams that supply nitrate to seaside lagoons. Approximately 50% of Virginia's Eastern Shore is agricultural land, with 80% of agricultural area in row crops [*USDA Census of Agriculture*, 2002]. Cropland is preferentially situated on well drained soils [*Phillips, et al.*, 1993] where nitrate fertilizers readily leach to generally aerobic groundwater [*Denver, et al.*, 2003]. Commercial fertilizer use (59%) and manure application to land (35%) account for over 94% of the nitrogen load to catchments on the Delmarva Peninsula (the geographic region encompassing the eastern shores of Delaware, Maryland, and Virginia) [*Brakebill and Preston*, 1999]. Agriculturally derived nitrogen has leached to the unconfined Columbia aquifer [*Denver*, 1989], where nitrate concentrations often exceed the US EPA drinking water standard of 10 mg NO_3^--N L^{-1} [*Denver, et al.*, 2003].

The Columbia aquifer is composed of Pleistocene-aged unconsolidated sands (generally 8-30 m thick; [*Calver*, 1968; *Mixon, et al.*, 1989]) with high hydraulic conductivity ($5.53 \times 10^{-5} \pm 1.56 \times 10^{-8}$ m s^{-1}; [*Hubbard et al.*, 2001]). The aquifer is generally aerobic, resulting in little attenuation of nitrate concentrations during transport through groundwater. Nitrate in groundwater discharges to coastal streams and the adjacent lagoons where it can have deleterious ecological effects [*Burkholder et al.*, 1995]. Groundwater discharge supplies the majority of flow to streams on the Delmarva Peninsula [*Bachman, et al.*, 1998] and represents a potentially large source of nitrogen to down-gradient systems. Groundwater nitrate concentrations are expected to increase substantially in the coming decades as groundwater systems come closer to steady state with the large inputs of agricultural nitrogen (Chapter 2).

4.2.2 Conceptualization of Groundwater Flow and Estimation of Potential Evapotranspiration (PET)

Previous measurements of hydraulic head in the subsurface of the Cobb Mill Creek watershed indicated a groundwater flow regime similar to that depicted in Figure 4-1. Data supporting such a flow pattern were presented in Chapter 3.

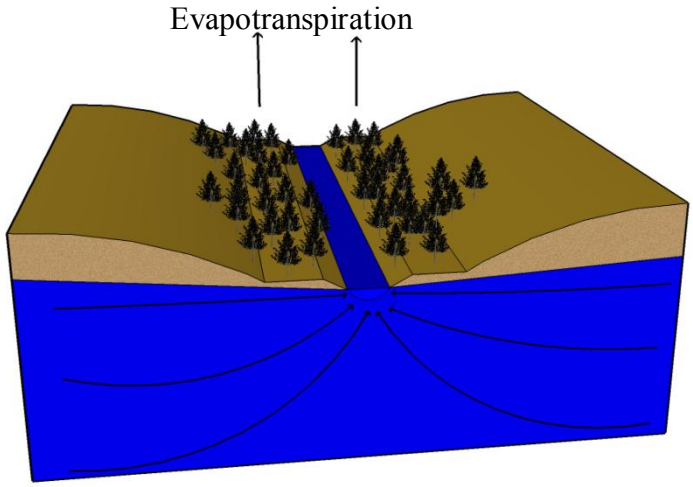

Figure 4-1: Generalized view of groundwater flow in a near-stream region. The brown and tan regions depict the vadose zone, whereas the blue regions denote the groundwater-stream system. Arrows indicate fluxes of water.

The stream's floodplain has a very low gradient, is forested, and remains saturated throughout the year. The average width of the forested floodplain is 125 m, i.e. 62.5 m on each side of the stream. The dimensions of the floodplain were determined by outlining the low-lying areas adjacent to the stream in a digital elevation model of Cobb Mill Creek in ArcGIS 9.0. The catchment is generally flat except for a prominent slope that separates the floodplain from the upland farm areas. This break in slope was used as the outlining feature of the floodplain.

Potential evapotranspiration (PET) was estimated with the Penman-Monteith equation (as in Campbell and Norman [1998]) and used as a specified flux condition in the vadose zone of the numerical groundwater flow model. The definitions of variables used in Equation (41) are listed in Table 4-1.

$$PET = \left[\frac{s}{s+\gamma^*} \left(R_{abs} - \varepsilon_s \sigma T_a^4 - G \right) \frac{m_w}{\rho_w} \right] + \left[\frac{\gamma^*}{s+\gamma^*} \left(\frac{\lambda g_v D}{p_a} \right) \frac{m_w}{\rho_w} \right] \quad (41)$$

Estimation of riparian zone PET with the Penman-Monteith equation is justified by its close agreement with two other methods of estimating total daily riparian zone ET at Cobb Mill Creek (Appendix 2). The first of the two ancillary methods was based on observed diurnal fluctuations in stream flow and is described in greater detail by Bond et al. [2002]. The second method was based on a mass-balance for chloride across the riparian zone of Cobb Mill Creek, similar to the approach developed by Claassen and Halm [1996].

Table 4-1. Variables and Parameters Used in the Calculation of PET

Parameter or Variable	Symbol	Value	Units
Absorbtivity	a	0.85	unitless
Reference Vapor Pressure	e_0	0.611	kPa
Actual Vapor Pressure	e_a	variable	kPa
Saturation Vapor Pressure	e_s	variable	kPa
Stomatal Conductance	g_v	variable	mol m^{-2} s^{-1}
Molecular Weight of Water	m_w	18.016	g mol^{-1}
Atmospheric Pressure	p_a	100	kPa
Slope of the Saturation Vapor Pressure Curve	s	variable	K^{-1}
Horizontal Wind Speed	u	variable	m s^{-1}
Vapor Pressure Deficit	D	variable	kPa
Soil Heat Flux	G	variable	W m^{-2}
Total Incoming Solar Irradiance	R	variable	W m^{-2}
Absorbed Solar Radiation	R_{abs}	variable	W m^{-2}
Gas Constant for Water Vapor	R_v	461	J K^{-1} kg^{-1}
Temperature Offset for Reference Vapor Pressure	T_0	273	K
Air Temperature	T_a	variable	K
Apparent Psychrometric Constant	γ^*	variable	K^{-1}
Surface Emissivity	ε_s	1	unitless
Latent Heat of Vaporization	λ	43.5	kJ mol^{-1}
Density of Water	ρ_w	1000	kg m^{-3}
Stefan-Boltzman Constant	σ	5.67×10^{-8}	W m^{-2} K^{-4}

Meteorological data from the Hog Island, VA weather station (the closest station with a continuous record) was used for PET determinations with the Penman-Monteith Equation from 7/16/2003 to 7/23/2003. Total incoming solar irradiance, air temperature, horizontal wind speed, and relative humidity were measured at hourly intervals. Barometric pressure was assumed to be 100 kPa, because it was not measured during the desired time interval.

There are several variables that were calculated from well-known relationships in meteorology texts (e.g. Stull [1995]). Absorbed solar radiation (R_{abs}) was estimated as:

$$R_{abs} = aR \tag{42}$$

The vapor pressure deficit, D, is:

$$D = e_s - e_a . \tag{43}$$

Saturation vapor pressure, e_s, was calculated from hourly data at the Hog Island meteorological station from the Clausius-Clapeyron Equation,

$$e_s = e_0 \exp\left[\frac{\lambda}{R_v}\left(\frac{1}{T_0} - \frac{1}{T_a}\right)\right]. \tag{44}$$

The slope, s, of the saturation vapor pressure curve is the derivative of Equation (44).

$$s = \frac{\lambda}{R_v}\frac{e_s}{p_a T_a^2} \tag{45}$$

The psychrometric constant and stomatal conductance were estimated as described by Campbell and Norman [1998]

$$\gamma^* = 6.67 \times 10^{-4}\left(1 + \frac{u}{3}\right) \tag{46}$$

$$g_v = \frac{0.12u}{0.6 + 0.2u} \quad (47)$$

4.2.3 Numerical Simulation of Groundwater Flow

A 2-D, time-dependent saturated-unsaturated groundwater flow equation was solved numerically to examine the effect of ET on groundwater discharge to Cobb Mill Creek. I adopted the notation used by Neuman and Witherspoon [1971], with the variables defined in Table 4-2.

$$\frac{\partial}{\partial x_i}\left(K_r K_i \frac{\partial h_i}{\partial x_i} \right) = \left[S_w S_s + C(\psi) \right] \frac{\partial h}{\partial t} \quad (48)$$

Table 4-2. Variables and Parameters Used in the Numerical Groundwater Flow Model

Parameter or Variable	Symbol
Distance in either the horizontal or vertical coordinate directions	x_i
Principal components of the hydraulic conductivity tensor, aligned collinear with the x and z direction	K_i
Relative hydraulic conductivity, assumed to be a scalar function of water saturation	K_r
Water saturation, which varies between zero for dry conditions and 1 for saturated conditions	S_w
Specific storage	S_s
Porosity	n
Hydraulic head	h
Specific moisture capacity	C
Pressure head, equal to h-z, where z is elevation head	ψ
Time	t

Equation (48) was solved using the Galerkin weighted residual finite element approach [*Hornberger and Wiberg*, 2005] with a Douglas-Jones predictor-corrector method, as described in Gu [2007].

The two unknown variables in Equation (48) were estimated from the relationships developed by Cooley and Westphal [1974] relating pressure head (ψ), normalized water saturation (S_w), and relative hydraulic conductivity (K_r).

$$S_w = \frac{A}{(-\psi)^c + A} \tag{49}$$

$$K_r = S_w^d \tag{50}$$

The three parameters (A, c, and d) in Equations (49) and (50) were the same as those used by Gu [2007] to model transient saturated-unsaturated flow at Cobb Mill Creek ($A = 10$; $c = 4$; $d = 2$). Specific moisture capacity (C) is defined as follows.

$$C = n\frac{dS_w}{d\psi} \tag{51}$$

The model domain was a 2-D cross-section of a hillslope leading down to Cobb Mill Creek (Figure 4-2). The upslope boundary was a constant head boundary representing a static water table elevation of 10.7 m above the confining layer (chosen to mimic site conditions); the land surface, confining layer, and channel center boundaries were no-flow boundaries; the seepage face was assigned elevation head (i.e. land surface elevation) as its boundary condition; below static stream stage, the area of the streambed was assigned a constant head boundary condition to represent a static stream level. PET calculated from Equation (41) was applied as a time-dependent flux distributed throughout the unsaturated zone.

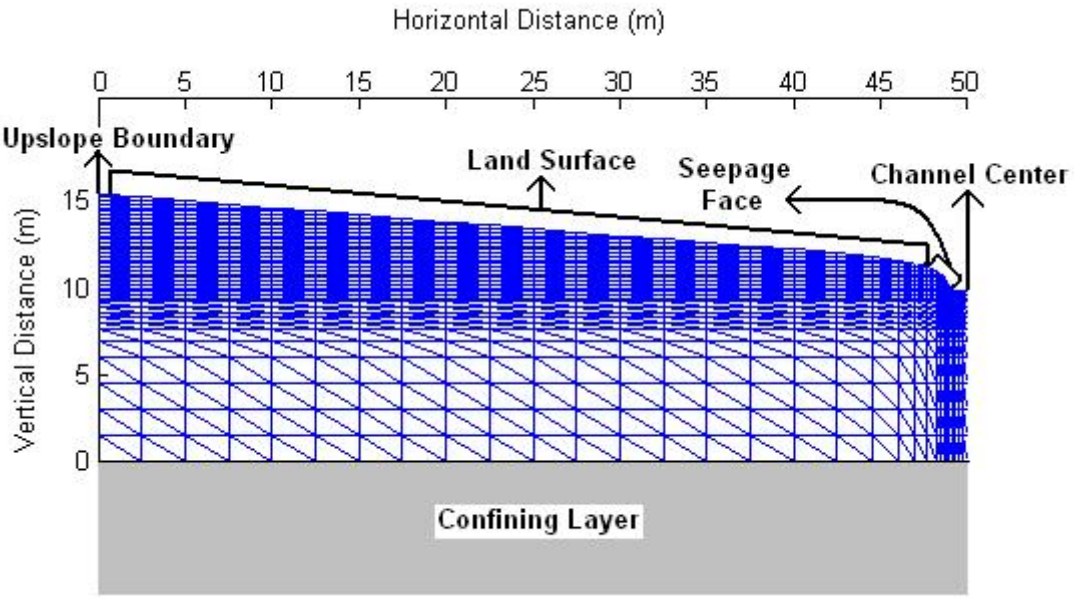

Figure 4-2: Schematic of the finite-element mesh used for the model of transient saturated-unsaturated groundwater flow. There is finer grid spacing near the water table and the stream because the largest hydraulic head fluctuations are expected in those areas. At the far right of the model grid is the stream channel and the upslope boundary is on the far left side. The confining layer is at the base of the grid and the land surface is the upper boundary. The seepage face on the stream bank is also labeled because there are special boundary conditions for that portion of the model.

The numerical simulations provided time series predictions of specific discharge through the streambed and stream bank driven by PET in the vadose zone. Specific discharge for all streambed and seepage face nodes were calculated from Darcy's law and then integrated to determine the total groundwater flux to Cobb Mill Creek. The head gradient was computed across a 15- to 20-cm layer of sediment directly beneath or adjacent to the stream (depending on grid spacing). This integrated specific discharge represents the groundwater discharge per unit stream length (q_w).

To compare these estimates to observed stream discharge required extrapolation of modeled specific discharge for this one cross-section to the approximately 2400-m stream channel. This was done by dividing the length of channel upstream of the

observation point into 1-m long increments (Δx). The time that stream water resides in each increment is $u/\Delta x$, where u is the mean stream velocity. The stream discharge at the observation point is the sum of all the incremental upstream contributions. This can be found with the following integral:

$$= \int \qquad -- \tag{52}$$

4.2.4 Quantitative Speculation on the Extent of Nitrate Removal

Predicted time series of specific discharge were used to drive the first-order rate law for nitrate removal in the streambed and stream bank. This model was used to speculate on the effect of diel flow variations on diel nitrate concentrations in the stream. A first-order kinetic rate law was adopted for describing the extent of nitrate removal in the near-stream zone due to its widespread use [*Boyer et al.*, 2006] and applicability to the streambed of Cobb Mill Creek (Chapter 3).

$$\frac{dN}{dt} = -kN \tag{52}$$

N is nitrate concentration and k is a first-order rate coefficient. Rearranging and integrating Equation (52) leads to a description of exponential decay over time.

$$N = N_0 e^{-kt} \tag{53}$$

Chapter 3 indicated that groundwater travel time (t) is a key control on the extent of nitrate removal and that a mean rate coefficient (k) reasonably describes the streambed as a whole. Thus, the temporal patterns predicted for groundwater travel time should drive temporal patterns in stream nitrate concentrations. Time (t) was approximated as the groundwater travel time through the streambed or stream bank, assuming that the

thickness of the nitrate reduction zone (L) is constant at 30 cm and specific discharge (q) varies through time according to the groundwater flow model predictions.

$$t = \frac{L}{q} \tag{54}$$

Analysis of streambed sediments at Cobb Mill Creek by Galavotti [2004] and Gu [2007] suggested that L could reasonably be assumed constant, such that t is approximately a function of q only. Specific discharge that was predicted by the numerical flow model (Section 4.2.3) was then used to speculate on diurnal variations in nitrate concentrations by applying the first-order rate law. The initial nitrate concentration entering the nitrate reduction zone, N_0, was assumed a constant 12.2 mg L^{-1}, the average nitrate concentration in four piezometers (12.2 ± 0.2 mg L^{-1}, n = 52) opened 40-80 cm beneath the streambed between October 2003 and May 2005.

The only remaining parameter for the first-order rate law is the rate coefficient, k. Measurements of groundwater travel times and of initial and final nitrate concentrations in groundwater seepage were reported in Chapter 3. For each seepage measurement made in Chapter 3, the reaction rate coefficient can be calculated by rearranging the first order rate law as follows.

$$k = -\frac{1}{t}\ln\left(\frac{N}{N_0}\right) \tag{55}$$

Data from all of the seepage meters produced a distribution of rate coefficients with a mean of 0.38 d^{-1} (Figure 4-3). This rate coefficient was used in the first-order rate law for nitrate removal and was held constant for all simulations in this chapter.

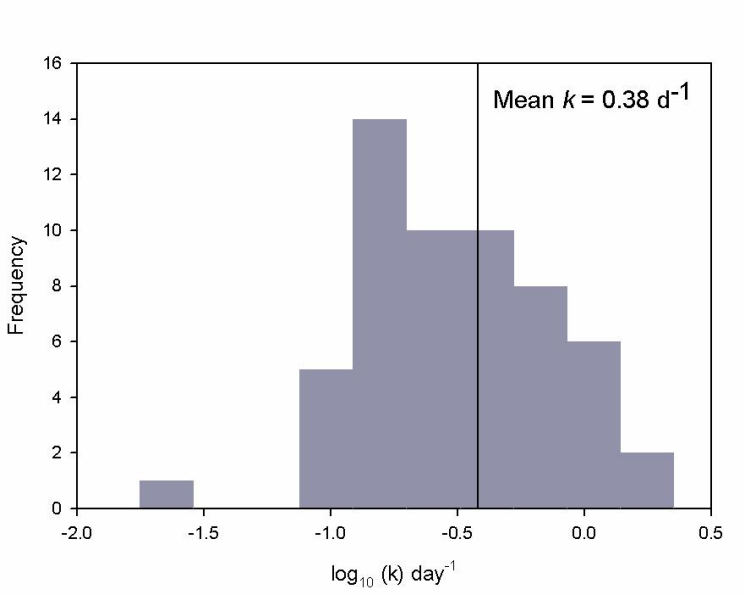

Figure 4-3: Histogram of first-order reaction rate coefficients for non-riparian influenced seepage through the streambed. Assuming a log-normal distribution the mean is 0.38 d^{-1}.

Transit time considerations were required to estimate actual stream nitrate concentrations in the same way that it was used to estimate stream flow. This provision allows for slow-moving streams to dampen diel signals, whereas swift streams allow the diel signals to persist. First, the nitrate flux per unit stream length (J_w) was calculated by integrating the modeled nitrate flux (qN) across the stream's width (w).

$$J_w = \int_0^w qN dw \tag{56}$$

Then, the stream nitrate flux at the observation point was calculated by integrating the nitrate fluxes per unit stream length down the channel (analogous to the stream flow calculation in Equation 52).

$$= \int \quad -- \tag{57}$$

Lastly, the predicted concentration of nitrate in the stream ( ) is calculated from the ratio of the nitrate flux (J) to stream flow (Q).

$$= - \quad (58)$$

4.3 Results

4.3.1 The Effect of ET on Groundwater Flow

The numerical flow model was solved from July 16 through July 22, 2003 (Julian days 197 to 203). There was no rain for that period, but there was one cloudy day, as indicated by the low solar irradiance on Julian day 200 (Figure 4-4D). Air temperatures varied diurnally with peaks in mid afternoon (Figure 4-4A). Relative humidity varied inversely with temperature, with the lowest relative humidity (i.e. highest vapor pressure deficit) on day 199 (Figure 4-4C). Wind speed was variable, but there was a persistent 48-hour period of low wind speeds on days 200 and 201 (Figure 4-4B). Those climate variables were used in Equation (41) to estimate PET.

PET was similar for most days with the noticeable exception of day 200 where PET was substantially lower (Figure 4-5). The low PET during that period resulted primarily from lower solar irradiance (Figure 4-4D), but also because of the low wind speeds (Figure 4-4B) and high relative humidity (Figure 4-4C). Moist, stagnant air prevents the vaporization and transport of water to the atmosphere. Output from the numerical flow model was driven by the record of PET in Figure 4-5.

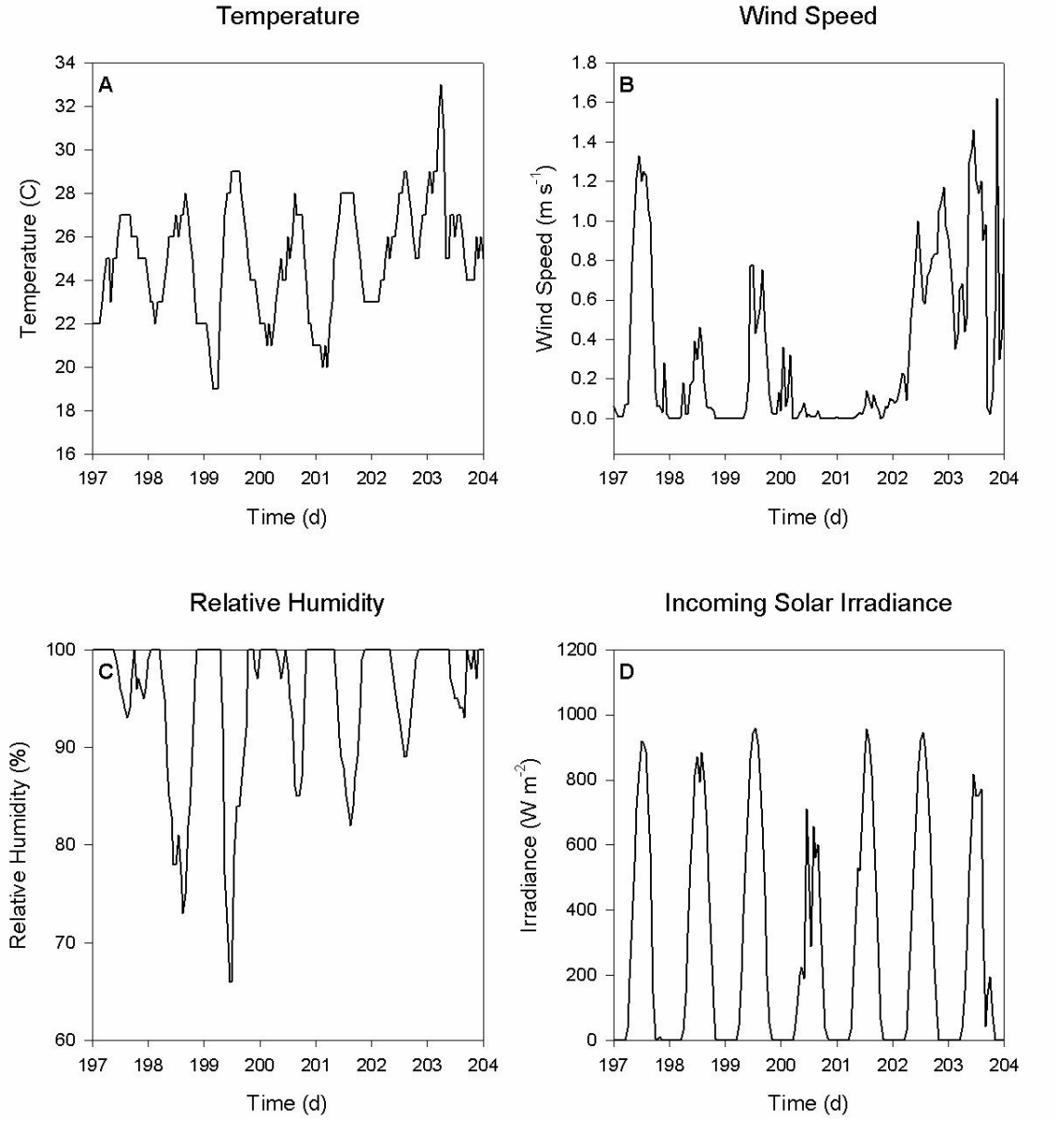

Figure 4-4. The records of temperature (A), wind speed (B), relative humidity (C), and incoming solar irradiance (D) were used to derive potential evapotranspiration that was input to the numerical flow model.

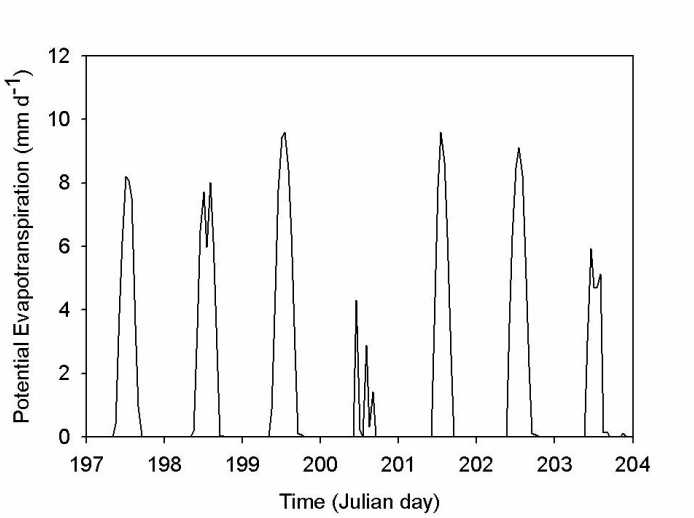

Figure 4-5. Modeled potential evapotranspiration (PET) was derived from the climatological conditions shown in Figure 4-4. The lowest PET was on day 200; the highest PET was on day 199.

There were diurnal fluctuations in modeled specific discharge, with peaks at 11:00 a.m. and troughs near 5:00 p.m. (Figure 4-6A). The best fit between observed and modeled stream discharge was found when the mean channel velocity was set to 0.09 m s^{-1}, giving a transit time of 7.4 hr. This velocity is similar to mean velocities measured when the stream was gaged (unpublished data). Modeled stream discharge was a factor of 4.6 lower than observations, but generally matched the shape of the observed hydrograph. The lack of a peak and trough on Julian day 200 (Figure 4-6) coincided with the low PET during that time (Figure 4-5).

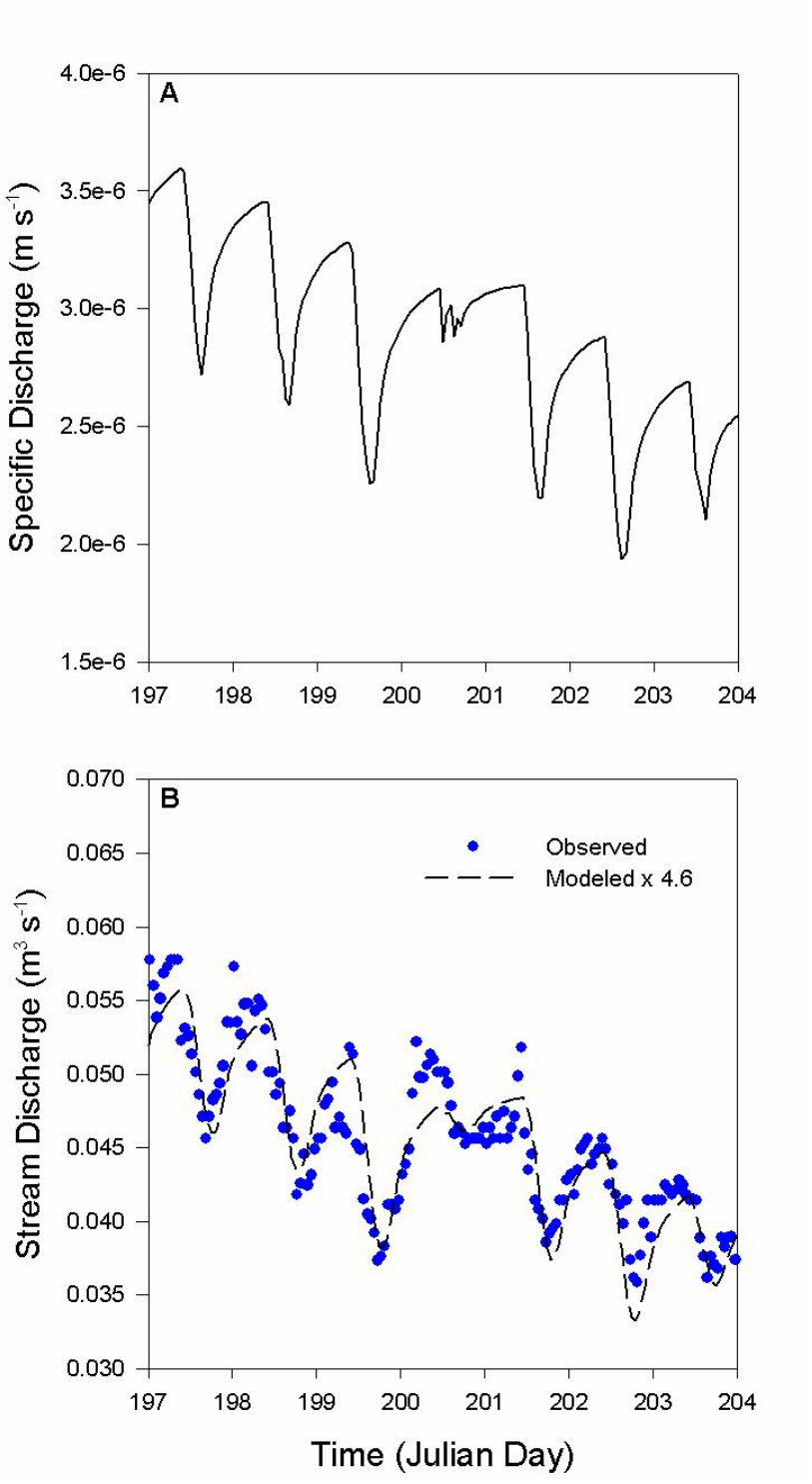

Figure 4-6. Average specific discharge for the modeled channel cross section exhibited a saw-toothed diurnal pattern (A). Upon integrating specific discharge through space and time, the observed (dotted line) and modeled (dashed line) stream discharge fluctuations were similar in shape, but different in magnitude (B). Modeled stream discharge was lower than that observed and to put both on the same scale for comparison, modeled discharge was multiplied by a factor of 4.6.

4.3.2 Predicted Diurnal Variations in Nitrate Concentrations

Predicted stream nitrate concentrations varied diurnally in response to ET cycles (Figure 4-7). The magnitude of the fluctuations depended on mean channel velocity, since this controlled the transit time (Figure 4-7). At low velocities, diurnal fluctuations were small (< 0.1 mg L^{-1}), whereas larger fluctuations occurred at higher velocities (~0.6 mg L^{-1}). In all cases, there was little diurnal fluctuation in nitrate concentrations on day 200. PET was low at that same time (Figure 4-5), causing only a small fluctuation in specific discharge (Figure 4-6A).

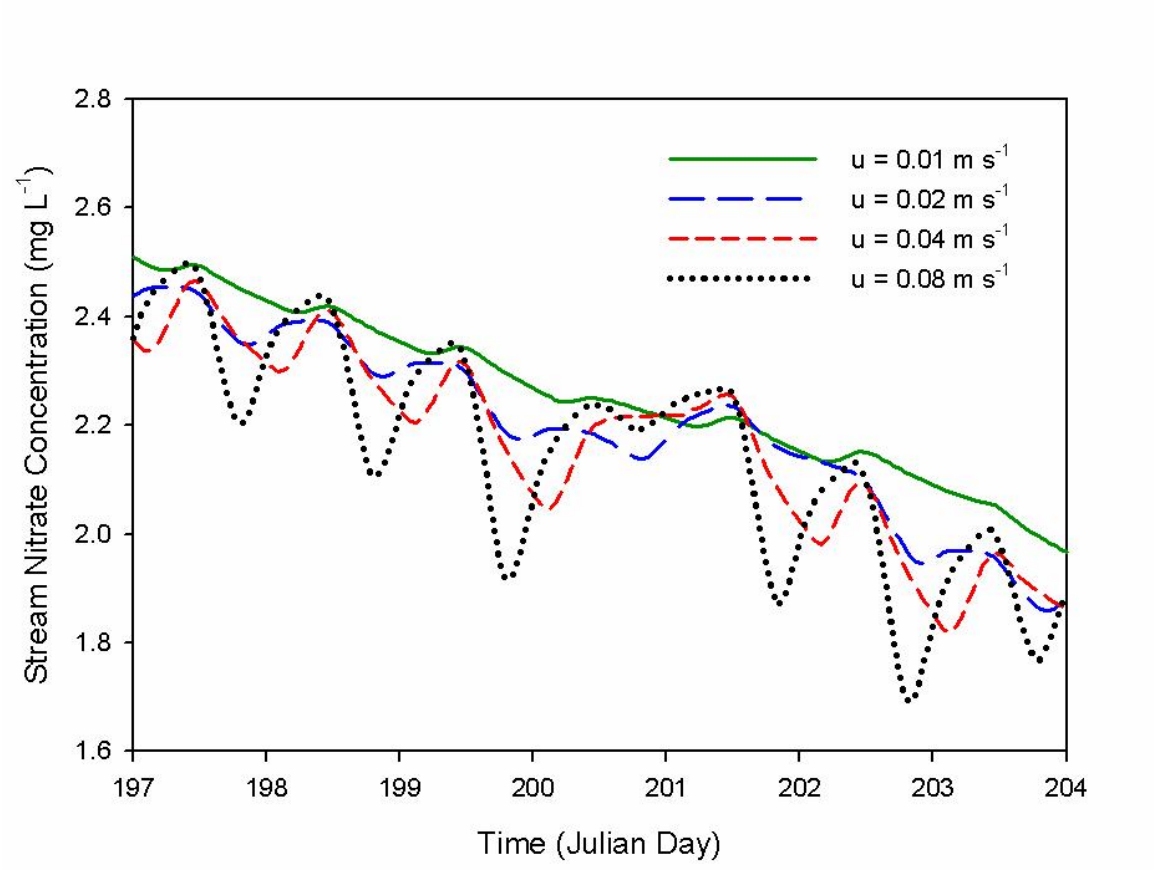

Figure 4-7: Modeled nitrate concentrations in stream water. Stream nitrate concentrations exhibit different temporal patterns depending on the mean channel velocity. This occurs as a result of temporal averaging of the diurnal pulse created by ET in the riparian zone. At low stream velocities,

these diurnal pulses get average out. But as stream velocity increases, these pulses can exit the catchment fast enough to experience little attenuation.

4.4 Discussion

4.4.1 Effect of ET on Groundwater and Stream Flow

The numerical groundwater flow model presented in this study demonstrates the effect of ET on groundwater and stream flow. The model was forced solely by meteorological data, so there is no inherent autocorrelation between modeled specific discharge and measured stream flow. Therefore, stream flow records are a strong test of the model's performance. The temporal pattern of measured stream discharge matched the model closely, although their magnitudes differed. This occurred, despite modeled specific discharge ($2 – 3.5 \times 10^{-6}$ m s^{-1}) being somewhat higher than the mean specific discharge measured with seepage meters in Chapter 3 (8.8×10^{-7} m s^{-1}).

The discrepancy in stream flow magnitude may be due to several factors. The numerical flow model was only a 2-D case, and it was assumed that this same 2-D cross section was consistent down the entire length of the stream. This assumption inherently ignores the third dimension and this could impart some errors to my model. The modeled area is just downstream of a large wetland and the geometry of this area may have some effect on the magnitude of groundwater discharge.

Another consideration is that specific discharge through the streambed and stream bank is not the only source of stream flow. Cobb Mill Creek begins as a large agricultural irrigation pond. Discharge from this pond was not available during the base-flow conditions modeled in this chapter, but measurements during storm events indicated that this pond can supply almost one-third of total stream flow (unpublished data). This alone does not account for the discrepancy, but it is likely a significant factor.

The other possible cause for the discrepancy between observed and modeled stream discharge is a shifting rating curve. Due to the sandy conditions in Cobb Mill Creek, it is difficult to establish a gaging station with a stable cross section. The current gaging station is located downstream of a double-barrel culvert that runs under VA Rt. 600, and that location is about 200 m upstream from the site described by the model. Although this is the most stable cross section available, it does not entirely prevent shifting of the rating curve over time. I had no way of determining or accounting for shifts in the rating curve and this affect may cause some bias in the observed discharge.

Diurnal variations in stream stage and also groundwater elevation have been documented by many others (e.g. [*Bond, et al.*, 2002; *Butler, et al.*, 2007; *Troxell*, 1936]). Although the concept of interactions between streams, groundwater, and ET was developed long ago (e.g.[*Troxell*, 1936; *White*, 1932]), the subject has gained more attention recently, as noted in the work of Butler et al. [2007] and Loheide et al. [2005]. For example, the method of estimating ET based on records of groundwater elevation was developed by White [1932] and has only recently been rigorously evaluated for its accuracy by Loheide *et al.* [2005].

Loheide et al. [2005] performed numerical simulations of saturated-unsaturated flow beneath vegetated areas of different geometries to test the White [1932] method for estimating ET. The authors found that the White [1932] method predicted ET to within 20% of the simulated value. Finer grained sediments resulted in larger fluctuations of the water table due to their lower specific yield (this is embedded in Equation (59) below). In sandy aquifers, the fluctuations are often less than 1 cm over the course of the day, whereas fluctuations in silty aquifers can be on the order of 10 cm.

The ET estimates at Cobb Mill Creek can be used in the White [1932] method (Equation (59)) to estimate the approximate fluctuations in the riparian groundwater table elevation.

$$ET = S_y\left(\frac{\Delta s}{t} + R\right) \tag{59}$$

The aquifer is primarily composed of sand. Specific yield for a sand was taken from Loheide et al. [2005] as 0.33. ET was set to 2 mm d^{-1}. The mean change in water table elevation is small over the course of a few days at Cobb Mill Creek, so $\Delta s/t$ can be ignored. With these assumptions, diurnal fluctuations in the riparian water table should be 7 mm d^{-1}. This fluctuation is an overestimate due to several reasons described in detail by Loheide et al. [2005], most important of which is that Equation (59) ignores the use of vadose-zone water by plants.

The estimated water table fluctuation suggests that the 2-5 cm diurnal variation in stream stage at Cobb Mill Creek is not a result of large-scale dewatering of the aquifer. Instead, the stage fluctuations must be a result of the diurnal patterns of specific discharge into the stream that are driven by time-dependent hydraulic head gradients. When specific discharge decreases, the stream drains at a rate determined by the channel slope and roughness. This draining cycle causes stream stage to drop sharply and to a greater extent than groundwater in the adjacent riparian zone.

In Chapter 3, specific discharge measurements from the streambed may have been affected by temporal variation in groundwater discharge. Those measurements were made in the late summer after prolonged rainless periods and diurnal fluctuations in specific discharge likely occurred. Modeled specific discharge decreased each day by

about 30% from its daily maximum (Figure 4-6A). Seepage measurements were generally taken between 8 a.m. and 2 p.m., but because of the spatial variations in flow rates, the seepage meters did not always measure specific discharge for the same duration. The temporal error that this would impart on seepage measurements was not explicitly calculated, although its upper bound is approximately 30% for Cobb Mill Creek (*i.e.* the maximum daily fluctuation). This level of error is of similar in magnitude to the error in successive seepage meter measurements at a single location in the streambed (Figure 3-3A). More importantly, the amount of temporal variation in specific discharge is small relative to the spatial variability. Specific discharge measured in Chapter 3 varied by orders of magnitude over distances of decimeters and this large spatial variability likely overshadowed any effects of temporal variability on the measurements.

4.4.2 Temporal Variations in Nitrate Concentrations

Stream nitrate concentrations responded to two effects. The diurnal patterns in groundwater travel time that were driven by ET caused fluctuations in stream nitrate concentrations over the same timescale. The specific discharge pattern in Figure 4-6A does not have the same shape as stream nitrate concentrations, however. This difference is due to in-stream averaging of the specific discharge signal and this averaging depends on mean channel velocity. At lower channel velocity, a parcel of water propagating down the stream experiences a larger segment of the specific discharge time series. The parcel averages over this time period and when it is large enough, the diurnal fluctuations disappear (*e.g.* when u = 0.01 in Figure 4-7). Conversely, at higher channel velocities, the stream nitrate concentration more closely resembles the pattern in specific discharge.

My simulated stream nitrate concentrations suggest that ET in the riparian zone affects nitrate concentrations in groundwater seepage in two ways. First, it causes a diurnal saw-tooth pattern in nitrate concentrations. Second, that saw-tooth pattern is overlain on a generally decreasing trend in nitrate concentrations through time (Figure 4-7). The cumulative effect of ET is then to draw down the water table in a single day and then over a longer multi-day period. The drawing down of the water table increases the residence time of groundwater in nitrate reduction zones and, therefore, reduces the concentration of nitrate discharging from the groundwater system.

My findings at Cobb Mill Creek suggest that there are multiple benefits of forested riparian zones on nitrogen retention in addition to plant uptake. Forests in the riparian zone have ET rates close to their potential due to wet soils and shallow water table conditions (Appendix 2). This wet environment allows trees to pump water at a maximal rate and this greatly reduces groundwater flow rates near the stream. As groundwater flow rates decrease, more nitrogen is removed in the reduced sediments of the riparian zone and streambed. These reduced conditions themselves exist because of the organic matter inputs from the forest. Thus, forested riparian zones provide the fuel to drive denitrification in the near-stream zone and they also draw down the water table during the growing season, which enhances the extent of nitrate removal that occurs. These effects, combined with nitrogen taken up by the plants themselves, provide strong support for the expanded use of forested riparian zones in mitigating nitrogen transfer to down-gradient systems.

5.0 References

Angier, J., G. McCarty, and K. Prestegaard (2005), Hydrology of a first-order riparian zone and stream, mid-Atlantic coastal plain, Maryland, *Journal of Hydrology*, *309*, 149-166.

Bachman, L., B. Lindsey, J. Brakebill, and D. Powars (1998), Ground-water discharge and base flow nitrate loads of nontidal streams, and their relation to a hydrogeomorphic classification of the Chesapeake Bay watershed, Middle Atlantic Coast, 71 pp, U.S. Geological Survey Water Resources Investigations Report 98-4059.

Barnes, D. (2004), Use of benthic macroinvertebrates to assess impacts of agricultural land use in nontidal coastal plain streams, Masters Thesis, 151 pp, University of Virginia, Charlottesville, VA.

Bastviken, D., P. Sanden, T. Svensson, C. Stahlberg, M. Magounakis, and G. Oberg (2006), Chloride-retention and release in a boreal forest soil: Effects of soil water residence time and nitrogen and chloride loads, *Environmental Science & Technology*, *40*, 2977-2982.

Bohlke, J. (2002), Groundwater recharge and agricultural contamination, *Hydrogeology Journal*, *10*, 153-179.

Bohlke, J., and J. Denver (1995), Combined use of groundwater dating, chemical, and isotopic analyses to resolve the history and fate of nitrate contamination in two agricultural watersheds, Atlantic coastal plain, Maryland, *Water Resources Research*, *31*, 2319-2339.

Bond, B., J. Jones, G. Moore, N. Phillips, D. Post, and J. McDonnell (2002), The zone of vegetation influence on baseflow revealed by diel patterns of streamflow and vegetation water use in a headwater basin, *Hydrological Processes*, *16*, 1671-1677.

Boyer, E. W., R. B. Alexander, W. J. Parton, C. S. Li, K. Butterbach-Bahl, S. D. Donner, R. W. Skaggs, and S. J. Del Gross (2006), Modeling denitrification in terrestrial and aquatic ecosystems at regional scales, *Ecological Applications*, *16*, 2123-2142.

Brakebill, J., and S. Preston (1999), Digital data used to relate nutrient inputs to water quality in the Chesapeake Bay watershed, version 1.0, U.S. Geological Survey Open-File Report 99-60.

Brann, D., D. Holshouser, and G. Mullins (2000), *Virginia Cooperative Extension Agronomy Handbook*, Virginia Polytechnic Institute and State University, Blacksburg, VA.

Bridge, J. (1977), Flow, bed topography, grain size and sedimentary structure in open channel bends: a three-dimensional model, *Earth Surface Processes*, *2*, 401-416.

Burkholder, J., H. Glasgow, and C. Hobbs (1995), Distribution and environmental conditions for fish kills linked to a toxic ambush predator dinoflegellate, *Marine Ecology Progress Series*, *124*, 43-61.

Burns, D. (1998), Retention of NO_3^- in an upland stream environment: A mass balance approach, *Biogeochemistry*, *40*, 73-96.

Burt, T. P. (1979), Diurnal variations in stream discharge and throughflow during a period of low flow, *Journal of Hydrology*, *41*, 291-301.

Butler, J., G. Kluitenberg, D. Whittemore, S. Loheide, W. Jin, M. Billinger, and X. Zhan (2007), A field investigation of phreatophyte-induced fluctuations in the water table, *Water Resources Research*, *43*, doi:10.1029/2005WR004627.

Calver, J. (1968), Groundwater resources of Accomack and Northampton Counties Virginia, 113 pp, Virginia Department of Conservation and Economic Development, Virginia Division of Mineral Resources, Report 9.

Campbell, G., and J. Norman (1998), *An introduction to environmental biophysics*, 286 pp., Springer-Verlag, New York, NY.

Caraco, N., and J. Cole (1999), Human impact on nitrate export: an analysis using major world rivers, *Ambio*, *28*, 167-170.

Cardenas, B., and V. Zlotnik (2003), Three-dimensional model of modern channel bend deposits, *Water Resources Research*, *39*, 1141, doi:1110.1029/2002WR001383.

Cardenas, M., and J. Wilson (2004), Impact of heterogeneity, bed forms, and stream curvature on subchannel hyporheic exchange, *Water Resources Research*, *40*, W08307.

Chen, A., and S. Wang (1999), Carbon, alkalinity and nutrient budgets on the East China Sea continental shelf, *Journal of Geophysical Research*, *104*, 20675-20686.

Cirmo, P., and J. McDonnell (1997), Linking the hydrologic and biogeochemical controls of nitrogen transport in near-stream zones of temperate-forested catchments: a review, *Journal of Hydrology*, *199*, 88-120.

Claassen, H., and D. Halm (1996), Estimates of evapotranspiration or effective moisture in Rocky Mountain watersheds from chloride ion concentrations in stream baseflow, *Water Resources Research*, *32*, 363-372.

Clement, J., L. Aquilina, O. Bour, K. Plaine, T. Burt, and G. Pinay (2003), Hydrological flowpaths and nitrate removal rates within a riparian floodplain along a fourth-order stream in Brittany (France), *Hydrological Processes*, *17*, 1177-1195.

Conant, B., J. Cherry, and R. Gillham (2004), A PCE groundwater plume discharging to a river: influence of the streambed and near-river zone on contaminant distributions, *Journal of Contaminant Hydrology*, *73*, 249-279.

Cooley, R., and J. Westphal (1974), An evaluation of the theory of ground-water and river-water interchange, Winnemucca reach of the Humboldt River, Nevada, 74 pp, National Technical Information Service, Springfield, VA, Technical Report Series H-W, Hydrology and Water Resources Publication No. 19.

Cooper, H., and M. Rorabaugh (1963), Groundwater movements and bank storage due to flood stages in surface stream, 343–366 pp, US Geological Survey Water Supply Paper 1536-J.

Denver, J. (1989), Effects of agricultural practices and septic-system effluent on the quality of water in the unconfined aquifer in parts of eastern Sussex county, Delaware, 66 pp, Delaware Geological Survey Report of Investigations 45, Newark, DE.

Denver, J., S. Ator, L. Debrewer, M. Ferrari, J. Barbaro, T. Hancock, M. Brayton, and M. Nardi (2003), Water quality in the Delmarva Peninsula: Delaware, Maryland, and Virginia, 1999-2001, US Geological Survey Circular 1228.

Efron, B., and R. Tibshirani (1993), *An introduction to the bootstrap*, 436 pp., CRC Press, Boca Raton, FL.

Fowler, D., C. Flechard, U. Skiba, M. Coyle, and J. N. Cape (1998), The atmospheric budget of oxidized nitrogen and its role in ozone formation and deposition, *New Phytologist*, *139*, 11-23.

Freeze, R., and J. Cherry (1979), *Groundwater*, 604 pp., Prentice-Hall, Englewood Cliffs, NJ.

Galavotti, H. (2004), Spatial profiles of sediment denitrification at the ground water - surface water interface in Cobb Mill Creek on the Eastern Shore of Virginia, Masters Thesis, 94 pp, University of Virginia, Charlottesville, VA.

Galloway, J. (1998), The global nitrogen cycle: changes and consequences, *Environmental Pollution*, *102*, 15-24.

Galloway, J., J. Aber, J. Erisman, S. Seitzinger, R. Howarth, E. Cowling, and B. Cosby (2003), The Nitrogen Cascade, *Bioscience*, *53*, 341-356.

Galloway, J., and E. Cowling (2002), Reactive nitrogen and the world: 200 years of change, *Ambio*, *31*, 64-71.

Galloway, J., W. Schlesinger, H. Levy, A. Michaels, and J. Schnoor (1995), Nitrogen fixation: anthropogenic enhancement-environmental response, *Global Biogeochemical Cycles*, *9*, 235-252.

Galloway, J. N., and G. E. Likens (1981), Acid Precipitation - the Importance of Nitric-Acid, *Atmospheric Environment*, *15*, 1081-1085.

Garcia-Ruiz, R., S. Pattinson, and B. Whitton (1998), Denitrification in river sediments: relationship between process rate and properties of water and sediment, *Freshwater Biology*, *39*.

Green, P., C. Vorosmarty, M. Meybeck, J. Galloway, B. Peterson, and E. Boyer (2004), Pre-industrial and contemporary fluxes of nitrogen through rivers: a global assessment based on typology, *Biogeochemistry*, *68*, 71-105.

Gu, C. (2007), Hydrological control on nitrate delivery through the groundwater-surface water interface, Dissertation, 247 pp, University of Virginia, Charlottesville, VA.

Gu, C., G. Hornberger, J. Herman, and A. Mills (2008), The effects of freshets on the flux of groundwater nitrate through streambed sediments, *Water Resources Research*, *44*, W05415, doi:05410.01029/02007WR006488.

Gu, C., G. Hornberger, A. Mills, J. Herman, and S. Flewelling (2007), Nitrate reduction in streambed sediments: effects of flow and biogeochemical kinetics, *Water Resources Research*, *43*, W12413,doi:12410.11029/12007WR006027.

Hager, T. (2008), *The alchemy of air : a Jewish genius, a doomed tycoon, and the scientific discovery that fed the world but fueled the rise of Hitler*, 316 pp., Harmony Books, New York.

Hedin, L., J. von Fischer, N. Ostrom, B. Kennedy, M. Brown, and G. Robertson (1998), Thermodynamic constraints on nitrogen transformations and other biogeochemical processes at soil-stream interfaces, *Ecology*, *79*, 684-703.

Hill, A. (1988), Factors influencing nitrate depletion in a rural stream, *Hydrobiologia*, *160*, 111-122.

Hill, A., K. Devito, S. Campagnolo, and K. Sanmugadas (2000), Subsurface denitrification in a forest riparian zone: interactions between hydrology and supplies of nitrate and organic carbon, *Biogeochemistry*, *51*, 193-223.

Hill, A., and K. Sanmugadas (1985), Denitrification rates in relation to stream sediment characteristics, *Water Research*, *19*, 1579-1586.

Hornberger, G., J. Raffensperger, P. Wiberg, and K. Eshleman (1998), *Elements of physical hydrology*, 302 pp., Johns Hopkins University Press, Baltimore, MD.

Hornberger, G., and P. Wiberg (2005), *Numerical Methods in the Hydrological Sciences*, 233 pp., American Geophysical Union, Electronic Book.

Howarth, R., G. Billen, D. Swaney, A. Townsend, N. Jaworski, K. Laytha, J. Downing, R. Elmgren, N. Caraco, T. Jordan, F. Berendse, J. Freney, V. Kudeyarov, P. Murdoch, and Z. Zhao-Liang (1996), Regional nitrogen budgets and riverine N & P fluxes for the drainages to the North Atlantic Ocean: natural and human influences, *Biogeochemistry*, *35*, 75-139.

Hubbard, S., J. Chen, J. Peterson, E. Majer, K. Williams, D. Swift, B. Mailloux, and Y. Rubin (2001), Hydrogeological characterization of the South Oyster Bacterial Transport Site using geophysical data, *Water Resources Research*, *37*, 2431-2456.

Jacobs, T., and J. Gilliam (1985), Riparian losses of nitrate from agricultural drainage waters, *Journal of Environmental Quality*, *14*, 472-478.

Kellman, L., and C. Hillaire-Marcel (1998), Nitrate cycling in streams: using natural abundances of nitrate N15 to measure in-situ denitrification, *Biogeochemistry*, *43*, 273-292.

Kennedy, C., D. Genereux, D. Corbett, and H. Mitasova (2007), Design of a light-oil piezomanometer for measurement of hydraulic head differences and collection of groundwater samples, *Water Resources Research*, *43*, W09501.

Kozlowski, T. (1997), *Physiology of Woody Plants*, Academic Press, San Diego, CA.

Lee, D. (1977), A device for measuring seepage flux in lakes and estuaries, *Limnology and Oceanography*, *22*, 140-147.

Lee, D., and H. Hynes (1978), Identification of groundwater discharge zones in a reach of Hillman Creek in Southern Ontario, *Water Pollution Research Canada*, *13*, 121-133.

Legout, C., J. Molenat, L. Aquilina, C. Gascuel-Odoux, M. Faucheux, Y. Fauvel, and T. Bariac (2007), Solute transfer in the unsaturated zone-groundwater continuum of a headwater catchment, *Journal of Hydrology*, *332*, 427-441.

Lischeid, G., A. Kolb, C. Alewell, and S. Paul (2007), Impact of redox and transport processes in a riparian wetland on stream water quality in the Fichtelgebirge region, southern Germany, *Hydrological Processes*, *21*, 123-132.

Loheide, S., J. Butler, and S. Gorelick (2005), Estimation of groundwater consumption by phreatophytes using diurnal water table fluctuations: A saturated-unsaturated flow assessment, *Water Resources Research*, *41*, doi:10.1029/2005WR003942.

McCarty, G., J. Angier, C. Rice, and K. Bialek (2008), Impact of temporal and spatial variations in agrochemical fluxes within the riparian buffer on exports from a first order watershed, paper presented at AWRA Specialty Conference on Riparian Processes, American Water Resources Association, Norfolk, VA.

McMahon, P., and J. Bohlke (1996), Denitrification and mixing in a stream-aquifer system: effects on nitrate loading to surface water, *Journal of Hydrology*, *186*, 105-128.

Mills, A., G. Hornberger, and J. Herman (2008), Sediments in low-relief costal streams as effective filters of agricultural nitrate, in *American Water Resources Association*, Virginia Beach, Virginia.

Mixon, R., C. Berquist, W. Newell, G. Johnson, D. Powars, J. Schindler, and E. Rader (1989), Geologic map and generalized cross sections of the coastal plain and adjacent parts of the Piedmont, Virginia, US Geological Survey, Miscellaneous Investigation Series Map I-2033, Washington, DC.

Murdoch, P. S., and J. L. Stoddard (1992), The Role of Nitrate in the Acidification of Streams in the Catskill Mountains of New-York, *Water Resources Research*, *28*, 2707-2720.

Neuman, S., and P. Witherspoon (1971), Analysis of nonsteady flow with a free surface using the finite element method, *Water Resources Research*, *7*, 611-623.

Nixon, S. (1995), Coastal marine eutrophication: a definition, social causes, and future concerns, *Ophelia*, *41*, 199-219.

Nixon, S. (1996), The fate of nitrogen and phosphorus at the land-sea margin of the North Atlantic Ocean, *Biogeochemistry*, *35*, 141-180.

Ocampo, C. J., C. E. Oldham, and M. Sivapalan (2006), Nitrate attenuation in agricultural catchments: Shifting balances between transport and reaction, *Water Resources Research*, *42*.

Olson, M., J. Herman, A. Sofranko, and A. Mills (2006), Nitrate loading as a function of stream discharge along the Eastern Shore of Virginia, in *Geological Society of Americal, Annual Meeting*, Geological Society of America, Abstracts with Programs, v. 38, no. 7, p. 39, Philadelphia, PA.

Pfenning, K., and P. McMahon (1996), Effect of nitrate, organic carbon, and temperature on potential denitrification rates in nitrate-rich riverbed sediments, *Journal of Hydrology*, *187*, 283-295.

Phillips, O. (2003), Groundwater flow patterns in extensive shallow aquifers with gentle relief: theory and application to the Galena/Locust Grove region of eastern Maryland, *Water Resources Research*, *39*, WR001261.

Phillips, P., J. Denver, R. Shedlock, and P. Hamilton (1993), Effect of forested wetlands on nitrate concentrations in ground water and surface water on the Delmarva Peninsula, *Wetlands*, *13*, 75-83.

Richardson, D. (1994), Hydrogeology and analysis of the ground-water-flow system of the Eastern Shore, Virginia, USGS, United States Government Printing Office.

Rowland, F. S. (1991), Stratospheric Ozone Depletion, *Annu. Rev. Phys. Chem.*, *42*, 731-768.

Russell, K., W. Keene, J. Maben, J. Galloway, and J. Moody (2003), Phase partitioning and dry deposition of atmospheric nitrogen at the mid-Atlantic U.S. coast, *Journal of Geophysical Research*, *108*, 4656, doi:4610.1029/2003JD003736.

Schmidt, I., O. Sliekers, M. Schmid, E. Bock, J. Fuerst, J. Kuenen, M. Jetten, and M. Strous (2003), New concepts of microbial treatment processes for the nitrogen removal in wastewater, *FEMS Microbiology Ecology*, *27*, 481-492.

Scholefield, D., T. Le Goff, J. Braven, L. Ebdon, T. Long, and M. Butler (2005), Concerted diurnal patterns in riverine nutrient concentrations and physical conditions, *Science of the Total Environment*, *344*, 201-210.

Seitzinger, S. (1988), Denitrification in freshwater and coastal marine ecosystems: ecological and geochemical significance, *Limnology and Oceanography*, *33*, 702-724.

Seitzinger, S., and A. Giblin (1996), Estimating denitrification in North Atlantic continental shelf sediments, *Biogeochemistry*, *35*, 235-260.

Seitzinger, S., J. A. Harrison, J. K. Bohlke, A. F. Bouwman, R. Lowrance, B. Peterson, C. Tobias, and G. Van Drecht (2006), Denitrification across landscapes and waterscapes: A synthesis, *Ecological Applications*, *16*, 2064-2090.

Seitzinger, S., R. Styles, E. Boyer, R. Alexander, G. Billen, R. Howarth, B. Mayer, and N. Van Breemen (2002), Nitrogen retention in rivers: model development and application to watersheds in the northeastern USA, *Biogeochemistry*, *57/58*, 199-237.

Shaw, S. B., A. A. Harpold, J. C. Taylor, and M. T. Walter (2008), Investigating a high resolution, stream chloride time series from the Biscuit Brook catchment, Catskills, NY, *Journal of Hydrology*, *348*, 245-256.

Silverman, B. (1981), Using kernel density estimates to investigate multimodality, *Journal of the Royal Statistical Society, Series B*, *43*, 97-99.

Smil, V. (1999), Nitrogen in crop production: An account of global flows, *Global Biogeochemical Cycles*, *13*, 647-662.

Smith, M., and J. Tiedje (1979), Phases of denitrification following oxygen depletion in soil, *Soil Biology and Biochemistry*, *11*, 261-267.

Smith, R., G. Schwarz, and R. Alexander (1997), Regional interpretation of water-quality monitoring data, *Water Resources Research*, *33*, 2781-2798.

Spalding, R., and M. Exner (1993), Occurrence of nitrate in groundwater--A review, *Journal of Environmental Quality*, *22*, 392-402.

Squillace, P. (1996), Observed and simulated movement of bank-storage water, *Ground Water*, *34*, 121-134.

Stanhope, J. (2003), Relationships between watershed characteristics and base flow nutrient discharges to Eastern Shore coastal lagoons, Virginia, Masters Thesis, 168 pp, The College of William and Mary, Yorktown, VA.

Stull, R. (1995), *Meteorology Today for Scientists and Engineers*, West Publishing Co., St. Paul, MN.

Swank, W., and W. Caskey (1982), Nitrate depletion in a second-order mountain stream, *Journal of Environmental Quality*, *11*, 581-584.

Tesoriero, A., H. Liebscher, and S. Cox (2000), Mechanism and rate of denitrification in an agricultural watershed: electron and mass balance along groundwater flow paths, *Water Resources Research*, *36*, 1545-1559.

Thornthwaite, C. W. (1948), An approach toward a rational classification of climate, *Geographic Review*, *38*, 55-94.

Thornthwaite, C. W., and J. R. Mather (1955), The Water Balance, *Publications in Climatology*, *VIII*, 1-104.

Thornthwaite, C. W., and J. R. Mather (1957), Instructions and tables for computing potential evapotranspiration and the water balance, *Publications in Climatology*, *X*, 311.

Tomer, M. D., and M. R. Burkart (2003), Long-term effects of nitrogen fertilizer use on ground water nitrate in two small watersheds, *Journal of Environmental Quality*, *32*, 2158-2171.

Trapp, H. (1992), Hydrogeologic Framework of the Northern Atlantic Coastal Plain in Parts of North Carolina, Virginia, Maryland, Delaware, New Jersey, and New York, Department of Interior, United States Government Printing Office.

Troxell, H. (1936), The diurnal fluctuations in the ground-water and flow of the Santa Ana river and its meaning, *Eos Tansactions of the American Geophysical Union*, *17*, 496-504.

Vitousek, P. M., J. D. Aber, R. W. Howarth, G. E. Likens, P. A. Matson, D. W. Schindler, W. H. Schlesinger, and D. G. Tilman (1997), Human alteration of the global nitrogen cycle: Sources and consequences, *Ecological Applications*, *7*, 737-750.

Vroblesky, D., and W. Fleck (1991), Hydrogeologic Framework of the Coastal Plain of Maryland, Delaware, and the District of Columbia, Department of Interior, United States Government Printing Office, Washington D.C.

White, W. (1932), A method of estimating ground-water supplies based on discharge by plants and evaporation from soil--Results of investigations in Escalante Valley, Utah, 105 pp, U.S. Geological Survey Water Supply Paper 659-A.

Willems, H., M. Rotelli, D. F. Berry, E. P. Smith, R. B. Reneau, and S. Mostaghimi (1997), Nitrate removal in riparian wetland soils: effects of flow rate, temperature, nitrate concentration and soil depth, *Water Research*, *31*, 841-849.

Winter, T., J. Harvey, O. Franke, and W. Alley (1998), Ground water and surface water: A single resource, 79 pp, United States Geological Survey Circular 1139.

Xu, S. P., A. C. Leri, S. C. B. Myneni, and P. R. Jaffe (2004), Uptake of bromide by two wetland plants (Typha latifolia L. and Phragmites australis [Cav.] Trin. ex Steud.), *Environmental Science & Technology*, *38*, 5642-5648.

Zumft, W. (1997), Cell biology and molecular basis of denitrification, *Microbiology and Molecular Biology Reviews*, *61*, 533-616.

Appendix 1: Data

Table A1.1: Seepage Meter Data

Sampling Date	Specific Discharge (cm s^{-1})	Chloride Concentration (mg L^{-1})	Nitrate Concentration (mg L^{-1})	Dissolved Organic Carbon Concentration (mg L^{-1})
8/11/2006	3.7E-04	13.5	9.6	NS
8/11/2006	6.3E-04	13.6	6.1	NS
8/11/2006	8.2E-04	13.6	5.6	NS
8/11/2006	7.4E-05	19.0	4.8	NS
8/11/2006	3.8E-04	18.5	7.8	NS
8/11/2006	1.2E-04	14.1	4.0	NS
8/11/2006	1.9E-04	14.8	4.7	NS
8/11/2006	1.7E-04	20.0	1.8	NS
8/11/2006	2.8E-04	14.5	4.6	NS
8/11/2006	3.1E-04	21.6	10.0	NS
8/11/2006	5.6E-04	15.0	5.9	NS
8/11/2006	6.5E-04	15.3	5.5	NS
8/11/2006	6.4E-04	18.5	7.4	NS
8/11/2006	2.5E-04	15.0	4.6	NS
8/11/2006	1.2E-04	24.2	1.6	NS
8/11/2006	2.6E-04	14.8	4.4	NS
9/9/2006	3.8E-05	22.5	1.8	7.6
9/9/2006	4.4E-05	23.7	1.6	12.3
9/9/2006	2.5E-04	24.3	0.7	6.7
9/9/2006	2.9E-05	20.7	1.4	12.6
9/9/2006	1.4E-04	23.0	18.9	11.8
9/9/2006	4.2E-04	NS	NS	6.0
9/9/2006	6.9E-05	23.8	0.6	6.6
9/9/2006	5.4E-05	20.9	7.9	15.6
9/9/2006	4.2E-04	24.6	1.5	13.1
9/9/2006	6.1E-05	23.8	10.9	9.9
9/9/2006	1.8E-05	NS	NS	NS
9/9/2006	1.7E-04	23.4	1.0	16.8
9/9/2006	4.5E-04	15.3	9.4	5.6
9/9/2006	2.0E-04	23.6	2.6	4.3
9/9/2006	2.6E-04	17.9	3.2	3.7
9/9/2006	3.2E-04	20.0	0.7	4.7
9/21/2006	3.8E-05	29.2	0.4	9.7
9/21/2006	1.3E-04	23.9	5.2	6.2
9/21/2006	6.8E-05	25.8	4.2	6.0
9/21/2006	6.9E-05	NS	NS	NS
9/21/2006	6.0E-05	26.6	0.4	18.5
9/21/2006	3.9E-04	28.3	0.5	5.4
9/21/2006	1.5E-04	23.9	3.7	5.1
9/21/2006	1.1E-04	29.7	0.3	5.5
9/21/2006	1.5E-04	27.0	1.4	4.4

Sampling Date	Specific Discharge (cm s^{-1})	Chloride Concentration (mg L^{-1})	Nitrate Concentration (mg L^{-1})	Dissolved Organic Carbon Concentration (mg L^{-1})
9/22/2006	2.7E-04	28.5	1.3	8.1
9/22/2006	3.5E-04	26.1	4.8	5.9
9/22/2006	1.5E-04	27.6	0.7	8.3
9/22/2006	1.9E-03	26.9	3.1	5.0
9/22/2006	2.8E-04	27.2	0.6	6.6
9/22/2006	5.1E-04	28.8	1.2	7.1
9/22/2006	5.6E-03	29.6	2.0	10.1
9/22/2006	1.2E-04	28.4	2.0	9.6
9/22/2006	2.7E-04	28.1	3.1	6.6
7/10/2007	2.9E-04	25.0	7.7	5.7
7/10/2007	3.8E-05	25.6	6.6	5.8
7/10/2007	1.6E-04	24.9	7.9	4.5
7/10/2007	4.1E-04	29.5	ND	12.4
7/10/2007	4.8E-05	19.5	0.0	14.2
7/10/2007	1.4E-03	29.5	0.4	2.7
7/10/2007	1.3E-05	27.0	ND	15.2
7/10/2007	5.3E-04	22.3	6.5	5.4
7/10/2007	5.1E-05	26.0	ND	10.9
7/10/2007	1.5E-04	NS	NS	NS
7/10/2007	2.8E-04	22.1	6.2	5.7
7/10/2007	3.2E-04	27.3	2.8	6.7
7/10/2007	3.3E-04	24.5	4.6	4.5
7/10/2007	3.4E-05	27.0	5.9	5.8
7/10/2007	6.1E-04	23.7	5.6	3.7
7/10/2007	2.3E-05	NS	NS	NS
7/10/2007	3.3E-05	NS	NS	NS
7/10/2007	1.3E-04	15.7	1.9	11.1
7/10/2007	7.1E-05	15.4	2.6	19.1
7/10/2007	2.6E-04	23.8	0.2	16.7
7/26/2007	6.7E-05	39.5	0.1	10.5
7/26/2007	3.5E-05	36.5	0.1	11.7
7/26/2007	2.2E-04	34.1	0.1	30.0
7/26/2007	2.8E-06	NS	NS	7.7
7/26/2007	ND	NS	NS	NS
7/26/2007	5.1E-06	NS	NS	NS
7/26/2007	5.8E-04	32.7	5.3	10.0
7/26/2007	2.5E-05	26.0	0.8	8.1
7/26/2007	2.5E-05	27.5	0.3	12.4
7/26/2007	2.2E-04	27.9	0.9	11.3
7/26/2007	5.5E-05	30.8	0.0	23.4
7/26/2007	2.3E-05	28.5	0.0	9.4
7/26/2007	1.0E-03	33.7	0.4	18.6
7/26/2007	1.3E-04	34.8	ND	19.3
7/26/2007	5.2E-05	34.1	0.1	12.8
7/26/2007	ND	NS	NS	NS
7/26/2007	1.4E-05	NS	NS	NS
7/26/2007	1.5E-04	33.1	ND	6.6

Sampling Date	Specific Discharge (cm s^{-1})	Chloride Concentration (mg L^{-1})	Nitrate Concentration (mg L^{-1})	Dissolved Organic Carbon Concentration (mg L^{-1})
7/26/2007	2.6E-06	NS	NS	NS
7/26/2007	7.3E-05	33.2	0.1	23.0
7/26/2007	1.4E-04	34.2	ND	14.6
7/26/2007	6.8E-05	34.9	ND	12.8
7/26/2007	3.7E-05	36.0	0.0	15.8
7/26/2007	7.1E-06	NS	NS	NS
7/26/2007	6.7E-06	NS	NS	NS
7/26/2007	2.7E-05	30.1	0.3	10.3
7/26/2007	6.6E-05	34.0	0.0	14.0
7/26/2007	1.1E-04	34.6	0.0	7.0
7/26/2007	7.1E-05	31.8	0.0	16.0
7/26/2007	9.7E-05	35.4	ND	22.7
7/26/2007	6.2E-05	36.0	0.2	17.3
7/26/2007	5.1E-05	33.0	0.0	25.2
7/26/2007	5.4E-05	33.1	0.0	11.1
7/26/2007	1.9E-04	34.1	ND	20.1
7/26/2007	5.2E-05	34.4	0.3	11.7
7/26/2007	2.8E-05	32.6	0.0	20.9
7/26/2007	1.5E-05	31.8	0.1	6.2
7/26/2007	6.7E-06	NS	NS	NS
7/26/2007	3.5E-05	31.5	0.1	7.4
7/26/2007	4.3E-05	NS	NS	NS
7/26/2007	2.8E-05	35.3	ND	14.2
7/26/2007	1.0E-04	34.6	0.0	24.5
7/26/2007	2.3E-04	34.1	0.0	9.8
7/26/2007	6.0E-05	34.0	0.1	9.3
7/26/2007	2.8E-05	29.6	0.1	11.4
7/26/2007	ND	NS	NS	NS
8/2/2007	7.6E-05	18.9	ND	7.8
8/2/2007	7.2E-05	17.9	3.1	5.3
8/2/2007	6.8E-04	16.2	10.7	8.8
8/2/2007	1.6E-05	19.1	ND	13.9
8/2/2007	2.5E-05	17.8	1.5	8.5
8/2/2007	1.3E-04	25.4	1.3	12.7
8/2/2007	1.3E-04	15.0	6.6	9.7
8/2/2007	1.9E-05	26.2	0.3	10.3
8/2/2007	8.1E-05	18.7	4.2	8.1
8/2/2007	1.7E-04	19.0	7.6	5.4
8/2/2007	5.0E-05	22.7	ND	16.4
8/2/2007	1.3E-04	21.8	0.3	8.5
8/2/2007	7.8E-05	17.2	2.4	10.8
8/2/2007	3.5E-04	17.9	9.1	6.9
8/2/2007	2.2E-05	22.8	0.0	6.6
8/2/2007	4.1E-05	22.8	0.4	4.8
8/2/2007	8.4E-05	17.5	6.6	10.7
8/2/2007	2.6E-05	22.5	0.2	17.8
8/2/2007	1.2E-04	17.5	6.9	6.9

Sampling Date	Specific Discharge (cm s^{-1})	Chloride Concentration (mg L^{-1})	Nitrate Concentration (mg L^{-1})	Dissolved Organic Carbon Concentration (mg L^{-1})
8/2/2007	4.0E-06	27.3	0.2	6.5
8/2/2007	9.4E-06	NS	NS	NS
8/2/2007	1.1E-05	NS	NS	NS
8/2/2007	1.9E-04	15.5	8.8	3.3
8/2/2007	3.9E-05	15.7	1.0	5.5
8/2/2007	1.1E-04	14.6	6.4	4.1
8/2/2007	1.9E-04	15.2	6.1	3.2
8/2/2007	5.9E-05	29.1	ND	15.5
8/2/2007	2.3E-05	24.1	ND	10.6
8/2/2007	2.0E-05	27.9	ND	10.0
8/2/2007	1.6E-05	18.3	0.2	6.9
8/2/2007	1.0E-04	14.6	6.1	6.0
8/2/2007	9.8E-05	23.1	0.8	8.9
8/2/2007	1.2E-05	23.8	ND	NS
8/2/2007	5.4E-04	17.3	11.8	5.9
8/2/2007	3.4E-04	24.4	0.5	8.1
8/2/2007	1.0E-04	18.3	2.9	9.4
8/2/2007	1.0E-04	24.2	ND	8.9
8/2/2007	2.8E-05	23.1	0.0	9.5
8/2/2007	2.8E-04	16.4	6.3	10.7
8/2/2007	4.5E-04	24.5	0.7	12.2
8/2/2007	1.3E-04	21.2	1.7	15.8
8/25/2007	6.8E-05	17.6	ND	NS
8/25/2007	4.5E-04	15.9	4.4	NS
8/25/2007	3.3E-04	15.3	4.9	NS
8/25/2007	5.0E-05	15.9	0.2	NS
8/25/2007	2.8E-05	18.5	1.8	NS
8/25/2007	7.3E-05	16.1	5.1	NS
8/25/2007	2.4E-04	15.7	4.9	NS
8/25/2007	2.6E-04	16.2	3.4	NS
8/25/2007	5.7E-05	20.5	ND	NS
8/25/2007	2.9E-05	15.4	1.9	NS
8/25/2007	2.6E-05	16.2	0.9	NS
8/25/2007	6.8E-05	18.6	0.4	NS
8/25/2007	1.9E-04	13.7	2.9	NS
8/25/2007	2.6E-05	15.1	1.3	NS
8/25/2007	2.5E-05	14.1	0.3	NS
8/25/2007	1.1E-05	14.6	0.5	NS
8/25/2007	1.6E-04	15.7	3.5	NS
8/25/2007	3.0E-04	16.9	1.8	NS
8/25/2007	3.0E-06	20.0	0.3	NS
8/25/2007	7.1E-06	21.2	0.8	NS
8/25/2007	ND	NS	NS	NS
8/25/2007	2.4E-04	NS	NS	NS
8/25/2007	8.7E-06	NS	NS	NS
8/25/2007	ND	NS	NS	NS
8/25/2007	1.9E-05	NS	NS	NS

Table A1.2: Surface Water Samples

Sampling Date	Sampling Location	Chloride Concentration (mg L^{-1})	Nitrate Concentration (mg L^{-1})	Dissolved Organic Carbon Concentration (mg L^{-1})
11/30/2003	Stream	23.5	2.2	NS
12/19/2003	Stream	27.0	2.5	NS
1/30/2004	Stream	30.6	4.0	NS
6/15/2004	Stream	32.8	3.1	NS
7/27/2004	Stream	33.1	3.3	NS
10/16/2004	Stream	30.3	2.2	NS
2/17/2005	Stream	31.3	2.6	NS
3/31/2005	Stream	28.0	2.5	NS
9/9/2006	Stream	23.0	1.8	10.9
9/21/2006	Stream	30.1	2.0	10.2
9/21/2006	Pond	24.6	0.8	NS
9/22/2006	Pond	24.2	0.8	17.9
9/22/2006	Stream	29.4	1.9	NS
7/10/2007	Stream	28.5	3.5	7.6
7/26/2007	Stream	27.1	4.8	NS
8/2/2007	Stream	28.5	4.3	5.9
8/25/2007	Stream	27.2	4.4	NS

Table A1.3: Nitrate Concentrations in Groundwater

Location	11/30/2003	12/19/2003	1/30/2004	6/15/2004	7/27/2004	10/16/2004	1/29/2005	2/17/2005	3/31/2005	5/16/2005
N1A	4.8	2.4	8.5	4.7	4.9	4.2	7.0	6.1	5.9	NS
N1B	10.0	11.0	10.7	6.2	5.7	6.1	7.1	6.8	7.3	NS
N1C	11.9	13.0	14.3	13.3	11.7	10.2	8.5	8.1	9.0	NS
N1W	11.2	13.4	11.7	2.7	2.6	8.3	8.3	7.5	7.8	NS
N3A	NS	6.6	10.4	7.9	7.3	4.1	3.0	3.5	4.4	3.4
N3B	8.7	11.6	10.7	11.4	11.3	3.0	5.3	4.9	5.4	7.4
N3C	11.9	13.9	11.3	11.6	11.2	7.2	7.4	7.0	7.6	8.6
N3W	9.6	11.6	11.4	11.7	11.4	3.8	6.1	5.2	5.3	7.6
N4A	1.3	4.3	7.5	5.3	4.8	2.5	2.6	2.7	3.6	5.5
N4B	0.8	1.6	7.3	8.2	8.0	2.0	3.2	3.6	4.0	8.3
N4C	0.1	0.4	6.2	6.5	7.2	0.9	1.9	2.2	3.3	9.3
N4W	1.3	2.0	7.5	8.1	7.6	2.1	2.7	2.9	4.1	8.9
N5A	1.8	1.6	1.9	8.7	8.7	1.3	0.6	0.4	0.4	0.6
N5B	2.9	7.7	1.8	9.9	9.2	1.9	1.9	1.5	1.2	1.9
N5C	9.7	9.6	9.9	11.5	11.5	4.3	5.5	3.5	2.4	4.6
N5W	1.4	7.2	0.9	8.5	7.9	0.3	0.0	0.3	0.0	0.4
N6A	4.8	9.7	8.8	6.0	5.8	2.2	5.9	5.6	4.0	2.9
N6B	6.4	9.6	12.4	9.5	9.3	4.5	7.3	7.1	5.5	4.6
N6C	8.9	12.7	13.4	11.0	10.9	6.6	8.4	8.1	7.0	6.4
N6W	6.2	11.1	13.8	6.9	6.7	4.6	5.8	6.8	6.4	6.0
N7A	10.7	13.4	15.1	6.4	7.3	4.2	6.2	5.4	7.0	7.4
N7B	11.5	13.1	17.0	14.3	13.9	10.9	9.0	9.0	10.5	9.1
N7W	13.5	15.0	16.6	10.7	10.0	8.8	7.4	8.0	10.3	8.8
N8W	0.3	0.4	0.7	2.1	2.0	0.3	0.0	0.3	0.4	0.0
N9A	3.3	3.4	7.8	1.2	1.6	2.6	1.1	2.3	2.5	1.4
N10A	6.2	2.8	15.4	8.6	7.8	6.5	7.7	7.6	5.6	6.4
N10W	2.4	1.0	13.5	5.0	3.7	3.2	5.1	4.3	2.1	4.3
N11W	NS	NS	NS	8.3	7.9	5.6	7.8	9.0	8.4	6.5
N12W	NS	NS	NS	10.7	9.9	8.0	4.3	5.6	6.1	5.0
N13W	NS	NS	NS	1.0	0.5	2.7	2.4	2.2	1.3	2.0
N14W	NS	NS	NS	NS	NS	10.4	8.4	NS	9.8	9.1
N15W	NS	NS	NS	NS	NS	2.9	3.7	3.8	3.5	3.2
N16W	NS	NS	NS	5.3	4.3	0.3	0.3	0.6	1.0	2.7

Location	11/30/2003	12/19/2003	1/30/2004	6/15/2004	7/27/2004	10/16/2004	1/29/2005	2/17/2005	3/31/2005	5/16/2005
HT	NS	NS	NS	4.0	4.8	NS	3.6	4.3	6.6	4.3
S1A	11.3	11.7	12.7	9.2	11.8	10.7	11.7	14.5	14.6	13.3
S1B	11.3	12.3	12.6	9.4	11.7	10.9	13.6	14.1	13.8	13.8
S2A	11.2	11.8	13.6	10.0	10.9	10.6	11.1	13.1	13.7	13.7
S2B	11.3	12.2	13.0	11.3	12.1	9.9	11.7	13.5	13.7	13.5
S3A	NS	NS	NS	NS	NS	1.6	3.2	3.6	3.9	3.7
S3B	NS	NS	NS	NS	NS	1.2	2.4	1.9	2.1	2.1
S4A	NS	NS	NS	NS	NS	8.2	6.6	9.7	9.4	8.9
S4B	NS	NS	NS	NS	NS	7.4	10.5	10.5	9.8	9.6

Table A1.4: Chloride Concentrations in Groundwater

Location	11/30/2003	12/19/2003	1/30/2004	6/15/2004	7/27/2004	10/16/2004	1/29/2005	2/17/2005	3/31/2005	5/16/2005
N1A	31.2	57.9	39.4	33.8	36.0	28.3	15.3	15.3	16.5	NS
N1B	19.0	31.1	35.2	38.7	40.4	21.8	14.2	14.3	14.7	NS
N1C	16.4	25.2	26.8	24.9	23.9	16.9	13.0	13.4	13.4	NS
N1W	17.2	26.1	34.7	41.6	45.0	19.8	13.9	13.9	14.1	NS
N3A	NS	52.8	36.3	44.5	50.9	41.5	25.4	27.1	23.3	31.4
N3B	22.2	30.0	37.4	36.0	39.7	29.9	15.8	15.9	16.0	24.2
N3C	17.3	26.5	32.9	24.5	26.6	16.8	13.5	13.5	14.2	16.9
N3W	22.7	31.0	33.9	34.6	37.7	27.7	14.0	15.4	16.1	24.0
N4A	25.4	35.1	39.2	31.2	34.2	26.8	30.3	30.6	24.5	20.0
N4B	25.7	35.9	39.8	35.0	36.9	27.1	24.1	22.2	19.8	17.7
N4C	26.8	33.9	39.6	35.2	40.9	27.8	23.5	26.7	22.0	15.2
N4W	26.5	42.6	39.5	32.0	33.0	26.9	30.0	28.6	22.5	16.7
N5A	36.9	47.8	43.1	32.6	34.9	30.9	25.7	26.5	34.3	36.9
N5B	31.2	36.4	40.9	30.5	30.7	24.0	18.6	19.7	26.1	26.3
N5C	25.8	28.3	38.5	30.6	33.0	23.1	15.3	19.2	27.4	24.2
N5W	64.4	38.6	44.9	30.9	34.5	42.7	26.0	28.0	36.1	39.4
N6A	18.8	26.6	39.4	32.2	34.4	23.0	15.3	15.1	15.8	20.3
N6B	17.3	27.0	33.2	30.1	32.2	16.9	14.8	15.3	14.8	18.3
N6C	19.1	26.3	35.3	29.7	32.3	17.4	14.7	15.1	14.9	17.3
N6W	46.0	26.4	32.0	31.7	35.4	18.2	19.6	15.6	15.4	18.0
N7A	17.3	29.2	30.4	17.9	19.7	12.9	13.7	14.3	16.2	17.5
N7B	16.0	23.9	26.1	25.3	27.1	17.3	12.9	13.0	14.3	14.0
N7W	17.6	26.8	27.0	20.3	21.9	13.9	12.7	13.5	15.6	16.3
N8W	27.2	36.1	32.7	31.3	35.0	18.2	20.4	23.4	36.9	27.2
N9A	19.5	46.6	37.3	50.4	59.6	59.9	33.1	44.3	35.2	26.5
N10A	16.1	24.4	33.9	21.0	23.0	13.0	13.3	14.4	18.7	16.3
N10W	16.3	27.9	31.4	17.7	19.6	11.3	15.5	17.3	27.2	18.5
N11W	NS	NS	NS	17.1	18.7	19.8	18.9	20.0	23.4	22.8
N12W	NS	NS	NS	25.1	27.2	18.5	24.5	22.3	23.3	18.7
N13W	NS	NS	NS	33.1	36.5	21.0	19.3	27.9	25.8	24.4
N14W	NS	NS	NS	NS	NS	17.6	15.1	NS	20.4	16.2
N15W	NS	NS	NS	NS	NS	13.1	19.7	20.8	42.2	29.8
N16W	NS	NS	NS	28.2	32.1	38.5	29.5	30.7	29.4	18.6

Location	11/30/2003	12/19/2003	1/30/2004	6/15/2004	7/27/2004	10/16/2004	1/29/2005	2/17/2005	3/31/2005	5/16/2005
HT	NS	NS	NS	12.9	17.6	NS	12.4	13.9	17.0	13.6
S1A	11.4	18.7	16.8	14.5	17.3	18.2	19.7	23.9	22.9	21.2
S1B	11.3	17.5	16.8	14.3	17.4	18.3	21.3	23.1	21.1	22.5
S2A	12.5	16.8	17.8	14.3	15.0	15.1	17.6	20.2	20.2	21.3
S2B	14.2	17.4	17.1	15.8	16.3	16.2	18.8	20.6	19.7	21.0
S3A	NS	NS	NS	NS	NS	41.1	36.6	42.6	38.8	38.6
S3B	NS	NS	NS	NS	NS	40.2	39.1	44.5	40.4	41.5
S4A	NS	NS	NS	NS	NS	23.2	16.5	16.5	15.8	18.5
S4B	NS	NS	NS	NS	NS	24.0	16.5	17.3	15.4	17.4

Table A1.5: Sulfate Concentrations in Groundwater

Location	11/30/2003	12/19/2003	1/30/2004	6/15/2004	7/27/2004	10/16/2004	1/29/2005	2/17/2005	3/31/2005	5/16/2005
N1A	32.4	42.6	28.4	29.6	28.9	29.4	22.2	24.0	25.1	NS
N1B	19.1	22.6	24.7	26.7	28.1	26.2	23.1	23.6	23.3	NS
N1C	16.9	19.3	17.3	20.0	17.8	20.5	21.6	23.2	22.1	NS
N1W	17.8	19.6	24.1	27.9	30.8	24.4	21.4	23.1	23.0	NS
N3A	NS	36.7	26.6	34.4	39.8	41.7	29.4	29.9	30.0	33.1
N3B	23.9	21.8	27.1	32.9	33.3	29.4	22.8	24.4	24.5	32.8
N3C	19.5	20.3	21.3	22.9	22.1	25.3	21.2	23.1	22.5	24.9
N3W	24.4	21.8	20.6	32.7	32.0	30.6	21.6	24.2	24.2	32.0
N4A	29.7	28.1	22.9	26.7	26.8	31.6	25.5	27.0	24.9	28.3
N4B	32.9	32.2	23.1	29.6	28.3	33.8	26.3	27.9	25.9	25.9
N4C	32.1	32.2	25.4	27.0	32.8	32.8	27.3	28.1	26.1	23.1
N4W	33.2	26.7	23.3	25.8	24.2	32.4	25.7	27.1	25.5	24.8
N5A	24.9	26.9	23.3	21.5	21.2	21.7	14.4	15.6	13.7	15.5
N5B	24.6	23.7	23.1	20.6	19.3	23.0	21.5	21.8	18.7	20.8
N5C	22.7	22.5	20.6	19.0	19.8	22.3	20.5	19.4	16.5	20.2
N5W	36.2	21.8	21.9	21.8	23.0	6.2	13.0	14.4	13.0	14.4
N6A	24.7	21.6	21.7	25.7	25.7	25.0	22.9	24.8	24.3	25.4
N6B	24.1	21.9	21.2	22.2	22.4	26.4	23.4	25.8	24.3	25.2
N6C	22.2	20.7	20.1	21.4	22.4	24.9	22.5	24.9	26.2	24.3
N6W	23.4	21.1	23.1	32.1	33.3	26.5	20.5	25.0	27.0	24.9
N7A	16.9	19.3	22.6	22.5	24.0	26.6	23.0	25.6	26.3	24.2
N7B	16.5	18.9	22.2	19.7	20.2	20.9	22.7	24.4	26.5	23.5
N7W	16.1	18.8	21.5	22.0	23.1	21.5	21.9	23.9	25.5	22.7
N8W	14.4	27.4	32.2	23.9	25.0	16.8	20.5	24.9	24.8	21.1
N9A	24.6	23.7	31.9	33.9	43.0	28.3	32.9	32.9	37.9	28.9
N10A	18.2	22.5	27.3	24.4	25.2	23.9	25.4	28.0	31.8	28.3
N10W	16.8	20.3	31.7	27.9	29.1	25.6	27.7	30.2	31.3	29.4
N11W	NS	NS	NS	23.9	25.4	24.9	23.5	25.1	28.5	24.1
N12W	NS	NS	NS	21.0	21.8	22.0	23.6	25.2	27.0	23.4
N13W	NS	NS	NS	43.1	42.9	30.8	27.1	28.2	30.4	30.4
N14W	NS	NS	NS	NS	NS	21.5	22.6	NS	27.7	22.1
N15W	NS	NS	NS	NS	NS	28.8	24.2	26.6	29.2	24.1
N16W	NS	NS	NS	24.5	29.3	17.1	15.4	15.2	18.3	21.7

Location	11/30/2003	12/19/2003	1/30/2004	6/15/2004	7/27/2004	10/16/2004	1/29/2005	2/17/2005	3/31/2005	5/16/2005
HT	NS	NS	NS	15.3	21.6	NS	24.4	24.2	26.9	21.4
S1A	22.2	25.3	30.1	18.9	23.0	20.5	17.7	21.3	21.7	19.9
S1B	22.2	26.5	30.1	18.6	23.4	21.6	20.5	21.8	20.0	19.9
S2A	20.3	22.1	29.8	19.0	19.8	19.7	19.8	22.7	20.9	19.7
S2B	21.5	23.2	28.9	22.0	22.8	21.7	20.4	22.6	21.0	19.6
S3A	NS	NS	NS	NS	NS	71.0	64.6	68.7	64.1	63.8
S3B	NS	NS	NS	NS	NS	73.4	69.9	74.8	70.8	70.4
S4A	NS	NS	NS	NS	NS	28.9	16.7	22.8	22.7	21.5
S4B	NS	NS	NS	NS	NS	30.4	19.9	22.1	22.8	23.1

Appendix 2: Estimation of Riparian-Zone Evapotranspiration

1.0 Purpose

Riparian zone evapotranspiration was needed for modeling groundwater flow in Chapter 4. The Penman-Monteith equation was the method used to estimate ET in that chapter. In order to ensure that those ET estimates were appropriate for Cobb Mill Creek, I estimated riparian zone ET with two other methods: one based on a chloride mass balance and another based on stream flow oscillations. ET estimates were all similar (ranging from 1.6 to 2 mm d^{-1}), suggesting that any of the methods would work well for the riparian zone of Cobb Mill Creek.

2.0 Methods

2.1 Estimating ET from Stream Flow Oscillations

Diurnal oscillations in stream discharge have been observed by others (*e.g.* Troxell [1936], Burt [1979], and Bond *et al*. [2002]) and were shown to result from the diurnal cycles of ET [Czikowsky and Fitzjarrald, 2004]. Similar diurnal oscillations in stream discharge were found at Cobb Mill Creek. Bond *et al*. [2002] developed a simple method for estimating the magnitude of evapotranspiration from these diurnal cycles in the stream flow record. The method assumes that in the absence of ET there would be no diurnal cycles and stream flow would change more gradually in response to longer-term climatic forcing. Bond *et al*. [2002] assumed that this longer-term pattern was indicated by connecting the daily stream flow peaks (Figure A2.1). The rate of water loss to ET was the difference between these straight line segments and the observed stream discharge. Thus, the estimated ET is expressed as a volume per time. In order to

compare these ET estimates to others, it was converted to dimensions of L T^{-1} by dividing through by the floodplain area at Cobb Mill Creek (described below).

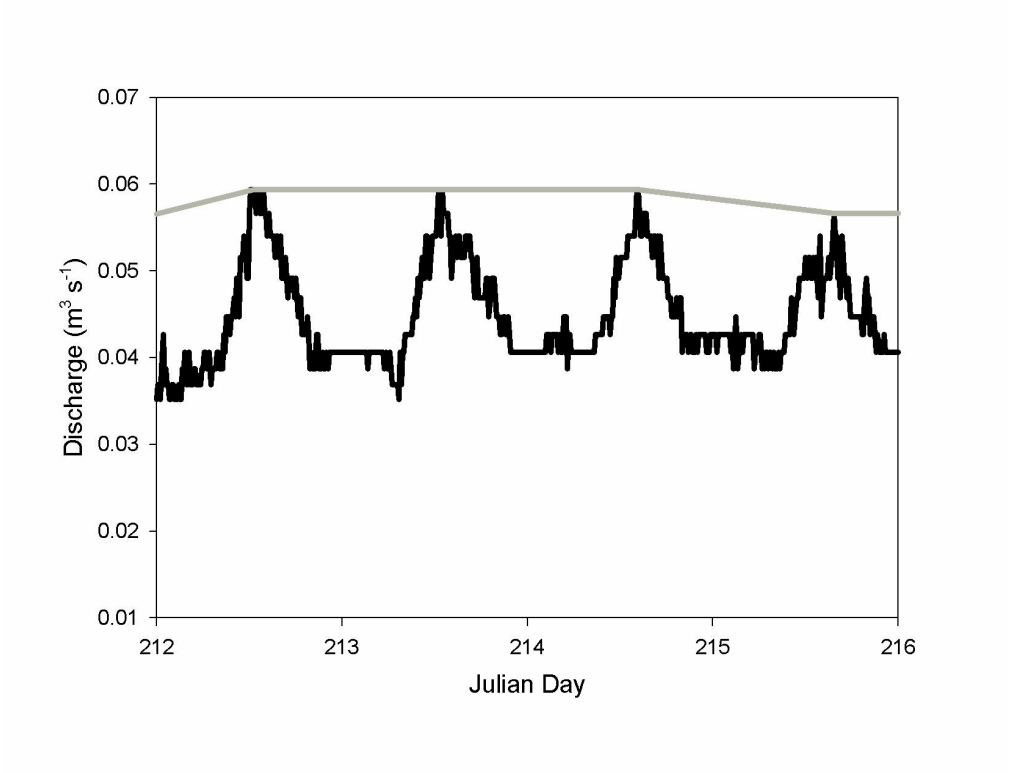

Figure A2.1: Four-day segment of the stream flow record at Cobb Mill Creek exhibiting diurnal fluctuations (solid black line). The gray line illustrates the assumed trend in stream flow in the absence of ET.

Stream discharge at Cobb Mill Creek was estimated from stream stage, measured continuously downstream of a double-barrel culvert running under VA route 600. A pressure transducer was installed in a stilling well to continuously measure total pressure (units = cm of water). A barometer was installed nearby to continuously record atmospheric pressure, which was needed to account for the effect of barometric pressure on stage measurements. Stream discharge was periodically measured at the same location and a rating curve was developed (Equation A2.1).

$$Q = 7x10^{-4} h^{11.846} \quad \text{(A2.1)}$$

Daily stream flow peaks were connected and the area between these straight line segments and the observed stream discharge indicated the rate of ET. This volumetric ET rate of water loss was converted to dimensions of L T^{-1} by dividing through by the area of the floodplain at Cobb Mill Creek.

The area of the floodplain, A_{fp}, was estimated by manually outlining the low-lying areas adjacent to Cobb Mill Creek on a digital elevation model of the catchment in ArcGIS 9.0 and calculating the area of the polygon produced. The area of the floodplain was 3 x 10^5 m^2, with a mean width of 125 m.

2.2 Estimating ET from Chloride Fluxes

Chloride mass balance was previously used by Claassen and Halm [1996] to estimate catchment-scale ET. Here, I present a similar method applicable to the floodplain (or riparian zone) of a stream. ET Estimates based on chloride fluxes assume an approximately steady input and conservative transport of chloride. As noted by Shaw et al. [2008], cycling of chloride between organic and inorganic forms occurs in soils and may complicate interpretations of chloride concentrations at short time scales. Over longer time scales, these short-term phenomena would cancel out and the conservative transport assumption would hold. Groundwater travel time across the floodplain of Cobb Mill Creek and other coastal plain streams is likely on the order of years, suggesting that an assumption of conservative chloride transport would be reasonable.

Groundwater exiting the riparian zone would have interacted with plant roots, potentially changing groundwater chloride concentrations through ET, root uptake, and root exudates. I assumed that root uptake and release of chloride would cancel out over the time scales of groundwater movement across the riparian zone. If that assumption

holds, then ET would result in a net removal of water from the system and effectively increase the concentration of chloride as groundwater moves across the riparian zone. Thus, a mass balance of chloride could be solved with estimates of groundwater chloride fluxes across the riparian zone.

To obtain chloride fluxes and then calculate ET, assume that each seepage meter location is the terminus of a stream tube that may or may not have been affected by evapotranspiration in the riparian zone. Each stream tube would have some initial discharge at its beginning and some final discharge (measured by the seepage meter) at the stream sediment surface. If no evapotranspiration extracted water from the stream tube, then the initial and final discharges would be equal. If the stream tube was affected by evapotranspiration, initial discharge into the stream tube would be equal to the sum of discharge measured by the seepage meter and discharge to the atmosphere resulting from evapotranspiration.

$$Q_i = Q_f + Q_{et} \tag{A2.2}$$

Q_i = flow rate into the stream tube

Q_f = measured seepage rate from the streambed

Q_{et} = rate of evapotranspiration

Equation A2.2 is a mass balance for water, assuming that water is incompressible. There is also a mass balance equation for chloride. Assuming that chloride behaves conservatively, the flux of chloride into the stream tube is equal to the flux of chloride out of the stream tube.

$$Q_i C_i = Q_f C_f \tag{A2.3}$$

C_i = chloride concentration at beginning of stream tube

C_f = chloride concentration measured at seepage meter

C_f and Q_f are measured with seepage meters and I assumed a constant value for C_i of 11.3 mg L^{-1}, the lowest groundwater chloride concentration observed between 11/30/2003 and 5/17/2005. It was assumed that this lowest concentration of chloride best represented groundwater unaffected by the riparian zone. An additional assumption used to estimate ET from chloride fluxes is that the spatial distribution of chloride concentrations discharging from the streambed does not change over the course of the day. With these assumptions, I combine Equations A2.2 and A2.3 to solve for Q_{et}.

$$Q_{et} = Q_f \left(\frac{C_f}{C_i} - 1 \right) \tag{A2.4}$$

The quantity Q_{et} is the reduction in discharge at each seepage meter due to ET. The Darcy's law analogy would be that ET reduces the hydraulic gradient toward the stream, thus reducing specific discharge. To factor out the dependence of Q_{et} on the size of seepage meter used, Q_{et} is divided by seepage meter area and expressed as q_{et}, which is the reduction in specific discharge from the streambed due to ET in the riparian forest. The average reduction in specific discharge from the streambed due to ET, $\overline{q_{et}}$, is related to the average rate of ET in the riparian zone.

To estimate the rate of ET from the riparian forest, $\overline{q_{et}}$ is converted to the rate of discharge of water to the atmosphere by multiplying by approximate streambed area.

$$Q_{ET} = \overline{q_{et}} wl \tag{A2.5}$$

w is mean stream width

l is stream length

Mean stream width is 1.5 m and stream length is 2400 m. The rate of discharge of water to the atmosphere is converted to the more common dimensions of length per time by dividing Q_{ET} by the approximate area of the floodplain, A_{fp}, in Cobb Mill Creek.

$$ET = \frac{Q_{ET}}{A_{fp}} \tag{A2.6}$$

Thus, an estimate of ET was achieved for each seepage meter and the collection of these values produced a distribution of ET rates.

2.3 Estimating Potential Evapotranspiration (PET)

The third method of estimating ET was the Penman-Monteith equation [*Campbell and Norman*, 1998].

$$PET = \left[\frac{s}{s+\gamma^*}\left(R_{abs} - \varepsilon_s \sigma T_a^4 - G\right)\frac{m_w}{\rho_w}\right] + \left[\frac{\gamma^*}{s+\gamma^*}\left(\frac{\lambda g_v D}{p_a}\right)\frac{m_w}{\rho_w}\right] \tag{A2.7}$$

This method relies solely on atmospheric data, thus providing a completely independent measure of ET from previous methods that used site-specific information on groundwater and stream flow.

The first term on the right hand side of Equation A2.7 describes the rate of ET due to net absorbed radiation. The second term on the right hand side describes the rate of ET due to latent heat loss. The Penman-Monteith equation accounts for stomatal and aerodynamic resistances to vapor transport from plant canopies to the atmosphere. The PET calculated by Equation A2.7 is more properly a reference ET, since the stomatal and aerodynamic resistances were selected for a completely closed, uniform, 12-cm-high canopy of grass with unlimited water supply. The reference ET represents a plausible upper limit for plant transpirable water. For the sake of simplicity, reference ET will be referred to as PET.

Meteorological data from the Hog Island VA, weather station (the closest station with a continuous record) was used for PET determinations with the Penman-Monteith Equation from July 1 to September 1 for 2006 and 2007. Total incoming solar irradiance, air temperature, horizontal wind speed, and relative humidity were measured at hourly intervals. Barometric pressure was assumed to be 100 kPa, since it was not measured during the desired time interval. Variations in barometric pressure have a very minor effect on PET estimates, so this simplification does not undermine their accuracy.

Equation 9 provides instantaneous estimates of PET. To compute daily PET, hourly instantaneous estimates were integrated for each day. The value of PET that was compared to the other two methods of estimating ET is the arithmetic mean of all daily PET estimates for the periods of July 1 to September 1 in 2006 and 2007.

3.0 Results

3.1 ET and PET Estimates

Each seepage meter provided an estimate of ET, and thus, a distribution of ET values was produced (Figure A2.2). This distribution was approximately log normal, with a mean of 2 mm d^{-1}. ET estimated from the stream stage record for a 5 day period from June 27 – July 2, 2003 was 1.6 mm d^{-1}. An average PET rate of 2 mm d^{-1} was obtained from July 1 to September 1 2006 and 1.9 mm d^{-1} from July 1 to September 1 2007 using the Penman-Monteith approach.

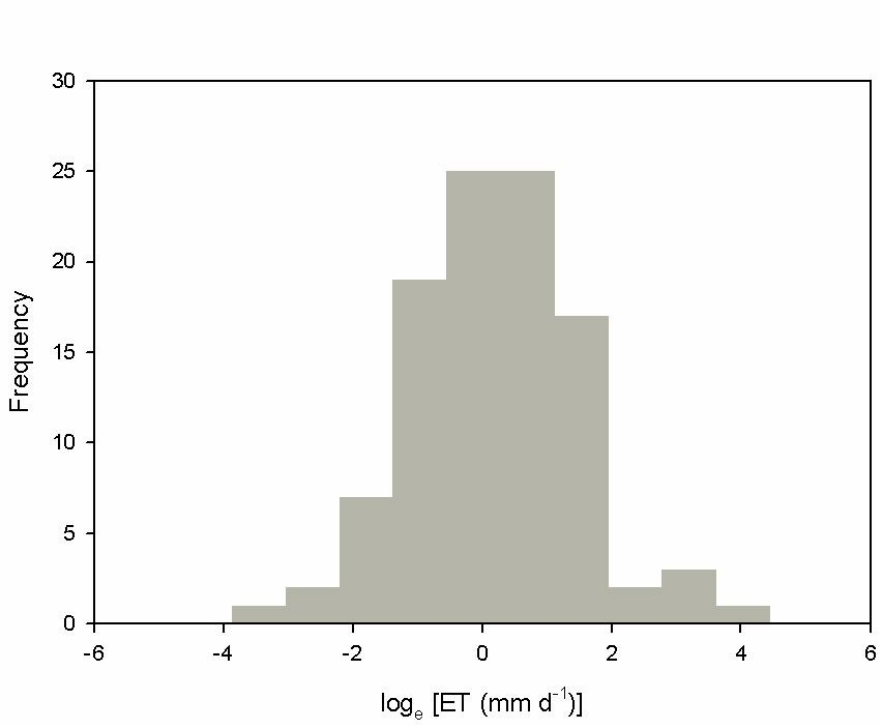

Figure A2.2: The distribution of ET calculated from chloride fluxes from the streambed.

4.0 Discussion

All three methods of estimating ET in this agree extremely well. Floodplain sediments in the riparian zone of Cobb Mill Creek are visibly moist throughout the year, even during periods of intense drought. The groundwater table is on the order of centimeters to decimeters below the ground surface in the riparian zone. Due to the moist conditions, riparian-zone vegetation likely has an abundant source of water throughout the entire growing season. Therefore, the close agreement between calculated rates of ET and PET is sensible.

Estimated ET from seepage meter measurements is likely a longer term average since travel times through the wide riparian zone are likely on the order of years. Assuming 60 m of riparian zone on each side of the stream (half of the total width of 125 m), travel time through the riparian zone for the mean rate of specific discharge measured

from the streambed would be almost 2 years. The calculation of travel time through the riparian zone assumes specific discharge is constant along flow tubes, although rates of specific discharge from the streambed are not likely to be constant along the entire length of a flow tube. Thus, the estimate of travel time through the riparian zone is more appropriately a rough order of magnitude estimate, but nonetheless illustrates the point that ET from chloride flux measurements is an average over a time scale of years.

The seepage meter ET estimates produced an interesting distribution of ET rates (Figure A2.2). Although the mean of this distribution agrees with the ET estimates from the other two methods, the limits of this distribution are extreme, ranging from 0.03 – 55 mm d^{-1}. The lower limit can be rationalized as a flow tube that completely bypassed the riparian zone, having never been affected by ET. The upper limit seems unrealistic. This upper limit may indicate that this seepage location was affected by short-term chloride cycling that can occur in soils.

There are processes in vegetated riparian soils that may affect chloride concentrations in groundwater. Controlled laboratory experiments have shown that soils can take up and release chloride after a step change in chloride inputs. Bastviken et al. [2006] showed that chloride uptake and release ultimately reached a steady state under conditions of constant flow and constant chloride inputs. Soils with temporal variability in groundwater residence times or transient chloride inputs will likely exhibit a dynamic pattern of chloride concentrations in groundwater [*Bastviken, et al.*, 2006]. This variability may be enhanced by plants that can take up and release halides in solution [*Xu, et al.*, 2004]. Water table dynamics may further contribute to non-steady-state conditions. Legout et al. [2007] found that chloride concentrations near the water table

decreased during times of the year when the water table rose and then increased when the water table declined. Since the riparian water table at Cobb Mill Creek is so close to the land surface and in contact with microorganisms and plant roots, these processes may contribute to dynamic short-term chloride cycling that is not fully understood. The transport of this water into seepage meters is a potential cause of the unrealistically high ET rates on the far right of the distribution in Figure A2.2.

Appendix 3: Approximation of specific discharge from the streambed of Cobb Mill Creek using shallow temperature profiles

Direct measurement of specific discharge with seepage meters is both time consuming and labor intensive. Alternative methods of obtaining these measurements that are more time and labor efficient are desirable. I explored the use of shallow temperature profiles for estimating specific discharge from the streambed of Cobb Mill Creek.

This approach is based on an analytical solution to the 1-D conduction-advection equation for heat that was presented by Bredehoeft and Papadopulos (1965) for steady vertical groundwater flow. Their solution takes the form,

$$\frac{T - T_0}{T_L - T_0} = \frac{\exp(\beta z / L) - 1}{\exp(\beta) - 1} \tag{A3.1}$$

where L is the maximum depth of temperature measurements, T_0 is the temperature at the top of the profile, T_L is the temperature at maximum depth (z), and β is a non-dimensional parameter defined as,

$$\beta = c_0 \rho_0 v_z L / \kappa \tag{A3.2}$$

where c_0 is the specific heat, ρ_0 is the density, and κ is the thermal conductivity of the bulk fluid-porous medium, and v_z is the vertical velocity of groundwater. Measured temperature profiles were converted to non-dimensional profiles by using the left side of Equation A3.1. A non-linear curve fitting algorithm was then used to find the optimal value of β for these curves. Then, the bulk physical properties of the fluid-porous

medium were estimated (c_0, ρ_0, κ) and Equation A3.2 was solved for the groundwater flow velocity at the location of each temperature profile.

This method is often used over depth intervals of meters to tens of meters in marine sediments (*e.g.* Tanaguchi *et al*. [2004]). I tested this method over depth intervals of tens of centimeters in the streambed of Cobb Mill Creek. Seepage meters were deployed to measure groundwater discharge from the streambed as previously described. On 8/11/2006 and 9/9/2006, eight of these seepage meters were carefully removed after flow rates were determined and then a thermocouple was used to measure temperature profiles directly beneath those seepage meters. The method of Bredehoeft and Papadopulos (1965) was used to calculate groundwater velocities from these temperature profiles, assuming a that $c_0\rho_0 = 4.18 \times 10^{-6}$ J K^{-1} m^3 and $\kappa = 2$ W m^{-1} K^{-1}, values similar to those used by Tanaguchi *et al.* [2004] for sandy sediments.

Groundwater velocities estimated from temperature profiles were compared with specific discharge from seepage meter measurements (Figure A3.1) and indicated that estimates from the two measurement methods were linearly related with a slope close to 1. This suggests that shallow temperature profiles can be used to accurately predict vertical groundwater velocities through the streambed of Cobb Mill Creek. This method is likely to work at other gaining streams within the Atlantic Coastal Plain.

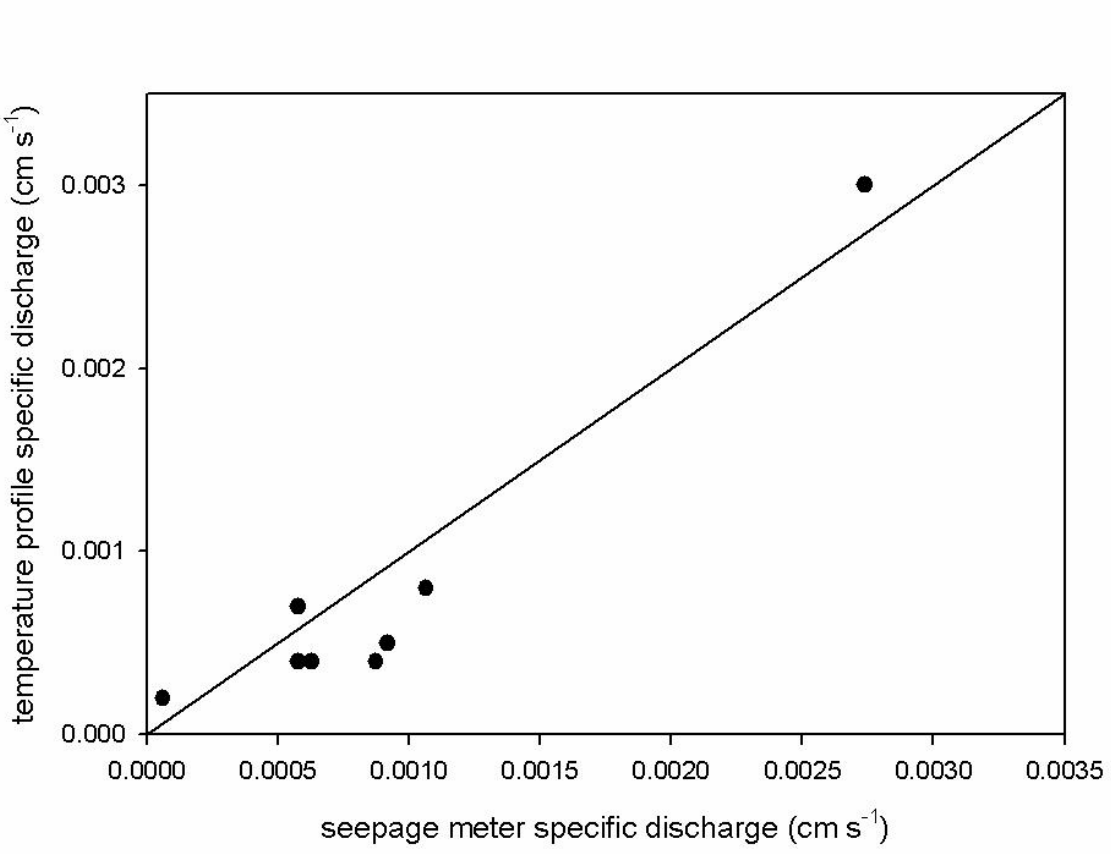

Figure A3.2. Comparison of specific discharge measured with seepage meters and estimated from streambed temperature profiles (solid circles). The straight line is a 1:1 line.